

**THEORETICAL ANALYSIS OF THE FLEXURAL STRENGTH AND
BEHAVIOUR OF UNBONDED PARTIALLY PRESTRESSED
CONCRETE BEAMS AND SLABS WITH AND WITHOUT
BONDED REINFORCEMENT**

A report submitted in partial fulfilment of the
requirement for the degree of
Master of Engineering
at the
University of Canterbury,
Christchurch,
New Zealand

by

TAN CHOR SUAN

February 1989

ABSTRACT

A modified version of the computer program written by Chan (1986) for the analysis of unbonded prestressed concrete members under third point loading was developed. The new program carries out the analysis more quickly and efficiently while still maintaining the required accuracy level.

The program was used to analyse twenty-two unbonded beams with bonded steel tested in China and twelve unbonded slabs with bonded steel and a further six unbonded slabs without bonded steel tested at the University of Canterbury. All analytical and experimental results were compared. The comparison revealed that the theoretical analyses gave good representation of the flexural behaviour of the unbonded concrete members both with and without bonded reinforcement.

The report confirms the Chinese finding that the combined reinforcement index has very significant effect on the ultimate tendon stress increase and moment capacity for the unbonded members. However, the effect of span-depth ratio on the flexural behaviour of unbonded partially prestressed concrete members was not significant. It is also confirmed that the unbonded members with bonded reinforcement behave in a more effective way than those without bonded reinforcement. The report recommends that bonded reinforcement should be used in design practice.

Two recommendations based on experimental results are proposed for the determination of ultimate moment capacity of unbonded partially prestressed concrete members. The proposed expressions for member without bonded reinforcement is given just for comparison and it is not recommended for use in practical design.

It is also recommended that the value of the combined reinforcement index chosen should be greater than 0.06 to prevent the occurrence of flexural instability and less than 0.305 for efficient design of the unbonded system. Value greater than 0.305 lead to a compression failure resulting in a low value of ultimate tendon stress increase and no increase in moment capacity.

ACKNOWLEDGEMENTS

I would like to take this opportunity to thank my two supervisors Dr. N. Cooke and Professor R. Park whom have given me invaluble encouragement ,advice and assistance.

LIST OF TABLES

TABLE		PAGE
7.1	Details of beams tested by Du and Tao (1984)	30
7.2	Comparison between experimental and predicted tendon stress increase and moment at failure	58
8.1	Detail of slabs tested by Yong (1980)	63
8.2	Comparison between experimental, analytical and predicted tendon stress and moment at ultimate	74
8.3	Detail of slabs tested by Savariar (1984)	76
8.4	Detail of slabs tested by Perumal (1986)	83
9.1	Comparison between experimental and predicted ultimate moment capacity by ACI 318-83 (1983) and proposed design equations (beams)	97
9.2	Comparison between experimental and predicted ultimate moment capacity by ACI 318-83 (1983) and proposed design equations (slabs)	98
9.3	Comparison between experimental and predicted increase in tendon stress at failure	99
9.4	Comparison between experimental and predicted ultimate moment capacity by ACI 318-83 (1983), Recommendations 1 and 2 . (beams)	100
9.5	Comparison between experimental and predicted ultimate moment capacity by ACI 318-83 (1983), Recommendations 1 and 2 . (slabs)	101
9.6	Comparison between experimental and predicted increase in tendon stress at failure, mean and standard deviation (beams)	102
9.7	Comparison between experimental and predicted increase tendon stress at failure, mean and standard deviation (slabs)	103
9.8	Comparison between experimental and predicted mean and standard deviation (all beams and slabs)	104

LIST OF FIGURES

FIGURE	PAGE
4.1 Section, strain, stress and component forces diagrams of a typical unbonded concrete section with bonded steel	10
5.1 Stress-strain relationship for concrete in compression	13
5.2 Stress-strain relationship for concrete in tension	15
5.3 Stress-strain relationship for reinforcing steel	16
5.4 Stress-strain relationship for prestressing steel as represented by the Ramberg-Osgood formula	18
5.5 Stress-strain relationship for prestressing steel (Perumal, Yong, Chan 1986, 1980, 1986)	20
5.6 Stress-strain relationship for prestressing steel (Savariar, Du and Tao 1984, 1984)	21
5.7 Effective embedment zone by CEP- FIP (1978)	22
6.1 Distribution of strain with and without external load	23
6.2 Stress, strain, section and component forces diagrams	26
7.1 Curve of increase in tendon stress at failure versus combined reinforcement index (Du and Tao , 1984)	31
7.2 Simplified load-deflection curve for unbonded beam with bonded reinforcement	32
7.3 Load-deflection curve (A-1)	34
7.4 Load-deflection curve (A-2)	35
7.5 Load-deflection curve (A-3)	36
7.6 Load-deflection curve (A-4)	37
7.7 Load-deflection curve (A-5)	38
7.8 Load-deflection curve (A-6)	39
7.9 Load-deflection curve (A-7)	40
7.10 Load-deflection curve (A-8)	41
7.11 Load-deflection curve (A-9)	42
7.12 Load-deflection curve (B-1, B-2, B-3, B-4)	43
7.13 Load-deflection curve (B-5, B-6, B-7, B-8, B-9)	44
7.14 Load-deflection curve (C-1, C-3, C-7, C-9)	45
7.15 Applied load/ Failure load vs Stress increase in Prestressing steel (A-1)	46
7.16 Applied load/ Failure load vs Stress increase in Prestressing steel (A-2)	47

7.17	Applied load/ Failure load vs Stress increase in Prestressing steel (A-3)	48
7.18	Applied load/ Failure load vs Stress increase in Prestressing steel (A-4)	49
7.19	Applied load/ Failure load vs Stress increase in Prestressing steel (A-5)	50
7.20	Applied load/ Failure load vs Stress increase in Prestressing steel (A-6)	51
7.21	Applied load/ Failure load vs Stress increase in Prestressing steel (A-7)	52
7.22	Applied load/ Failure load vs Stress increase in Prestressing steel (A-8)	53
7.23	Applied load/ Failure load vs Stress increase in Prestressing steel (A-9)	54
7.24	Applied load/ Failure load vs Stress increase in Prestressing steel (B-1, B-2, B-3, B-4)	55
7.25	Applied load/ Failure load vs Stress increase in Prestressing steel (B-5, B-6, B-7, B-8, B-9)	56
7.26	Applied load/ Failure load vs Stress increase in Prestressing steel (C-1, C-3, C-7, C-9)	57
7.27	Experimental and theoretical curve of tendon stress increase at failure vs combined reinforcement index (Du and Tao, 1984)	59
7.28	Theoretical curve of tendon stress increase at failure vs combined reinforcement index (Du and Tao, 1984)	60
7.29	Strain diagrams of unbonded beams with different q_0 values	61
8.1	Load-deflection curve (UB1, UB2)	64
8.2	Load-deflection curve (UB4, UB5)	65
8.3	Load-deflection curve (UB7, UB8)	66
8.4	Load-tendon stress curve (UB1, UB2)	67
8.5	Load-tendon stress curve (UB4, UB5)	68
8.6	Load-tendon stress curve (UB7, UB8)	69
8.7	Experimental and theoretical tendon stress increase at failure vs combined reinforcement index (slabs)	70
8.8	Theoretical tendon stress increase at failure vs combined reinforcement index (beams)	71
8.9	Experimental increase in tendon stress at failure vs l_e/d ratio (slabs)	72
8.10	Theoretical increase in tendon stress at failure vs l_e/d ratio (slabs)	73
8.11	Load-deflection curve (YUB3, YUB4)	77
8.12	Load-deflection curve (YUB5, YUB6)	78

8.13	Load-deflection curve (YUB7, YUB8)	79
8.14	Total load vs tendon stress increase curve (YUB3, YUB4)	80
8.15	Total load vs tendon stress increase curve (YUB5, YUB6)	81
8.16	Total load vs tendon stress increase curve (YUB7, YUB8)	82
8.17	Load-deflection curve (HUB3, HUB4)	85
8.18	Load-deflection curve (HUB5, HUB6)	86
8.19	Load-deflection curve (HUB7, HUB8)	87
8.20	Total load vs tendon stress increase curve (HUB3, HUB4)	88
8.21	Total load vs tendon stress increase curve (HUB5, HUB6)	89
8.22	Total load vs tendon stress increase curve (HUB7, HUB8)	90
9.1	Curve of tendon stress increase at failure vs combined reinforcement index for all experimental data with proposed design curves	95
9.2	The graph of $M_u / bd^2 f'_c$ vs combined reinforcement index	96

NOTATION

DIMENSION

A_s	= area of non-tensioned bonded reinforcement
A_{ps}	= area of prestressing steel
b, B	= width of section
c, x_1	= neutral axis depth
d_p	= depth from top compression fibre to depth of prestressing steel
d_s	= depth from top compression fibre to depth of bonded reinforcement
x	= depth to crack
l_e	= length of tendon from anchorage to anchorage

STRESS

f'_c	= compressive cylinder strength of concrete
f_{se}	= initial effective prestress prior to loading
f_{su}	= ultimate stress in unbonded tendon
f_{cr}	= cracking stress
f_y	= yield strength of reinforcing steel
E_s	= modulus of elasticity of steel
E_{sh}	= modulus of elasticity of steel
E_T	= tangent modulus of steel
E_c	= modulus of elasticity of concrete

STRAIN

ϵ_c	= concrete strain at the level of prestressing steel
ϵ_{su}	= total strain in the prestressing steel at ultimate capacity
ϵ_{cpi}	= initial effective strain at the level of prestressing steel
ϵ_{pi}	= initial tendon strain
ϵ_p	= total average tendon strain along the span length
ϵ_{cp}	= augmented concrete strain at tendon level
ϵ_{sh}	= steel strain at commencement of strain hardening
ϵ_{su}	= steel strain corresponding to f_{su}
ϵ, ϵ_s	= strain in steel
ϵ_y	= steel strain at first yield

ϵ_{cs} = ultimate concrete strain

ϵ_{cr} = cracking strain

NON-DIMENSIONAL FACTORS

q_e = $A_{ps} f_{se} / b d_p f'_c$

q_s = $A_s f_y / b d_s f'_c$

q_o = $q_e + q_s$

CONTENTS

CHAPTER		PAGE
1	INTRODUCTION	1
2	APPLICATION OF UNBONDED TENDONS IN PARTIALLY PRESTRESSED CONCRETE STRUCTURES	3
3	COMMENT ON RECENT CODE EXPRESSIONS AND EXPRESSION OBTAINED BY DU AND TAO (1984)	6
	3.1 ACI 318-83 (1982)	6
	3.2 NZS 3101 (1982)	6
	3.3 AS 1431-1378 (1978)	7
	3.4 British Standard Code of Practice CP 110 (1972)	7
	3.5 Comment on Recent Code Expressions and expression obtained by Du and Tao (1984)	8
4	FLEXURAL THEORY OF UNBONDED CONCRETE SECTION WITH BONDED REINFORCEMENT	10
5	STRESS-STRAIN RELATIONSHIP FOR CONCRETE, REINFORCING STEEL AND PRESTRESSING STEEL USED IN THE COMPUTER ANALYSIS AND EFFECTIVE EMBEDMENT ZONE	13
	5.1A Concrete in Compression	13
	5.1B Concrete in Tension	14
	5.2 Reinforcing Steel	16
	5.3 Prestressing Steel	18
	5.4 Effective Embedment zone	22
6	DESCRIPTION OF THE COMPUTER PROGRAM	23
	6.1 General Description	23
	6.2 Computer Analysis Procedure	25
7	DISCUSSION AND COMPARISON BETWEEN ANALYTICAL AND EXPERIMENTAL RESULTS FOR TESTS DONE BY DU AND TAO (1984)	29
8	DISCUSSION AND COMPARISON BETWEEN ANALYTICAL AND EXPERIMENTAL RESULTS FOR TEST DONE AT THE UNIVERSITY OF CANTERBURY	62

8.1	General	62
8.2	Unbonded Slabs tested by Yong (1980)	62
8.3	Unbonded Slabs tested by Savariar (1984)	75
8.4	Unbonded Slabs tested by Perumal(1986)	83
9	DESIGN RECOMMENDATIONS AND DISCUSSION OF RESULTS	91
10	SUMMARY, CONCLUSIONS AND SUGGESTIONS FOR FUTURE RESEARCH	105
10.1	Summary	105
10.2	Conclusions	106
10.3	Suggestions For Future Research	107
	REFERENCES	109
APPENDIX		
A	NOTATION	112
B	COMPUTER PROGRAM	114

CHAPTER 1

INTRODUCTION

Unbonded tendons are being used increasingly in partially prestressed concrete structures in many parts of the world. In Canada and USA more unbonded tendons are used in the floors and roofs of building than in any other type of structure. The practice started about 25 years ago, and it now represents the largest segment of post-tensioned construction in those countries. Over 55 million m² of post-tensioned unbonded building floors were completed in USA between 1965 and 1982 (ARTHUR E. ANDREW, 1987). Unbonded prestressed systems used in floors and roof slabs has proved to have advantage over other systems in the use of longer spans with fewer columns, thinner slab and giving greater flexibility of layout.

In China, unbonded systems have been used increasingly in many types of multi-storey buildings including factory buildings, residential buildings, public buildings, commercial buildings, parking garages, cold storage etc. They have devised ways of employing unbonded tendons in some unusual ways to overcome problems in certain types of structures. Unbonded systems have quickly gained popularity in China because it has been proved to be simpler in construction and more economical than the bonded system. Since 1987 a research programme, supported by the Chinese Government, in this area has been made to promote applications of unbonded system in China. More research is being done on the influence of earthquakes on the resistant behaviour of unbonded systems, the strength and crack behaviour of unbonded beams and the influence of non-prestressed steel on the ultimate stress increase of unbonded tendons.

The main objective of this research is to find out suitable design equations for the design of unbonded beams and slabs with bonded steel. The proposed design equation is based on the testing done in China and the University of Canterbury. It includes the main parameters which may influence the behaviour of unbonded prestressed concrete structures with bonded reinforcement. The main parameters are shown to be the area of the prestressing steel, the area of the bonded steel, span-depth ratio, cylindrical strength of the concrete, effective prestress in the tendon immediately before testing, tendon profile and the yield strength of the non-prestressed steel.

Chan et al (1986) developed a computer program for the analysis of unbonded slabs with and without bonded steel for uniform loading and third point loading. This program has been modified so as to reduced the computing time and still obtain good result for third point loading only. The

simplification is on third point loading is adequate for carrying out analyses on all the tests in the Chinese and University of Canterbury research programmes.

CHAPTER 2

APPLICATION OF UNBONDED TENDON IN PARTIALLY PRESTRESSED CONCRETE STRUCTURES

Unbonded tendon systems have been widely used in floor and roof slabs of many different types of buildings as an alternative to the conventional grouted tendon, which were too expensive to be used. Unbonded systems have some technical and commercial advantages over the bonded systems. The advantages are :-

- (a) Unbonded tendons are able to redistribute any local high stresses because the tendon is not bonded to the structure and hence decrease the local deflection of the structure. It is effective in the case where one floor is heavily loaded and the other floor is not loaded.
- (b) If a particular unit is damaged or cracked by impact or overloaded, it will close up again on removal of the overload.
- (c) Unbonded tendons have a smaller overall diameter than the bonded tendon and hence can be placed nearer to the face of the concrete which is limited by the codes in specifying the cover. This will provide a larger moment lever arm and hence increase the ultimate moment capacity of the concrete section.
- (d) Unbonded tendons can often lead to an increase in construction speed because of the delay caused by injecting cement grout and awaiting hardening are avoided.
- (e) The unbonded system has the advantage of simplicity in construction over the bonded system.
- (f) Unbonded tendons are simpler prefabricated and more easily have a lower frictional value.

By far the most common type of unbonded post-tensioned floor slab is the flat slab which is most generally adopted for apartment buildings, offices, hospitals, hotels etc. It is used in the United Kingdom for car-parks and office blocks.

The lift slab method is employed to reduce the cost of formwork and falsework, and has been extensively used in North America on multi-storey buildings, in the United Kingdom on multi-storey car-parks and in China on light industrial buildings (Arthur E. Andrew 1987 ; Du and Tao 1987). Waffle slabs are commonly used in buildings subjected to heavy loading where spans are similar in both directions. Continuous band is used in slabs where the

spans are predominantly in one direction and live loads are relatively light , for example in car parks, schools etc .

Unbonded post-tensioned two-way slabs are being used increasingly in office buildings, commercial buildings, parking garage constructions, cold storage plants etc. in China(Du and Tao 1987). In structures subjected to seismic loading the continuity of the roof slab is essential and can be obtained by post-tensioning tendons along the joints between adjacent slabs .

Unbonded tendons are utilized in ground slabs subjected to heavy loads , for example heavy duty pavement needed for warehouses with high stacking loads and fork-lift trucks, container terminals and airport hard standings. It is also used in ground slabs supported on piles and machinery foundation slabs subjected to heavy vibration such as engine test beds, drop hammers and printing presses. Unbonded tendons are particularly suitable for use in tanks and silos which will exert a uniform radial compression pressure and ensures the watertightness of tanks containing liquids. In remedial work for a sewage tank, bands of unbonded tendons can be used to strengthen the tank.

Practical experience has shown that post-tensioned unbonded floor slabs have behaved extremely well in earthquakes. In the case of the San Fernando earthquake which hit Los Angeles on 9th of February 1971, had the largest acceleration ever measured during an earthquake and had a severity of ground motion that was probably close to the maximum generated by any earthquake. This earthquake cause the loss of sixty four lives and around US \$ 1000 million damage. A post-earthquake survey (ESI Engineering Services INC 1971) was carried out on eighty projects constructed between 1967 and 1971 that were located within a twenty five mile radius of the area which recorded the largest acceleration. The projects tested included office buildings, hospitals, apartments, underground car parks and multi-storey car parks. Out of the eighty projects reviewed, only eight reported some damage to the structural system. Seven of them had the damage to shear wall and other rigid members. The last case was a structure in which continuous beams, supported on brick shear walls, carried one-way slabs. The shear walls failed, allowing some settlement of the slabs. None of the post-tensioned element were damaged; and after repairing the shear walls and pilasters, the building was put back into service.

It was found in the survey that properly detailed and constructed post-tensioned structures performed as well as or better than other types of structural systems. In a nine-storey car parking building in San Francisco, the seismic resistance was provided by the use of a prestressed concrete shear wall using unbonded tendons. The factor of safety against cracking is 1.65. After a severe earthquake, the unbonded tendons still remain elastic. This shows that structures containing them will suffer less damage and cost less to repair. In addition unbonded tendons don't suffer the problem of loss in bond with

cyclic loading which is faced by bonded tendons. The loss in bond will increase the possibility of corrosion if cracking develops.

The use of unbonded tendons in bridges is quite common in the United Kingdom and United States of America. Generally the cables are ^{within} outside the longitudinal web in a beam-and-slab construction or within the cell in the case of a box section . The use of external tendons means that unusually thin web sections can be a feature which greatly increases the strength to weight ratio and hence the structural efficiency. It also eliminates many of the problems of post-tensioning especially in segmental construction such as the maintenance of continuity of duct across joints between segments, frictional and grouting problem.

CHAPTER 3

COMMENT ON MOST RECENT CODE EXPRESSION AND EXPRESSION OBTAINED BY DU AND TAO (1983)

3.1 ACI 318-83 (1983)

The empirical expressions recommended by ACI 318 - 83 (1983) is mainly based on tests conducted by Mattock et al and is divided into two parts depending on the value of span-depth ratio as follows :-

For members with span-depth ratio less than or equal to 35

$$f_{su} = f_{se} + 68.9 \times (f'_c / 100 \rho_p) \text{ Mpa} \quad (3.1 a)$$

but f_{su} must be less than $f_{se} + 414 \text{ Mpa}$

For members with span-depth ratio greater than 35

$$f_{su} = f_{se} + 68.9 \times (f'_c / 300 \rho_p) \text{ Mpa} \quad (3.1 b)$$

but f_{su} must be less than $f_{se} + 207 \text{ Mpa}$

The ultimate stress obtained from expression 3.1a or 3.1b is used in determining the ultimate flexural capacity of the partially prestress member in the following expression

$$M_u = A_{ps} f_{su} (d_p - a/2) + A_s f_y (d_s - a/2) \quad (3.1c)$$

where

$$a = (A_{ps} f_{su} + A_s f_y) / (0.85 f'_c d) \quad (3.1d)$$

3.2 NZS 3101 (1982)

The New Zealand standard code has recommended a simplified expression based on ACI 318 - 83 (1983) . The expression for ultimate tendon stress is as follows:-

$$f_{su} = f_{se} + 100 \text{ Mpa} \quad (3.2)$$

The above empirical expression is for unbonded members with f_{se} of the prestressing steel greater than $0.5 f_{pu}$.

Similarly the value of f_{su} obtained from equation 3.2 is used in equations 3.1c and 3.1d to calculate the ultimate design moment strength.

3.3 AUSTRALIAN CONCRETE CODE : AS 1431- 1378 (1978)

The Australian code expression for calculating the ultimate tendon stress is adopted from the expression proposed by Warwaruk et al (1962) . The expression is as follows:-

$$f_{su} = f_{se} + 210 - (4.76\rho / f'_c) \times 10^5 \text{ Mpa} \quad (3.3a)$$

The expression for ultimate moment is

$$M_u = A_{ps} f_{su} d_p (1 - 0.6 q) + A_s f_y d (1 - 0.6 \times d_p / d) \quad (3.3b)$$

where

$$q = (A_{ps} f_{su} + A_s f_y) / b d_p f'_c \quad (3.3c)$$

The above expressions applies to members with span-depth ratios less than or equal to 40.

3.4 BRITISH CODE OF PRATICE CP 110 (1972)

Research done by F.N. Pannell is the basis of British code expression unbonded tendon member where

$$f_{su} / f_{se} = (1 + \lambda / q_e) / (1 + 2.5 \lambda) \quad (3.4a)$$

Where

$$\lambda = (7000 \times \rho_p) / f'_c \times (l_e / d) \quad (3.4b)$$

The expression for determining the ultimate moment is

$$M_u = f_{su} A_{ps} (d - 0.5 X)$$

Where X is the neutral axis depth.

3.5 COMMENT ON RECENT CODE EXPRESSIONS AND REGRESSIONS OBTAINED BY DU AND TAO (1984) .

It can be seen from the above four code expressions that most conservative results will be obtained from NZS 3101 (1982) code expression because f_{su} only depend on initial effective prestress . Other parameters like area of prestressing steel, area of bonded steel, crushing strength of concrete, yield strength of steel etc. , which will be crucial in determining the ultimate tendon stress, were not included. AS 1431 - 1378 (1978) code expression has all the other parameters as included in both ACI 318 - 83 (1983) and CP 110 (1972) code expressions except span-depth ratio. ACI 318-83 (1983) and CP 110 (1972) expressions which include the most number of parameters are still found to be conservative and inadequate in predicting the ultimate tendon stress.

Research done by Du and Tao on twenty-two unbonded partially prestressed beams has developed a new regression expression for determining the ultimate stress of prestressing steel. The expression is obtained from the graph of tendon stress increase at ultimate versus combined reinforcement index. The best straight line drawn among all the experimental data is

$$f_{su} = f_{se} + 786 - 1920 q_0 \quad (3.5a)$$

Where the combined reinforcement index q_0 is : -

$$q_0 = A_{ps} f_{se} / b d_p f'_c + A_s f_y / b d_s f'_c \quad (3.5b)$$

The above expression is limited to values of q_0 between 0.06 and 0.3 . The above expression contain two extra major parameters, the area and yield strength of reinforcing steel, which is not included in any of the above code

expressions and is shown to get less conservative results than ACI 318 - 83 (1983) and CP110 (1972) for unbonded beams with bonded steel. It should be noted that all the unbonded beams tested by Du and Tao have the same span-depth ratio of twenty. Hence the above expression obtained might not apply for a wide range of span-depth ratio unless its effect on flexural behaviour of unbonded beam with bonded steel is not significant.

Since present code expressions are still inadequate, an expression for f_{su} with more parameters of importance, covering a wider range of l_e/d ratio and q_0 values, should be found so as to obtain much better and less conservative result.

CHAPTER 4

FLEXURAL THEORY OF UNBONDED CONCRETE SECTION WITH BONDED STEEL .

The flexural theory of unbonded concrete section with bonded reinforcing steel introduced by Collins (1983) is used to calculate the ultimate moment of all slabs tested in this University by Yong (1980), Savariar (1984) and Perumal (1986), and beams tested in China by Du and Tao (1984), after obtaining the ultimate tendon stress from the proposed design equations 9.1 or 9.2 . It is found to give better result than equations 3.1c and 3.1d of ACI 318-83 (1983). The better results obtained by Collins (1983) is clearly shown in Table 9.1.

The basis of Collins' flexural theory in figure 4.1 below

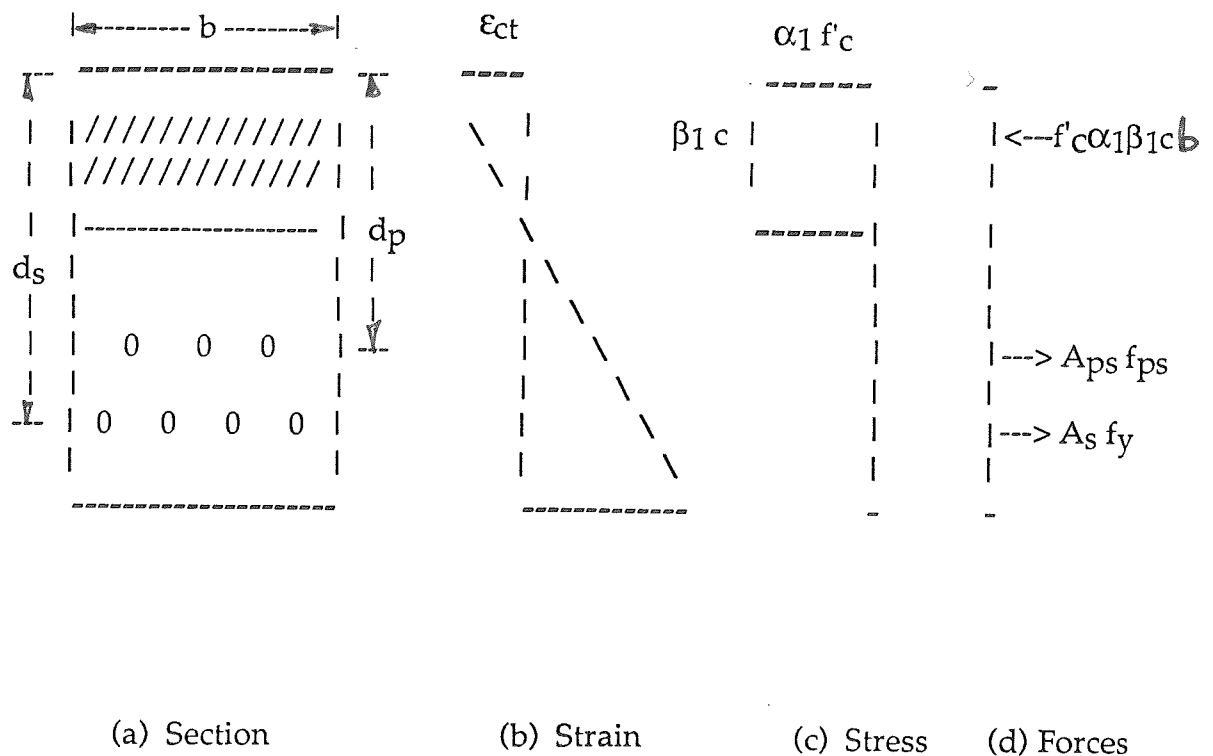


Figure 4.1 : Section, strain, stress and component forces diagrams of a typical unbonded concrete section with bonded steel.

The basis of Collins (1983) flexural theory for an unbonded concrete section with bonded reinforcement is based upon basic principles established

for reinforced concrete members , the most fundamental conditions of which are equilibrium of component forces and strain compatibility. These two conditions are used to solve for the unknown parameters. The main difference from the ACI 318-83 (1983) is the way he defines ^{the} stress block of ^{the} concrete compression area. The concrete compression stress area is modified to a rectangle block which has area equal to $\alpha_1 \beta_1 c f'_c$.

α_1 and β_1 is defined as :

$$\alpha_1 \beta_1 = \epsilon_{ct} / \epsilon_{cs} - 1/3 \times (\epsilon_{ct} / \epsilon_{cs})^2 \quad (4.1a)$$

and

$$\beta_1 = (4 - \epsilon_{ct} / \epsilon_{cs}) / (6 - 2 \times \epsilon_{ct} / \epsilon_{cs}) \quad (4.1b)$$

where

$$\epsilon_{cs} = 2 \times f'_c / E_c \quad (4.1c)$$

The value of neutral axis depth , c , can be determined from the equilibrium of component forces :-

$$f'_c \alpha_1 \beta_1 b c = A_{ps} f_{su} + A_s f_y \quad (4.1d)$$

or

$$c = (A_{ps} f_{su} + A_s f_y) / \alpha_1 \beta_1 f'_c b \quad (4.1e)$$

The ultimate moment is expressed by :-

$$M_u = A_{ps} f_{su} (d_p - \beta_1 c / 2) + A_s f_y (d_s - \beta_1 c / 2) \quad (4.1f)$$

where

$$\beta_1 c = (A_{ps} f_{su} + A_s f_y) / \alpha_1 b f'_c \quad (4.1g)$$

and

$$\alpha_1 = [\epsilon_{ct} / \epsilon_{cs} - 1/3 \times (\epsilon_{ct} / \epsilon_{cs})^2] / [(4 - \epsilon_{ct} / \epsilon_{cs}) / (6 - 2 \times \epsilon_{ct} / \epsilon_{cs})] \quad (4.1h)$$

In this research report ϵ_{ct} is taken to be 0.003 and value of E_c used for short term loading is $4200 \times \sqrt{f'_c}$.

Collins' (1983) flexural theory is also used to obtain the initial estimate of the of neutral axis depth in the computer analysis where c is given by equation (4.1e) .

CHAPTER 5

STRESS-STRAIN RELATIONSHIP FOR CONCRETE , REINFORCING STEEL AND PRESTRESSING STEEL USED IN THE COMPUTER ANALYSIS, AND EFFECTIVE EMBEDMENT ZONE .

5.1A CONCRETE IN COMPRESSION

For unconfined concrete in compression, the stress-strain relationship follows a second-order double parabola as shown in Figure 5.1 . It starts from zero strain value with zero concrete compressive stress , to strain value of ϵ_{cs} with at maximum concrete stress of f_{cs} which is the cylinder crushing strength of concrete and finally to the strain value of $2 \times \epsilon_{cs}$ with concrete compressive stress value falling back to zero.

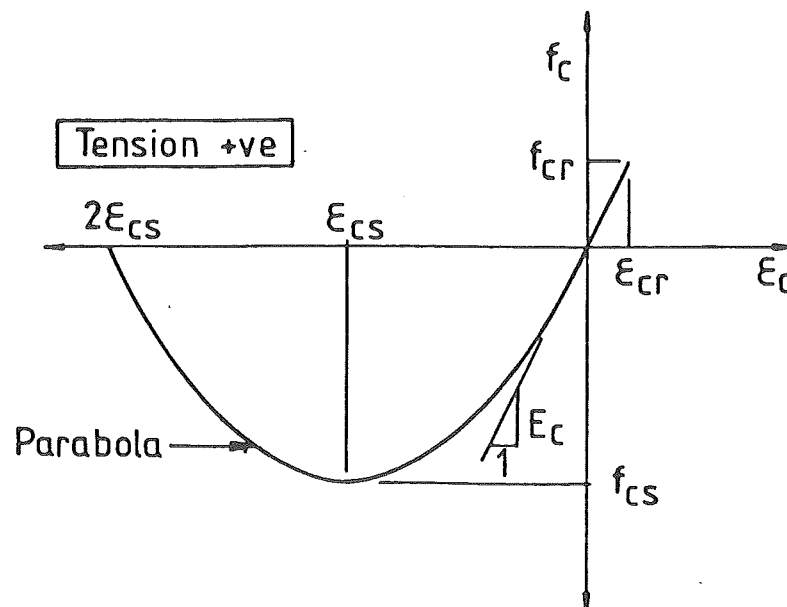


Figure 5.1 : Stress-strain relationship for concrete in compression.

the equation for the curve is as follows: -

$$f_c = f_{cs} [2 \times \epsilon_c / \epsilon_{cs} - (\epsilon_c / \epsilon_{cs})^2] \quad (5.1a)$$

where

$$\epsilon_{cs} = 2 \times f_{cs} / E \quad (5.1b)$$

$$f_{cs} = - f'_c \quad (5.1c)$$

For short term loading

$$E_c = 4200 \times \sqrt{f'_c} \quad (5.1d)$$

For long term loading

$$E_c = 1500 \times \sqrt{f'_c} \quad (5.1e)$$

5.1B CONCRETE IN TENSION

For concrete in tension, the stress-strain relationship is as shown in Figure 5.2. Initially the increase in concrete tensile stress is linear with a slope equal to that of concrete compressive curve at zero strain, that is E_c , until cracking stress is reached.

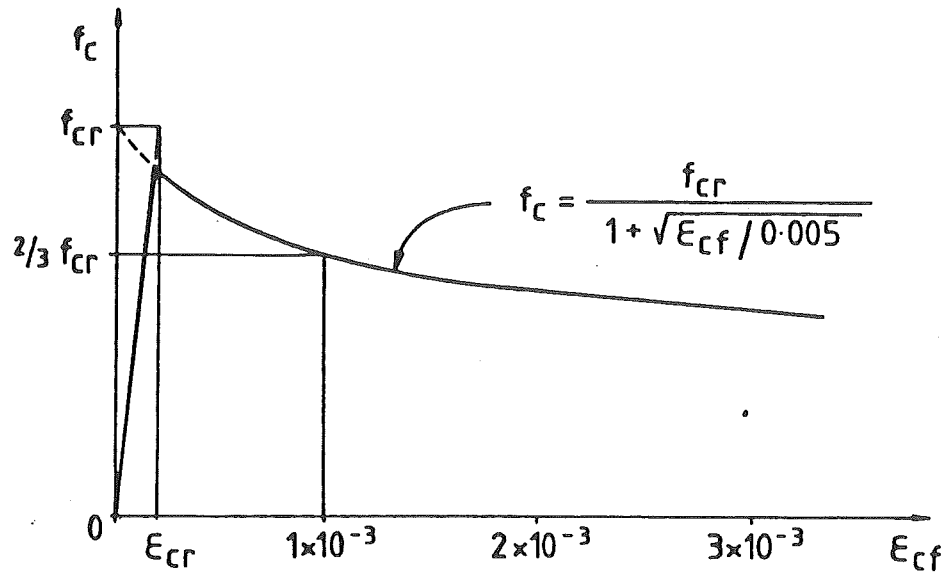


Figure 5.2 : Stress-strain relationship for concrete in tension.

The cracking stress for for short term loading is given by :-

$$f_{cr} = 0.4 \times \sqrt{f'_c} \quad (5.1f)$$

For strain value greater than ϵ_{cr} , the concrete tensile stress follows the stress-strain curve given by expression as follows:-

$$f_c = f_{cr} / (1 + \sqrt{\epsilon_{cf} / 0.005}) \quad (5.1g)$$

This curve when interpolated to zero strain value, has the stress value of f_{cr} and will decrease to a stress value of $2/3 \times f_{cr}$ at strain value of 0.001 .

5.2 REINFORCING STEEL

The stress-strain relationship used for reinforcing steel is mainly divided into three stages which is observed in the typical experimental test. The three stages are elastic loading, yielding and strain hardening as shown in Figure 5.3 .

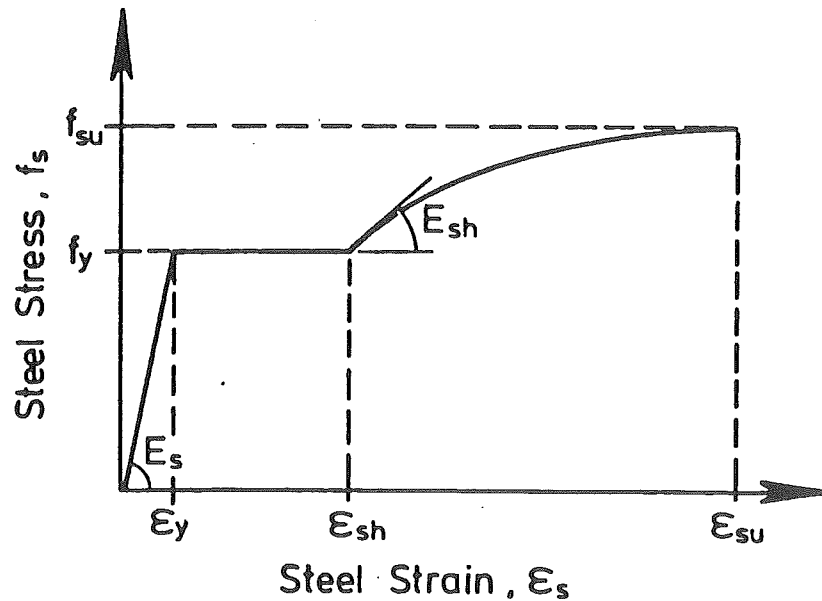


Figure 5.3 : Stress-strain curve reinforcing steel.

STAGE 1 : ELASTIC LOADING

In stage 1, the steel stress increase from zero value to yield stress f_y in a linear relationship with a slope equal to the elastic modulus of steel E_s .

The expressions for stress and the tangent modulus of steel are

$$f_s = E_s \epsilon_s \quad (5.2a)$$

The tangent modulus of elasticity E_T is given by :-

$$E_T = E_s$$

In the computer analysis E_s is taken as 200 GPa .

STAGE 2 : YIELD PLATEAU

This stage resembles a flat plateau as the steel stress remain unchanged while the steel strain is increasing.

In this case, we have

$$f_s = f_y \quad (5.2b)$$

And

$$E_T = 0$$

STAGE 3 : STRAIN HARDENING

When steel strain is greater than ϵ_{sh} the constant steel stress is finally over and the stress starts to increase again due to strain hardening behaviour of the reinforcing steel. It increases to ~~to~~ maximum steel stress f_{su} , in the form of power curve with ϵ_{su} corresponding to maximum steel strain. Fracture strain will occur at a strain larger than ϵ_{su} and at stress lower than f_{su} .

The expressions used for this portion of curve is as follows:-

$$(f_{su} - f_s) / (f_{su} - f_y) = (\epsilon_{su} - \epsilon_s) / (\epsilon_{su} - \epsilon_{sh}) \quad (5.2c)$$

Thus,

$$f_s = f_{su} + (f_y - f_{su}) \times [(\epsilon_{sh} - \epsilon_s) / (\epsilon_{su} - \epsilon_{sh})]^p \quad (5.3d)$$

Where p is the strain hardening power which can be found by differentiating equations 5.2d and substituting $\epsilon_s = \epsilon_{sh}$.

Thus,

$$p = E_{sh} [(\epsilon_{su} - \epsilon_{sh}) / (f_{su} - f_y)] \quad (5.2e)$$

The tangent modulus of elasticity can be obtained by manipulating equation 5.2d , and E_T is given by :-

$$E_T = E_{sh} [(f_{su} - f_s) / (f_{su} - f_y)] (1 - 1/p) \quad (5.2f)$$

Where E_{sh} is the initial slope at the strain value of ϵ_{sh} and can be determined experimently .

5.3 : PRESTRESSING STEEL

The stress-strain curve used by Chan et el is in the form of a single equation defined by the Ramberg - Osgood formula. A typical stress-strain relationship is as shown in Figure 5.4 .

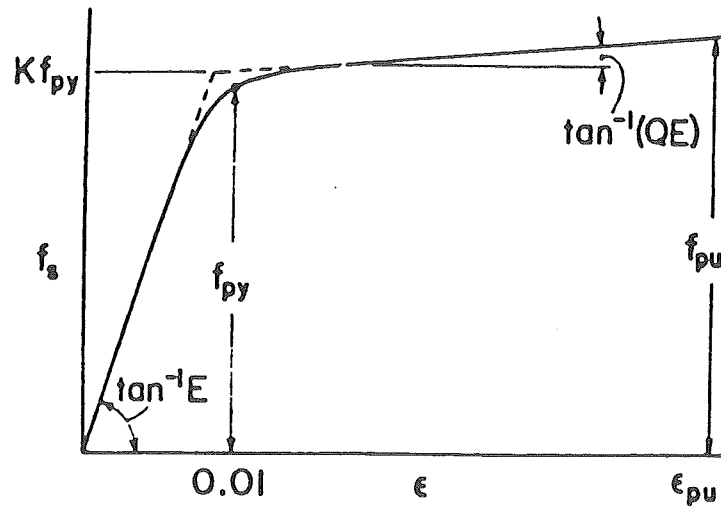


Figure 5.4 : Typical stress-strain curve for prestressing steel as represented by the Ramberg-Osgood formula.

Ramberg - Osgood formula is expressed as follows:-

$$f_s = \epsilon E_s \left\{ Q + (1-Q) / \left[1 + (\epsilon E / K f_{py})^{1/R} \right] \right\} \quad (5.3a)$$

where

$$Q = [(f_{pu} - K f_{py}) / (\epsilon_{pu} E - K f_{py})] \quad (5.3b)$$

f_{py} is the specified strength of prestressing steel and K is a coefficient which can be determined experimentally.

Figure 5.5 shows the stress-strain curves for prestressing steel used by Chan (1986) for the computer analysis of unbonded slabs tested by Perumal (1986), Savariar (1984) and Yong (1980). Chan (1986) found one Ramberg - Osgood formula for a prestressing strand diameter of 7.9 or 8mm and the other for a strand diameter of 12.48 to 12.7mm. I have found that these two curves show a much larger prestressing stress at a higher strain when compared to the stress-strain curves of Perumal (1986), Savariar (1986) and Yong (1986), obtained from typical experimental tests, as shown in Figures 5.5 and 5.6 .

I also found that the representation of prestressing stress-strain curve by a series of straight lines portions can be easily used in the computer programme and agree well with the typical stress-strain curves obtained from testing . The stress - strain curves in this analysis for test done at the University of Canterbury and in China are all shown in Figures 5.5 and 5.6. These are composed of a series of straight lines.

In the report by Du and Tao (1984), the shape of the prestressing stress-strain curves for group A,B and C were not given. The only information given for group A or C and B are the ultimate prestressing strength of 1790 and 1840 MPa , and the 0.2 % proof stress of 1465 and 1645 MPa respectively. These two stress-strain curves were obtained by matching a typical prestressing curve for 6.35mm diameter wire and Savariar's curve for 12.5mm diameter strand . It can be seen that the curves show similar shapes still maintaining the accurate values of 0.2 % proof stress and ultimate prestressing stress .

FIGURE 5.5 : STRESS-STRAIN CURVES FOR PRESTRESSING STEEL

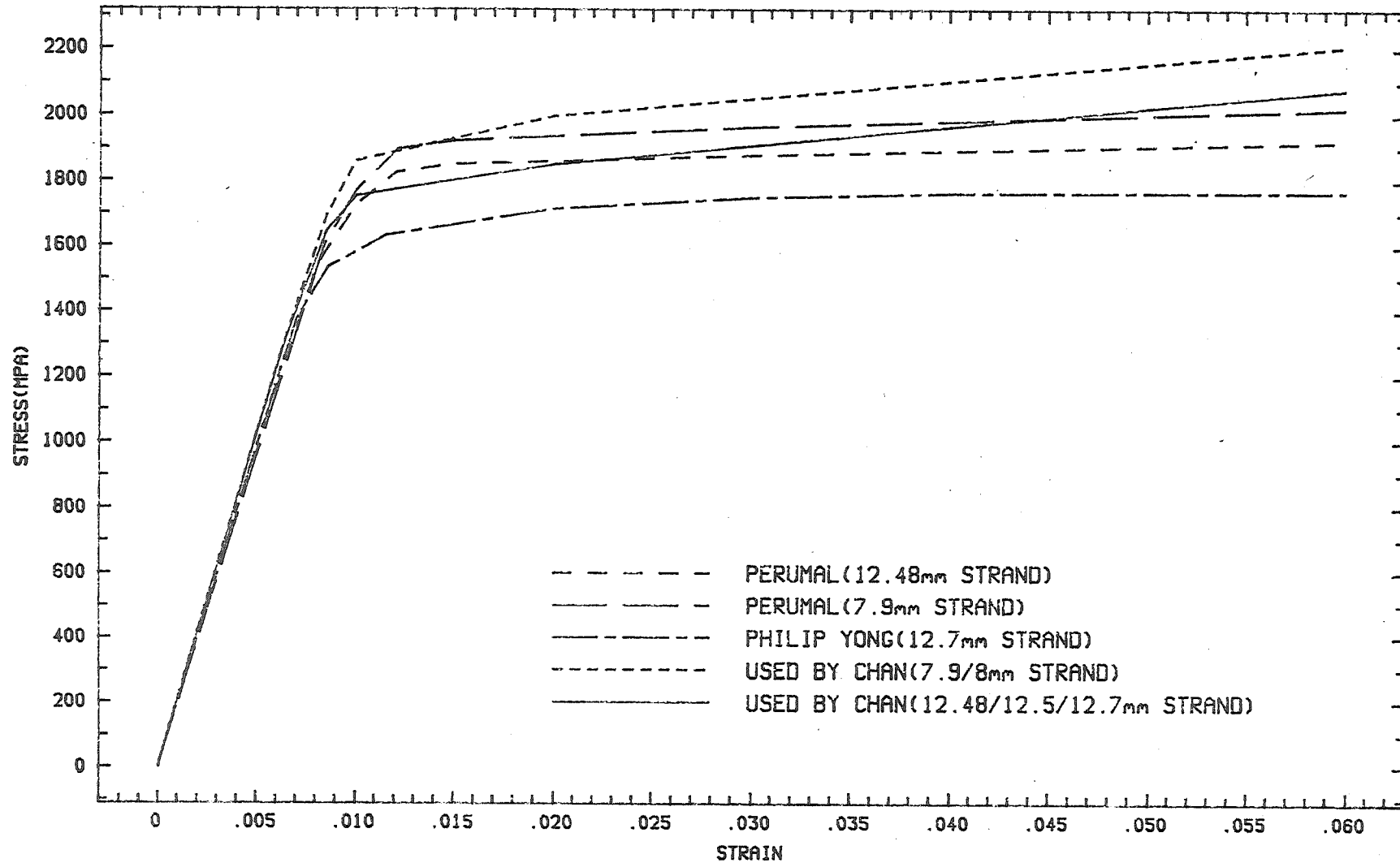
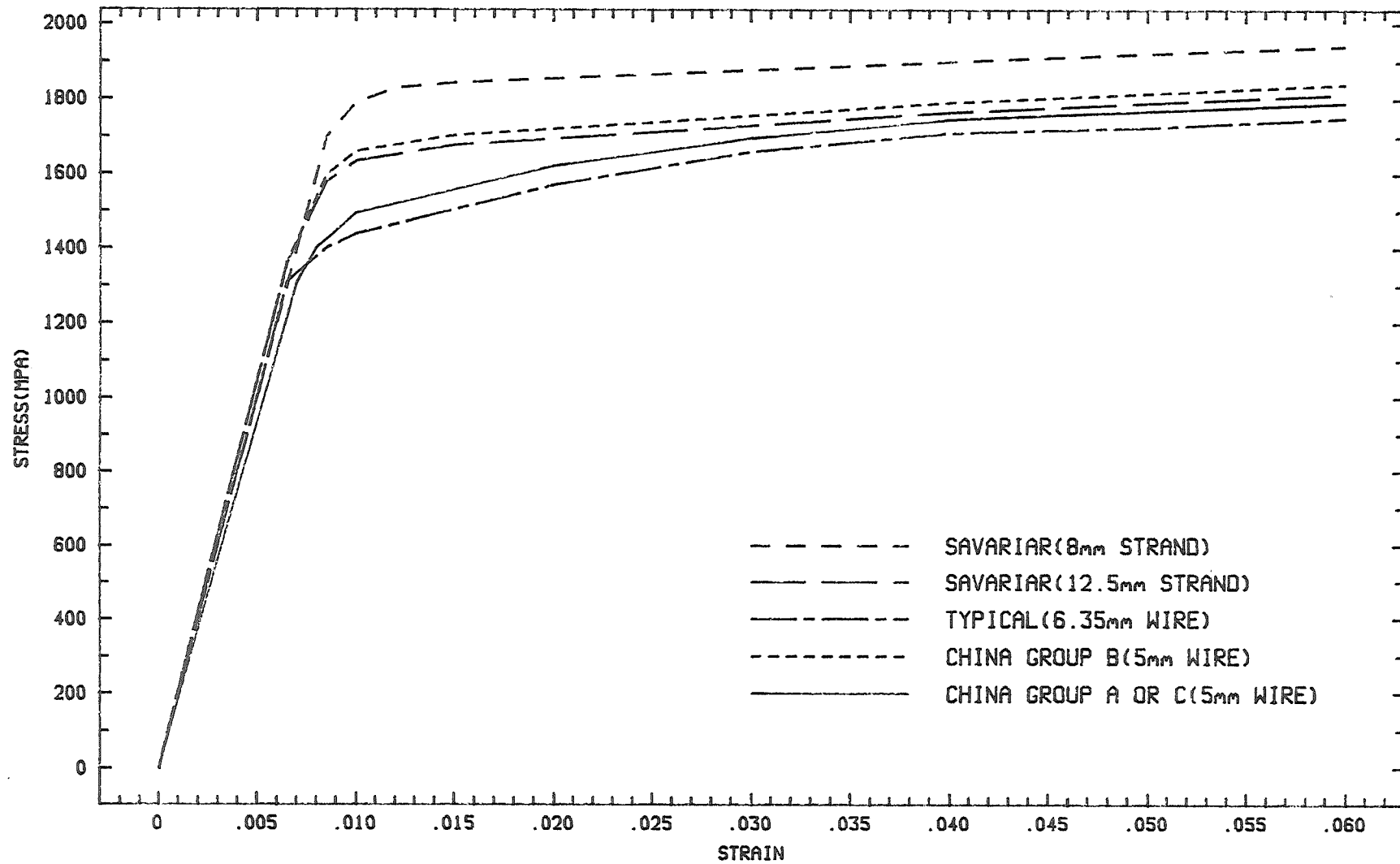


FIGURE 5.6 : STRESS-STRAIN CURVES FOR PRESTRESSING STEEL



5.4 EFFECTIVE EMBEDMENT ZONE

The area of effective embedment zone used complies with the requirement set by CEP - FIP code . Figure 5.7 shows the derivation of the effective embedment zone which is mainly based on arrangement or spacing and diameter of bars .

where

$BEZ = b_1 + b_2 + b_3$ is the width of the effective embedment zone .

$h_1 + h_2$ is the height of the effective embedment zone

ϕ is the diameter of the bar

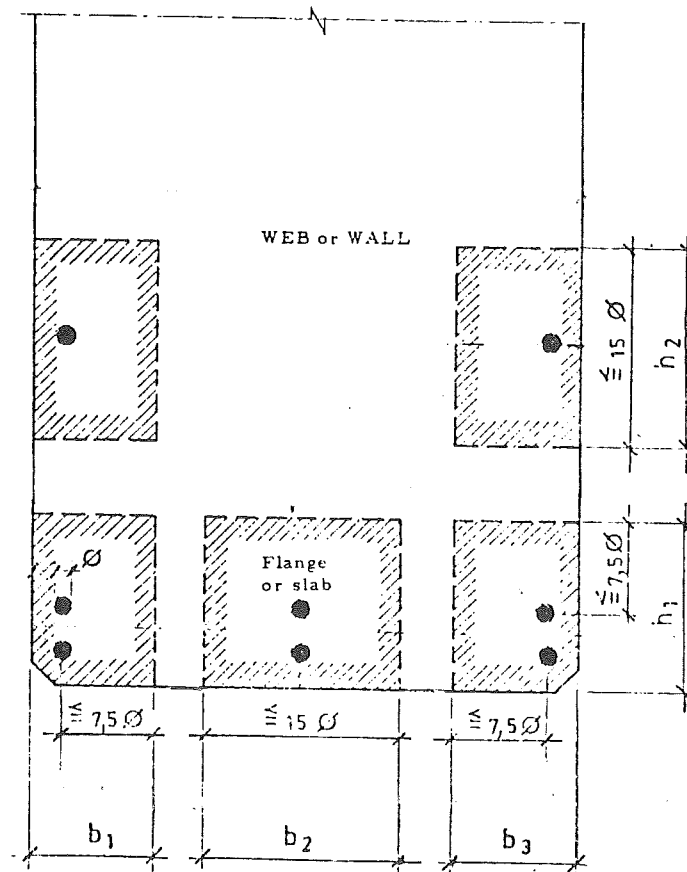


Figure 5.7 : Effective embedment zone as specified by code of CEP - FIB .

CHAPTER 6

DESCRIPTION OF THE COMPUTER PROGRAM

6.1 GENERAL DESCRIPTION

This program can be used to analyse the behaviour of unbonded beams or slabs either with or without bonded reinforcing steel and subjected to third point loading. A copy of the program is as attached in Appendix B. Chan (1986)'s program has been modified so as to achieve more efficient and accurate analysis. This has been achieved by removing part of the programme which analysed the behaviour of those slabs with parabolic profiles and those loaded by a uniformly distributed load. The numerical approach has also been changed radically in order to speed up the operation of the program. This program determines the magnitude of the ultimate load, the flexural capacity and the mid-span deflection at much faster rate while still maintaining the required accuracy level. The main purpose of the modification was to carry out the analysis of all the unbonded members tested at the University of Canterbury and in China, which were all under third point loading, so as to achieve a better understanding of the flexural behaviour and distinguish the main parameters which will affect the ultimate tendon stress increase and moment capacity of the members tested.

The basic assumptions still remain the same, that is, it is assumed that the initial strain distribution over the section with ^{and} ~~or~~ without external load is as shown in Figure 6.1.

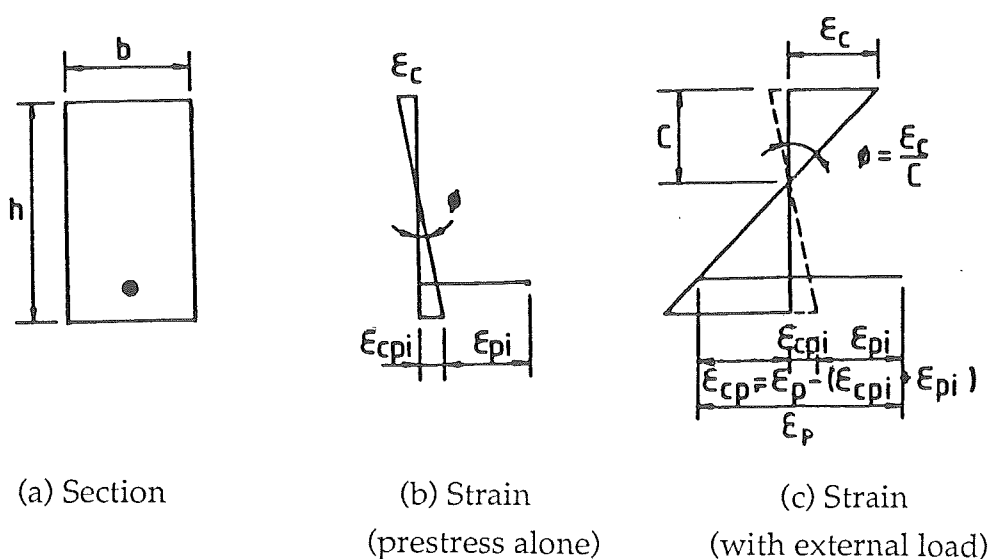


Figure 6.1 : Distribution of strain with and without external load.

ϵ_{pi} denotes the initial tendon tensile strain immediately before the application of external load. ϵ_{cpi} is the compression strain in the concrete at the level of prestress as a result of the action of the initial prestress alone. With the application of external load the concrete strain at the level of prestress changes from compressive to tensile. ϵ_{cp} denotes the tensile strain at the level of the tendon at a certain level of external load ^{and} ~~or~~ prestressing force and is determined from the following expression :-

$$\epsilon_{cp} = \epsilon_p - (\epsilon_{cpi} + \epsilon_{pi}) \quad (6.1)$$

ϵ_p is the prestressing strain at a certain level of prestressing force due to external loading. ϵ_{pi} and ϵ_p can be determined easily in the program from the appropriate prestressing stress-strain curve. In this program ϵ_p is calculated at each increment of prestressing force which indirectly implies that the external load also increases. At each increment of prestressing force a particular value of external load can be calculated by matching the total concrete strain at the level of prestressing steel between anchorages obtained from internal and external load to a satisfactory level of accuracy. This program uses an iterative process to find a particular external load which will satisfy the compatibility conditions resulting from each level of prestressing force until the ultimate load is reached, that is, when the top compressive strain ϵ_{ct} reaches 0.003 as specified in this project.

To calculate the strain at prestressing steel level caused by external load, it can't be assumed that the change in strain in the prestressing tendon is equal to the change in the strain in the surrounding concrete because the tendon which is unbonded is free to slip due to lack of frictional ^{bond} force. Hence the change in strain in all the points along the beam has to be considered. In order to simplify the calculations the beam is divided into as many sections as required to obtain a good estimate of the average strain along the beam. Strain values are calculated in all the sections and a linear relationship is assumed for strain between the sections. The average strain is obtained by equating the area of the strain diagram which varies at each section with the area of the constant average strain along the entire length.

6.2 COMPUTER ANALYSIS PROCEDURE

The main and basis steps in which the computer analysis will proceed are as follows: -

STEP 1

All data is input. These are (a) initial prestressing force and increment, (b) initial external load and increment, (c) cross section dimensions and span of the beam or slab, (d) effective embedment zone details, (e) area and profile of unbonded prestressing steel, (f) area and location of bonded reinforcing steel, (g) crushing strength of concrete, (h) number of divisions the span length is being divided into and finally (i) the minimum, maximum of the concrete top strain specified and the number of top strain increment.

STEP 2

The first level of prestressing force is set equal to the sum of initial prestressing force ^{plus} and ^{incremented} prestressing increment. The initial prestressing strain and prestressing strain at first level of prestressing force, are calculated from the appropriate stress-strain curve. Compressive concrete strain at the level of the prestressing steel is calculated from initial prestress only. Computation of equation 6.1 is then carried out to find the concrete strain at the level of prestressing steel due to first level of prestress.

STEP 3

Calculate the external moment resulting from the initial external load at each section along the span.

STEP 4

Calculate the moment, curvature and the concrete strain at the level of prestressing steel for each concrete top strain obtained from the minimum, maximum and at each interval between them. The minimum top strain must be less than -0.003 to achieve the failure load. The maximum top strain should be greater or equal to zero to cover for small external moment near the

supports and the number of top strain interval must be sufficient to obtain a good result. Forty-five divisions has been found to be reasonable in this analysis. The calculations are achieved as follows:-

STEP 4 a

Starting from maximum concrete top strain, estimate the neutral axis depth from Collins' (1983) equation 4.1e. Curvature, concrete bottom strain and depth to cracking strain can be estimated. All the component forces are then calculated ; these are, (a) concrete compressive force C , (b) reinforcing steel force T_3 , (c) concrete tensile force obtained from section with zero strain to cracking strain T_1 and (d) concrete tensile force obtained from section with effective embedment zone. All the component forces are as shown in Figure 6.2 together with stress, strain and section diagrams.

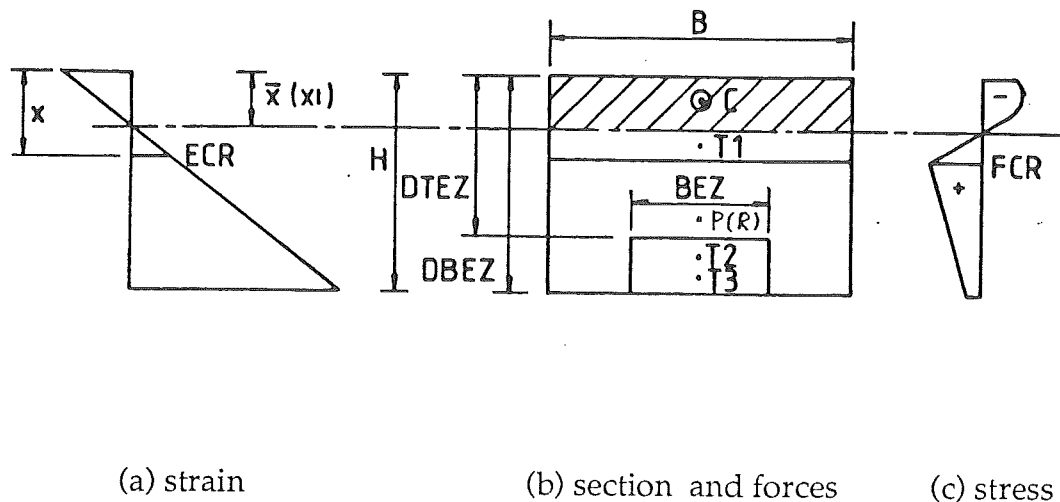


Figure 6.2 : Description of component forces with stress, strain and section diagram.

STEP 4 b

After all forces have been calculated, a test is performed to see whether the compressive force (C) is equal to the sum of tensile forces ($P(R) + T_1 + T_2 +$

T3) to within a specified limit. If the test fails, the concrete bottom strain is adjusted by a certain amount which will reduce the difference . Now all component forces have changed and new test is carried out. The process is repeated until the test is successful.

STEP 4c

Calculate the internal moment from the final component forces reached, the curvature and the concrete strain at the prestressing steel level.

STEP 4d

Starting with the next interval of concrete top strain, the same process is carried out as in steps 5, 6 and 7. It continues until the last interval which is the specified minimum top strain is reached. The data containing interval moments, curvatures, concrete strains at prestressing steel level and concrete specified top strains for all intervals are stored and tabulated in the order of increasing internal moment or decreasing top strain.

STEP 5

Beginning with external moment in step 3 calculated in the first section, a search is performed to match its value with the tabulated internal moments. The program starts with the lowest internal moment until it reaches an internal moment which is just larger than the required value. Linear interpolation is then used between the moment just lower and just larger to calculate the curvature, concrete strain at the prestressing steel level and the top strain associate this external moment. This process will be repeated until all sections specified have been covered.

STEP 6

Calculate the average concrete strain at the level of prestressing steel resulting from the external load. Another test is carried out to match the average strain at the level of the prestress obtained from the internal prestressing force with that obtained from external load. The two values must agree within a specified limit. Again, if the test fails the value of external load

will be adjusted and steps 5 and 6 will be repeated. New tests will continue to be carried until a satisfactory agreement is reached between the two values.

STEP 7

Calculation of the mid-span deflection is then performed by taking the first moment of the curvature diagram of half a span about the support. This is done section by section and summation is carried out in the end. Linear variation of curvature relationship is assumed between two adjacent sections.

STEP 8

This step starts with the second level of prestressing force obtained from summation of the first level of prestressing force and the specified increment of prestressing force and the former process from steps 4 to 7 will be repeated. The next level of prestressing force is then used until the corresponding concrete top strain reaches 0.003.

Tabulated results of all successive level of prestressing forces will be printed in the output. The printed results are plotted in graphs to compare with experimental results.

CHAPTER 7

DISCUSSION AND COMPARISON BETWEEN EXPERIMENTAL AND ANALYTICAL RESULTS FOR TESTS DONE IN CHINA BY DU AND TAO (1984)

Twenty-two unbonded partially prestressed concrete beams were tested by Du and Tao (1984). All the beams have the same breadth, depth, span, span-depth ratio, and were tested under third point loading. Unbonded prestressing steel and bonded reinforcing steel were all placed at 220 and 250mm respectively below the top of all the beam section. The beams are divided into three groups, group A, B and C as shown in table 7.1 .

The 0.2% proof stress for the prestressing steel of group A or C and group B were 1465 and 1645 MPa, and the elastic moduli of the prestressing wire were 205 and 210 MPa respectively. The ultimate strength of prestressing wire for group A or C were 1790 MPa and for group B were 1840 MPa .Group B has higher strength concrete and prestressing wire than group A while group C has larger yield strength of prestressing steel than group A. The combined reinforcement index q_0 , range from 0.0628 to 0.47 covering a sufficiently large range as used for practical design. The main objective of the tests was to find out the effect of concrete strength, amount and strength of bonded prestressing steel ,amount and yield strength of reinforcing steel used , on the behaviour of unbonded partially prestressed concrete beams.

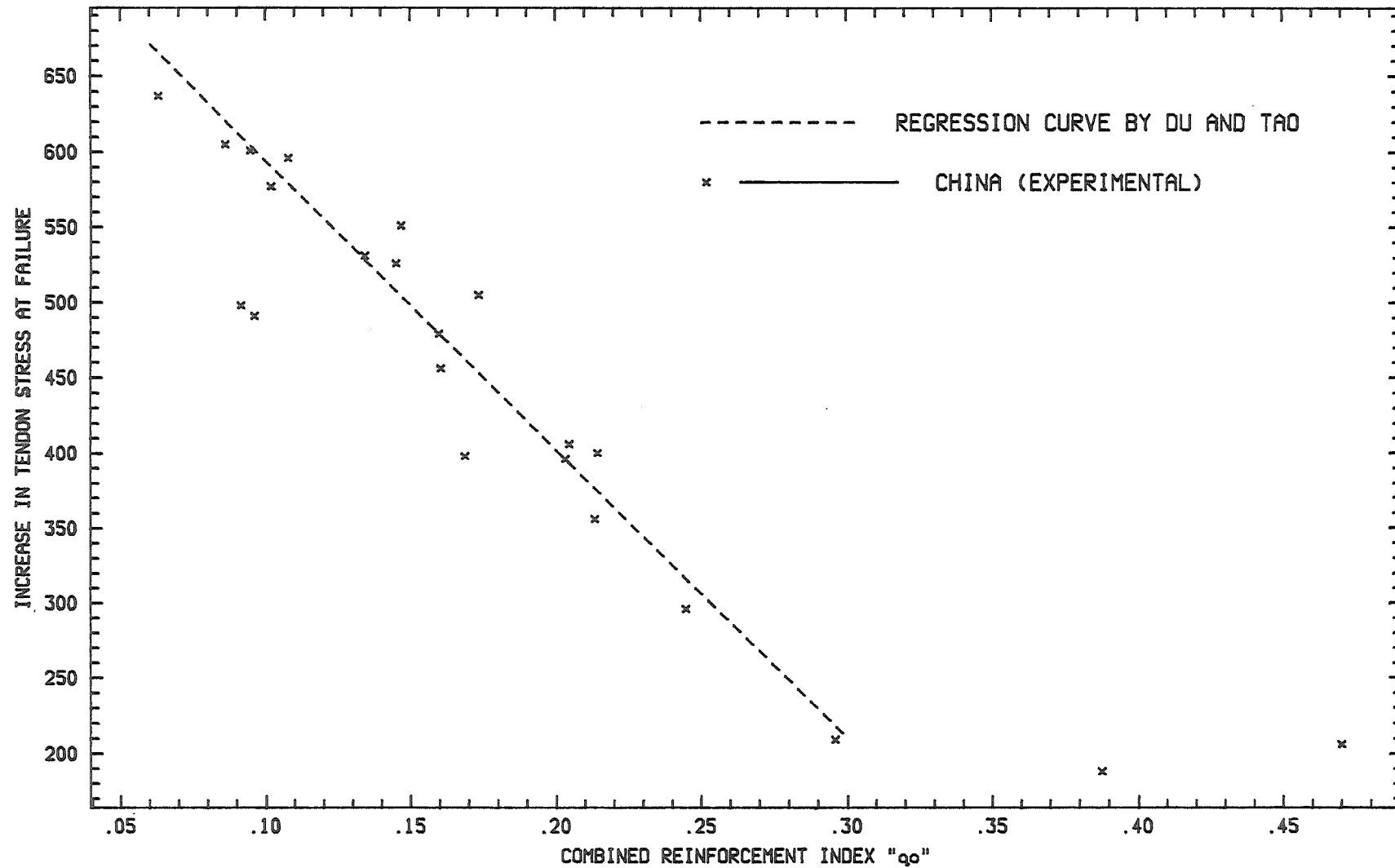
The experimental results show a generally linear relationship between increase in tendon stress and combined reinforcement index as shown in Figure 7.1 . The increase in tendon stress decreases linearly with increasing combined index value. But the relationship appears to be valid for q_0 values less than or equal to 0.3 . A regression formula was developed from these experimental results, as shown in equation 3.5a, to predict the increase in tendon stress for any unbonded partially prestressed beam with combined reinforcement index value ranging from 0.06 to 0.3 .

They also found that the load-deflection curves and the load-increase in tendon stress curves for beams with q_0 less than or equal to 0.2448, exhibited three distinct stages. The first , second, and third stages are uncracked elastic, cracked elastic and plastic flow respectively as shown in Figure 7.2 .

Table 7.1 : Details of test beams.

beam	f'_c	A_{ps}	f_{se}	A_s	f_y	q_o	q_e	q_s
	(MPa)	(mm ²)	(MPa)	(mm ²)	(MPa)			
A1	30.6	58.8	960	157	267	.0913	.0542	.0389
A2	30.6	98.0	904	157	430	.1450	.0822	.0627
A3	30.6	156.8	820	236	430	.2135	.1194	.0942
A4	30.6	58.8	869	157	430	.1077	.0464	.0613
A5	30.6	78.4	810	308	400	.1734	.0590	.1144
A6	30.6	156.8	854	462	400	.2959	.1243	.1716
A7	30.6	39.2	885	308	400	.1466	.0322	.1144
A8	33.1	58.8	894	462	400	.2033	.0451	.1586
A9	33.1	156.8	920	804	395	.3876	.1211	.2665
B1	45.8	58.8	1008	157	267	.0628	.0368	.0260
B2	45.8	98.0	987	157	430	.1019	.0600	.0419
B3	42.5	156.8	963	236	430	.1688	.1009	.0678
B4	42.5	58.8	1040	157	430	.0860	.0409	.0451
B5	42.5	78.4	989	308	400	.1342	.0518	.0824
B6	42.5	137.2	1002	462	400	.2144	.0919	.1235
B7	48.8	39.2	1002	308	400	.0946	.0229	.0717
B8	42.5	58.8	1002	462	400	.1598	.0390	.1208
B9	48.8	98.0	1050	804	395	.2448	.0600	.1849
C1	33.1	58.8	905	157	389	.0959	.0447	.0513
C3	33.1	156.8	825	236	485	.2046	.1086	.0961
C7	33.1	39.2	955	462	485	.1603	.0321	.1282
C9	33.1	156.8	903	804	505	.4700	.1215	.3485

FIGURE 7.1: INCREASE IN TENDON STRESS AT FAILURE VS COMBINED REINFORCEMENT INDEX



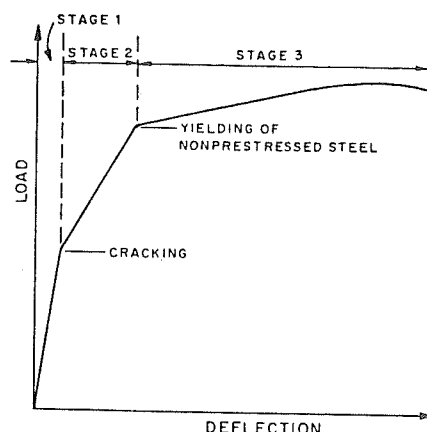


Figure 7.2 : Simplified load-deflection curve for unbonded beam with bonded steel .

For unbonded beams with q_0 values greater than or equal to 0.2959, the curves only show the first two stages because at high q_0 values the non-prestressing steel does not yield . Computer analyses have been carried out on all the beams tested and the analytical results obtained show this same trend for all the twenty-two beams analysed. I believe that the computer program is successful in predicting the actual flexural behaviour of the beams tested.

Analytical results are plotted in Figures 7.3 to 7.26 . Figures 7.3 to 7.11 show the comparison of experimental and analytical load-deflection curves for beams of group A. Close comparison is seen for all beams . Some beams show slightly less deflection calculated analytically. This means that the analytical beams are slightly stiffer for group A. Generally the theoretical analysis by computer program shows a good representation of actual beam behaviour for group A.

For group B and C, no experimental curves were given by the report presented by Du and Tao (1984), hence only analytical results are plotted. Figures 7.12 and 7.13

show load deflection curves of beams of group B. All the curves of group B beams show the three distinctive stages which is the typical behaviour of beams with low q_0 as expected. Figure 7.14 shows analytical curves for all beams of group C . Beam C9 is the only one showing two stages while the rest all show three stages.

Beam C9 is the only beam in group C with a high q_0 value and non-prestressing steel will not yield as predicted.

Analytical results of load-tendon stress increase plotted in Figure 7.15 to 7.23 also show close agreement with experimental results of beams in group

A. This means that the theoretical analysis by computer can also give good representation of actual relationship between tendon stress and external load for beams of group A. Most beams show slightly lower analytical values of increase in tendon stress than experimental data. This means that ultimate tendon stress obtained from the computer analysis will mainly be slightly conservative compared to that obtained from tests as shown in table 7.2. From table 7.2 we can also observed that the tendon stress at ultimate obtained from analytical results is much closer to the experimental results than that predicted from ACI 318-83 (1983) and NZS 3101(1982) code expressions and analytical ultimate moments show good comparison with the experimental ultimate moments. All ultimate moment capacities from the computer analysis show slightly lower values than experimental values even though some analytical ultimate tendon stresses are larger than experimental values, for instance, beams A1 and A6. Hence the computer analysis generally shows slightly less conservative results for ultimate moment and mostly lower values for ultimate tendon stress.

Figures 7.24 and 7.25 load-tendon stress increase curves for beams of group B. The three distinct stages are all clearly shown for all curves. This agrees with all load-deflection curves of group B in figures 7.12 and 7.13. Load-tendon stress increase curves for group C are plotted in Figure 7.26. Again three stages are shown for beams except beams C-9 which has large q_0 value and agree with figure 7.14 which shows load-deflection curves.

The analysis using the computer program gave satisfactory results for all beams tested in China. It give better results than predicted results by ACI 318-83 (1983) and NZS 3101(1982) code equations.

A comparison between the experimental and the analytical data for beams in groups A,B and C is made in Figure 7.27. All results are plotted in the graph of tendon stress increase at failure versus combined reinforcement index. Close agreement is observed for most beams. Both experimental and analytical data show the same trend for the relationship between tendon stress increase and combined reinforcement index where tendon stress increase values decrease linearly for q_0 values less than 0.3 and remain basically unchanged for q_0 values equal or greater than 0.3.

Analytical data conform more closely to the linear relationship than experimental results where analytical points are less scattered from a best straight line drawn. This is clearly shown by comparing Figure 7.28 and 7.1.

It should be noted that the values of tendon stress increase only change slightly or remain nearly constant for q_0 values greater than 0.2959 where the load-deflection curve started to show only two distinct stages. The decrease in tendon stress increase value with increasing q_0 can be explained by the lowering of neutral axis depth as the area of prestressing and reinforcing steel getting larger. Figure 7.29 shows clearly that the unbonded beam with a higher

FIGURE 7.3 : LOAD-DEFLECTION CURVE

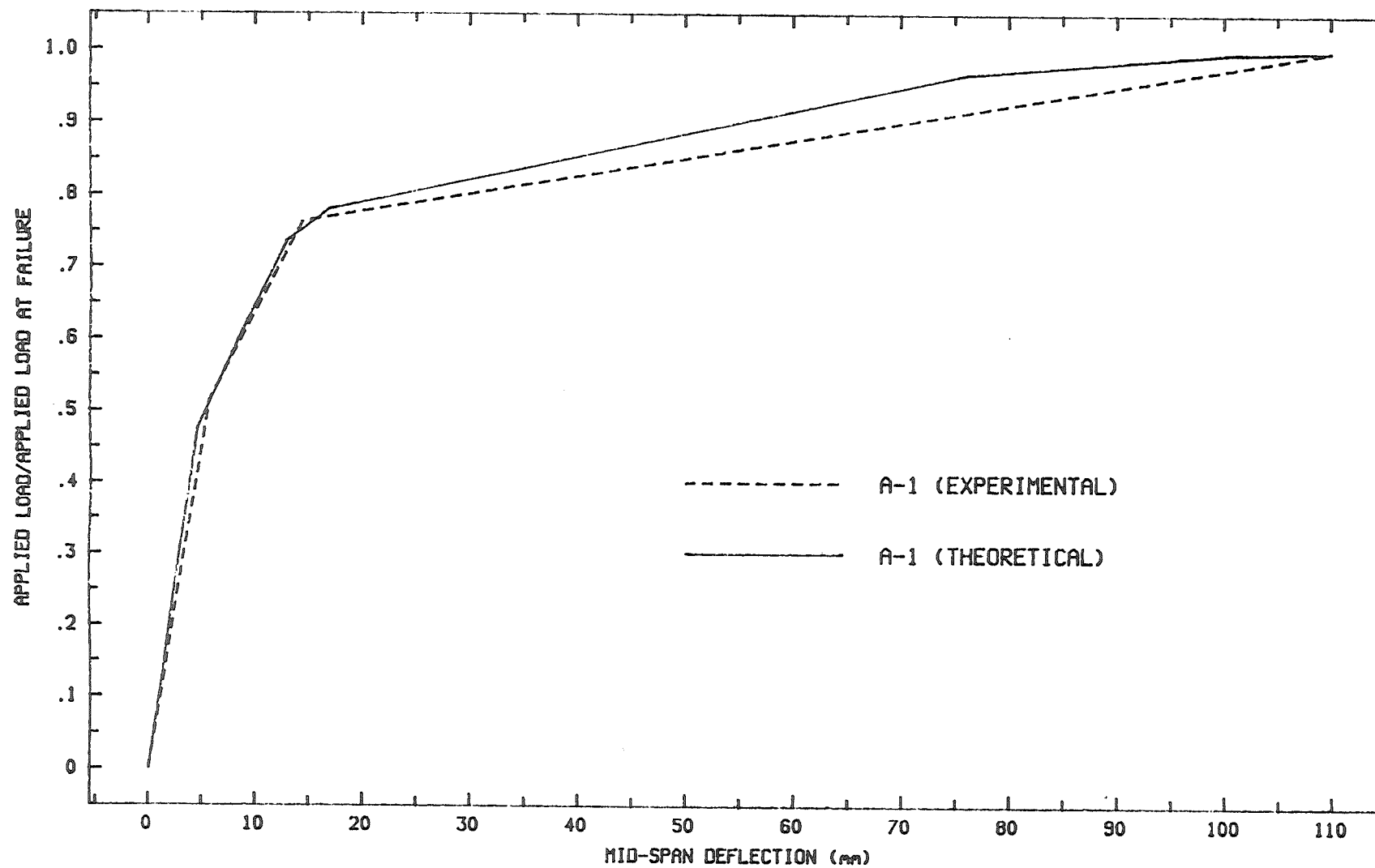


FIGURE 7.4: LOAD-DEFLECTION CURVE

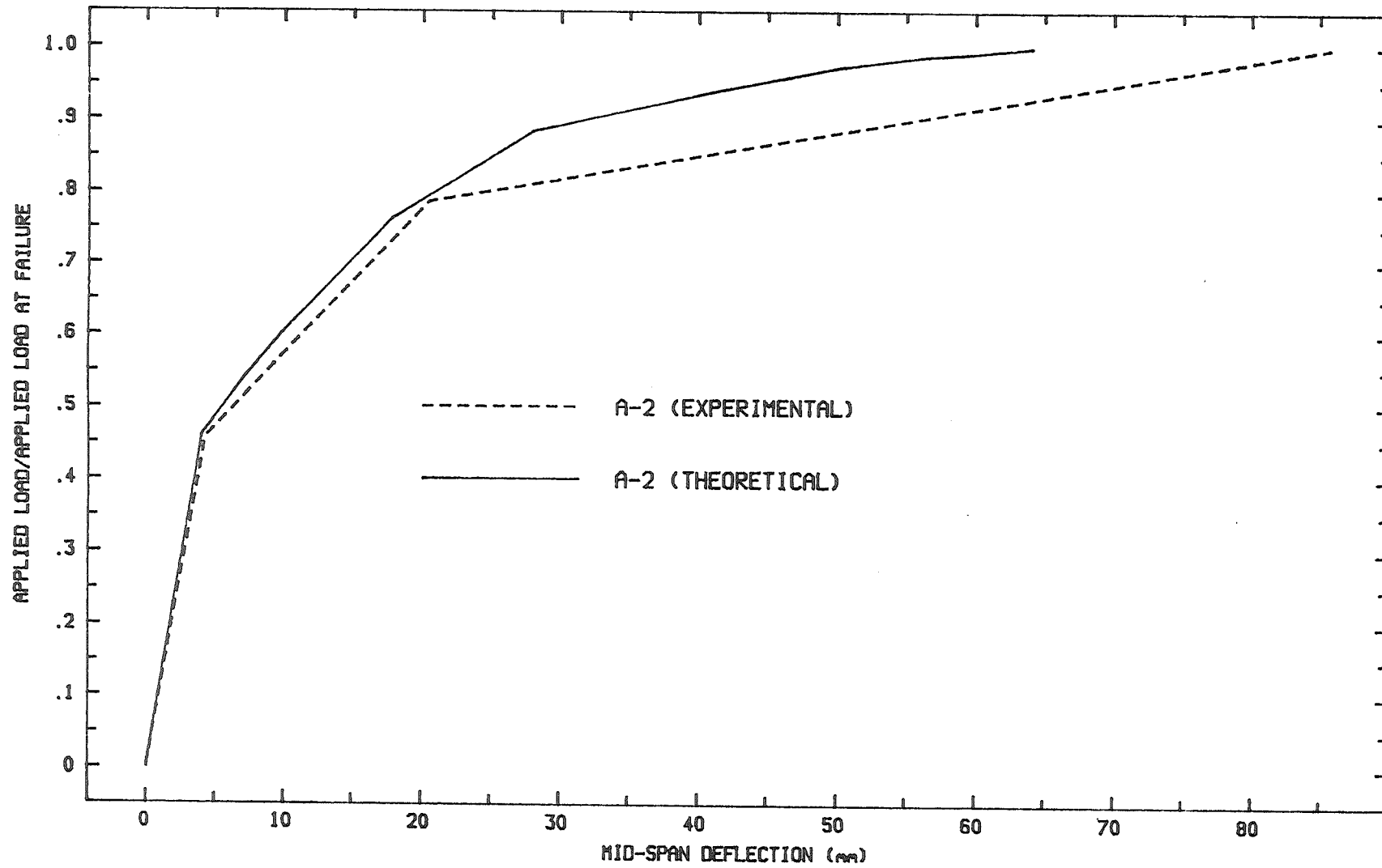


FIGURE 7.5 : LOAD-DEFLECTION CURVE

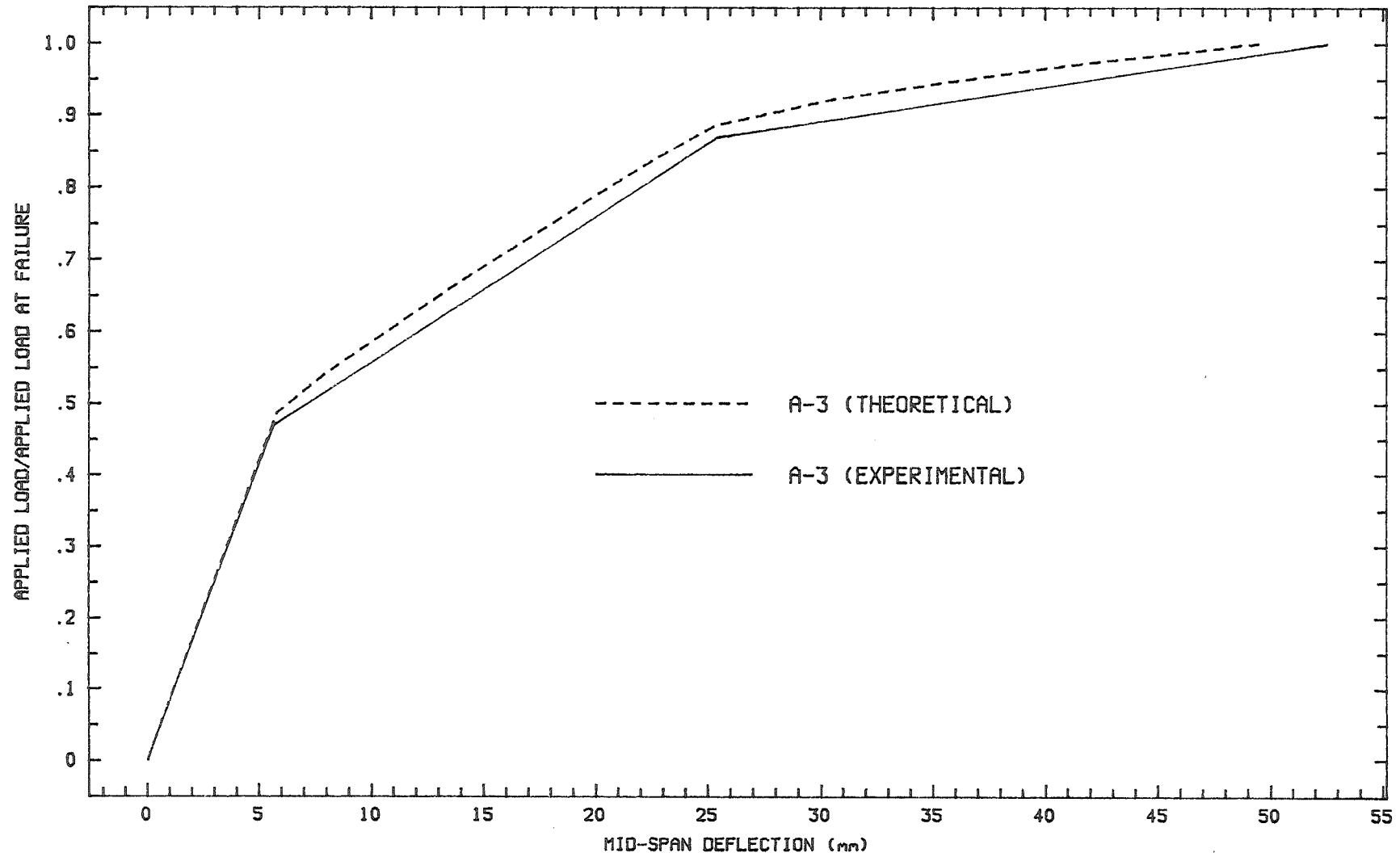


FIGURE 7.6 : LOAD-DEFLECTION CURVE

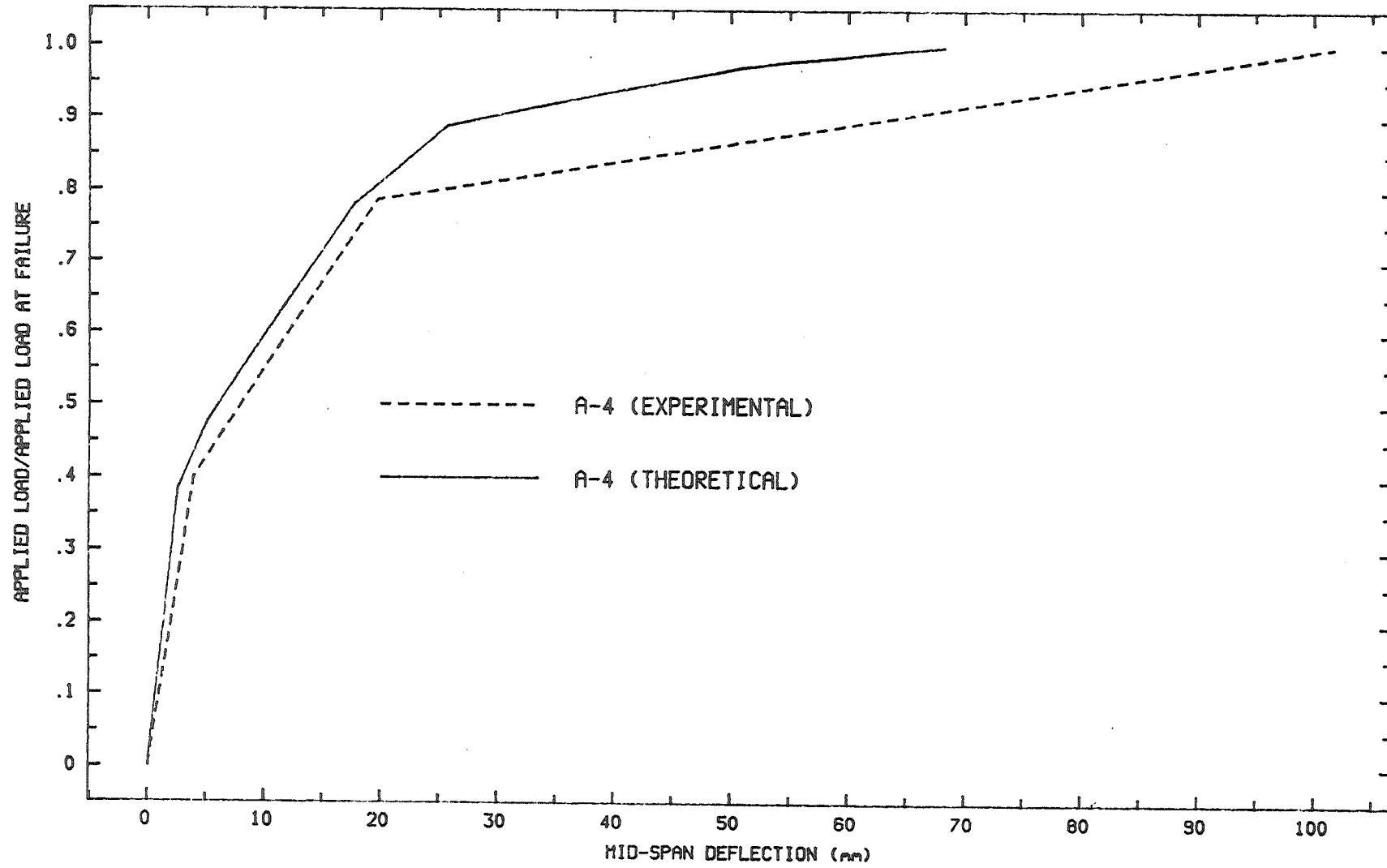


FIGURE 7.7 : LOAD-DEFLECTION CURVE

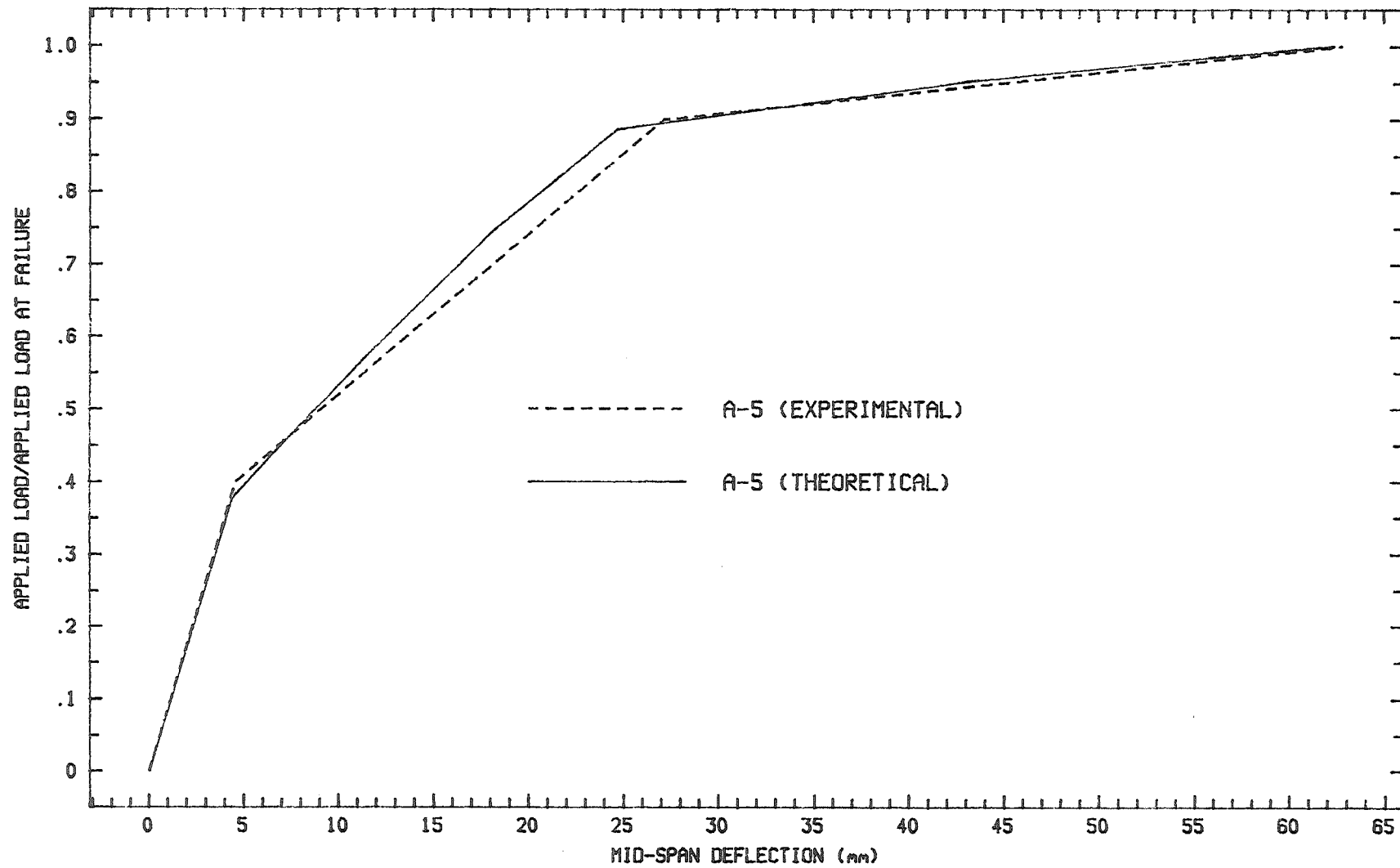


FIGURE 7.8 : LOAD-DEFLECTION CURVE

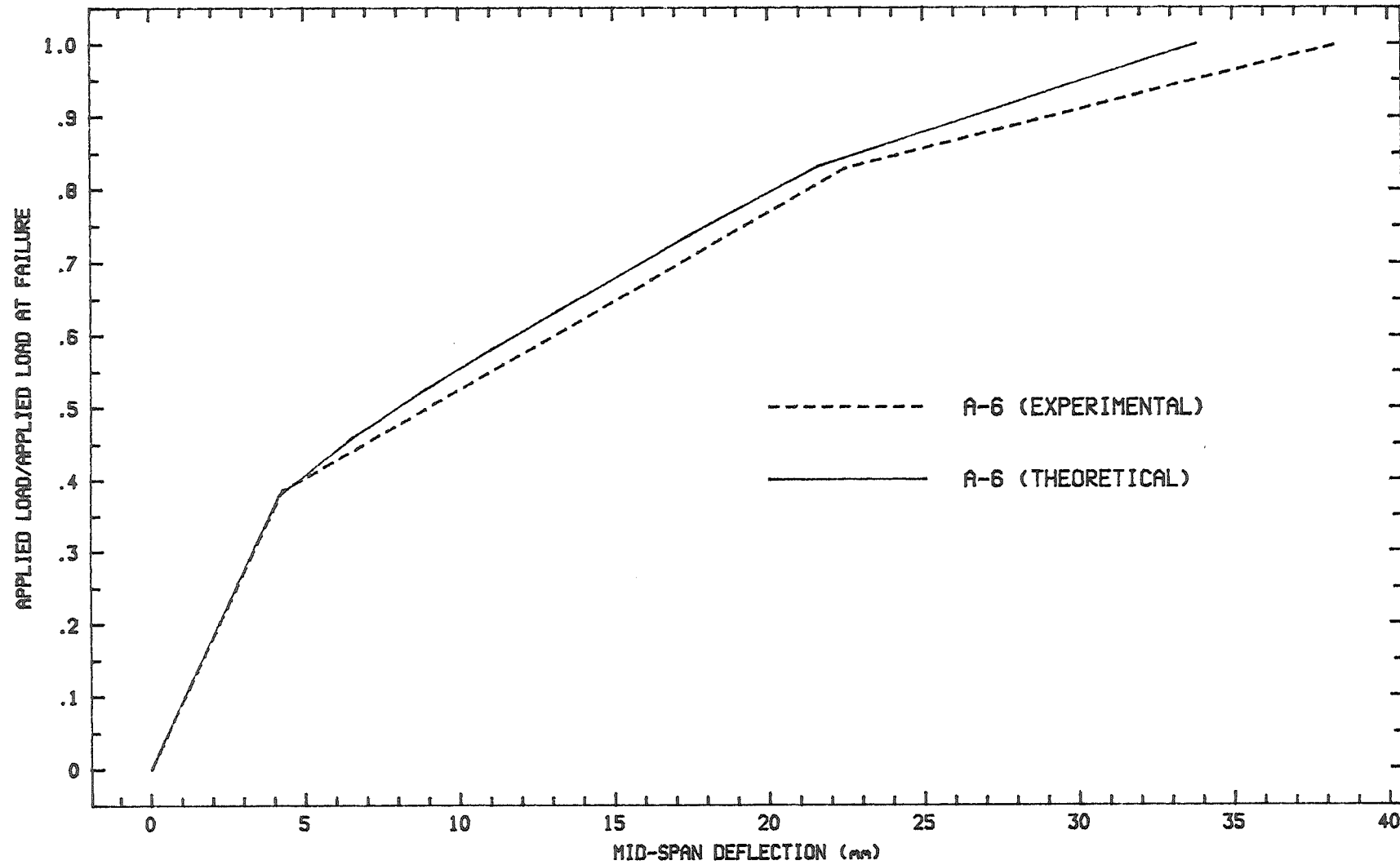


FIGURE 7.9 : LOAD-DEFLECTION CURVE

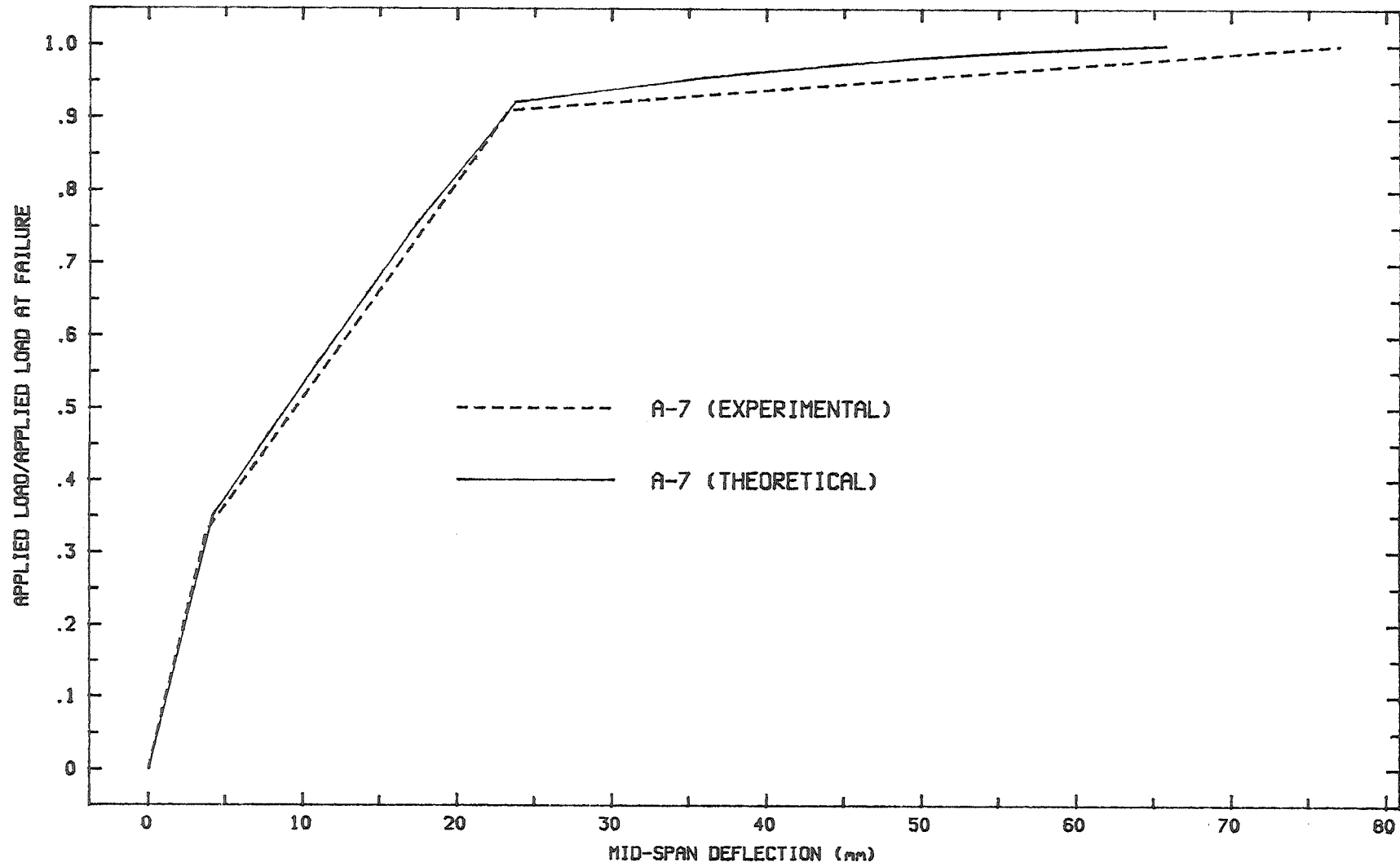


FIGURE 7.10 : LOAD-DEFLECTION CURVE

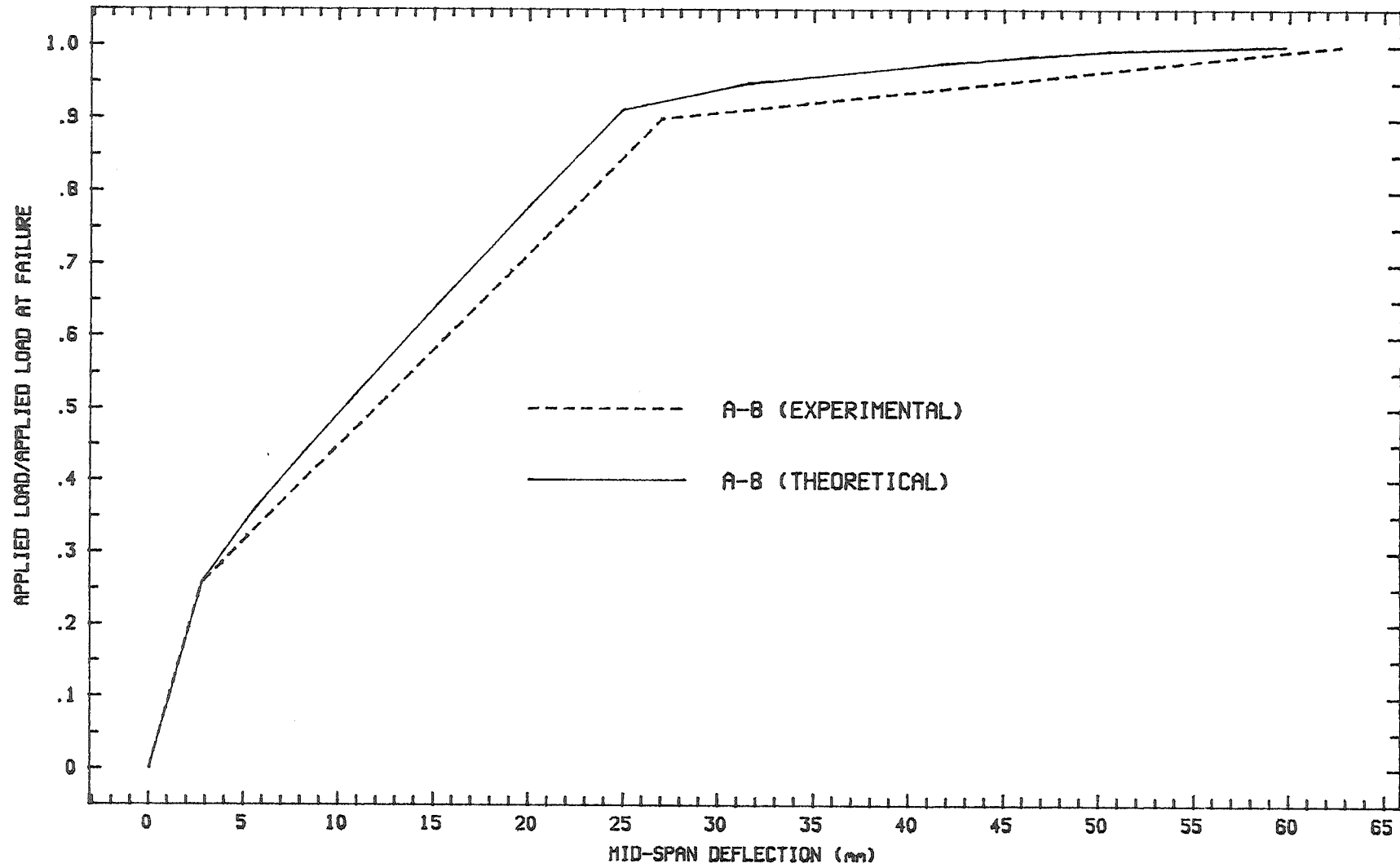


FIGURE 7.11 : LOAD-DEFLECTION CURVE

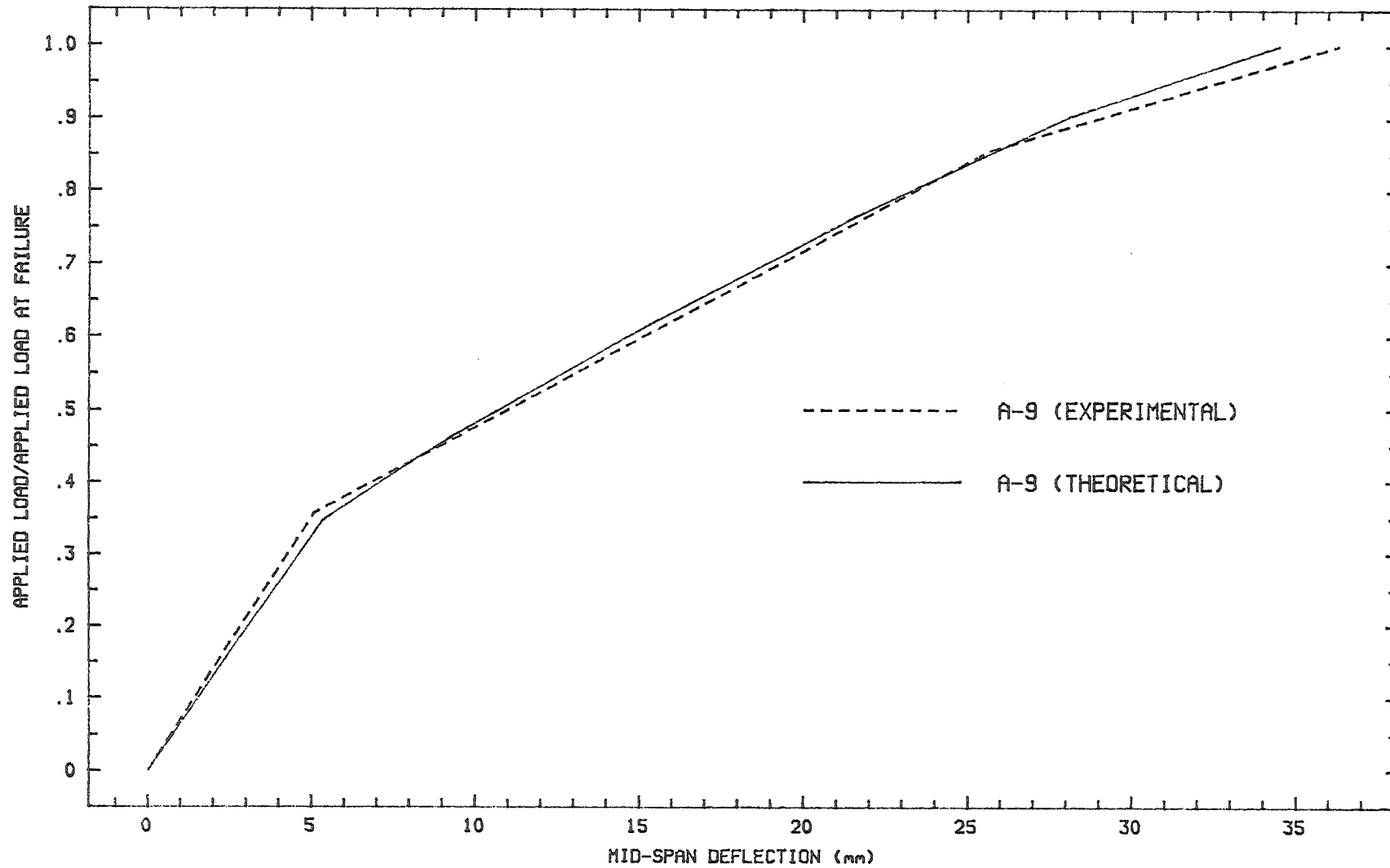


FIGURE 7.12: LOAD-DEFLECTION CURVE AT MID-SPAN

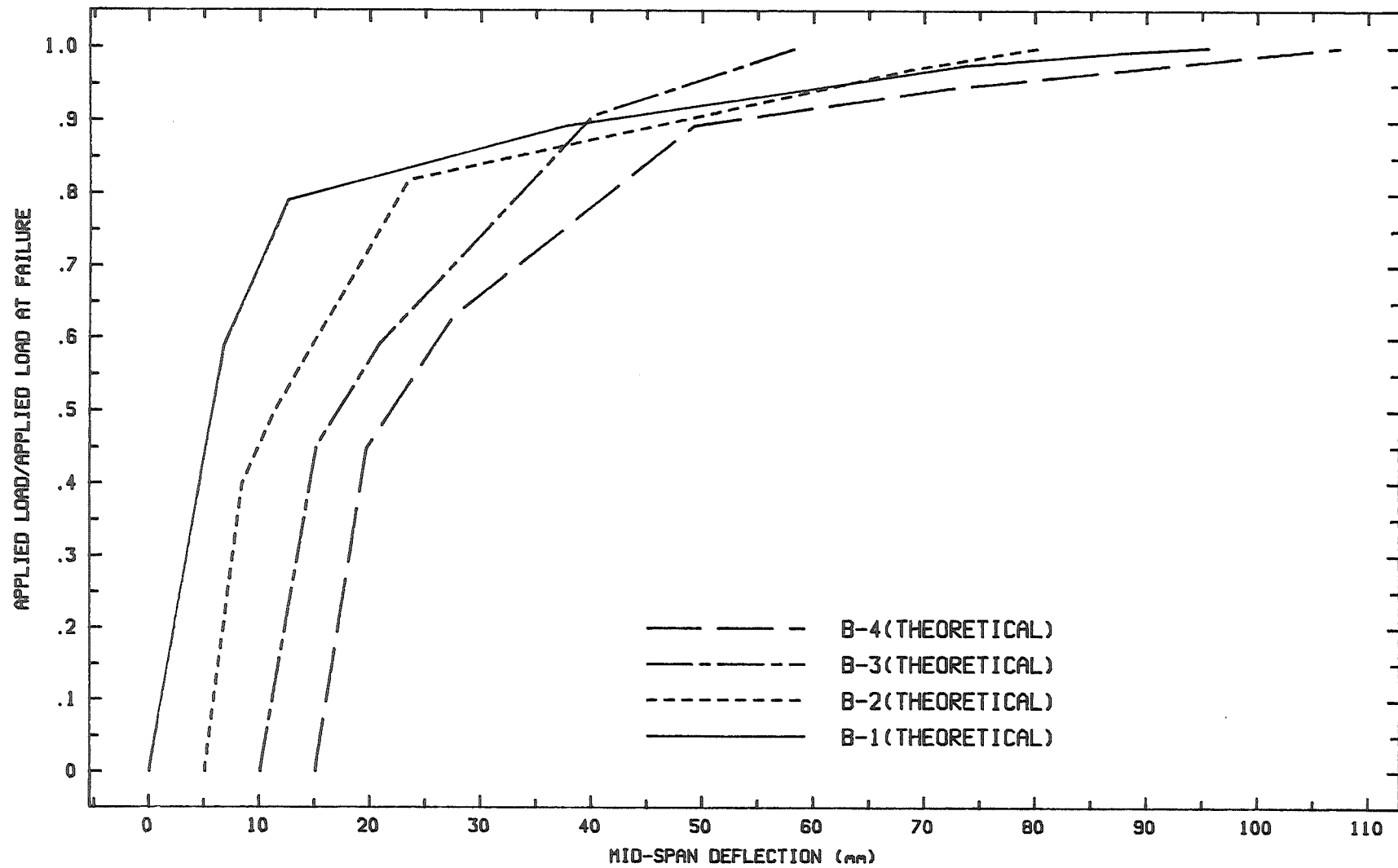


FIGURE 7.13: LOAD-DEFLECTION CURVE AT MID-SPAN

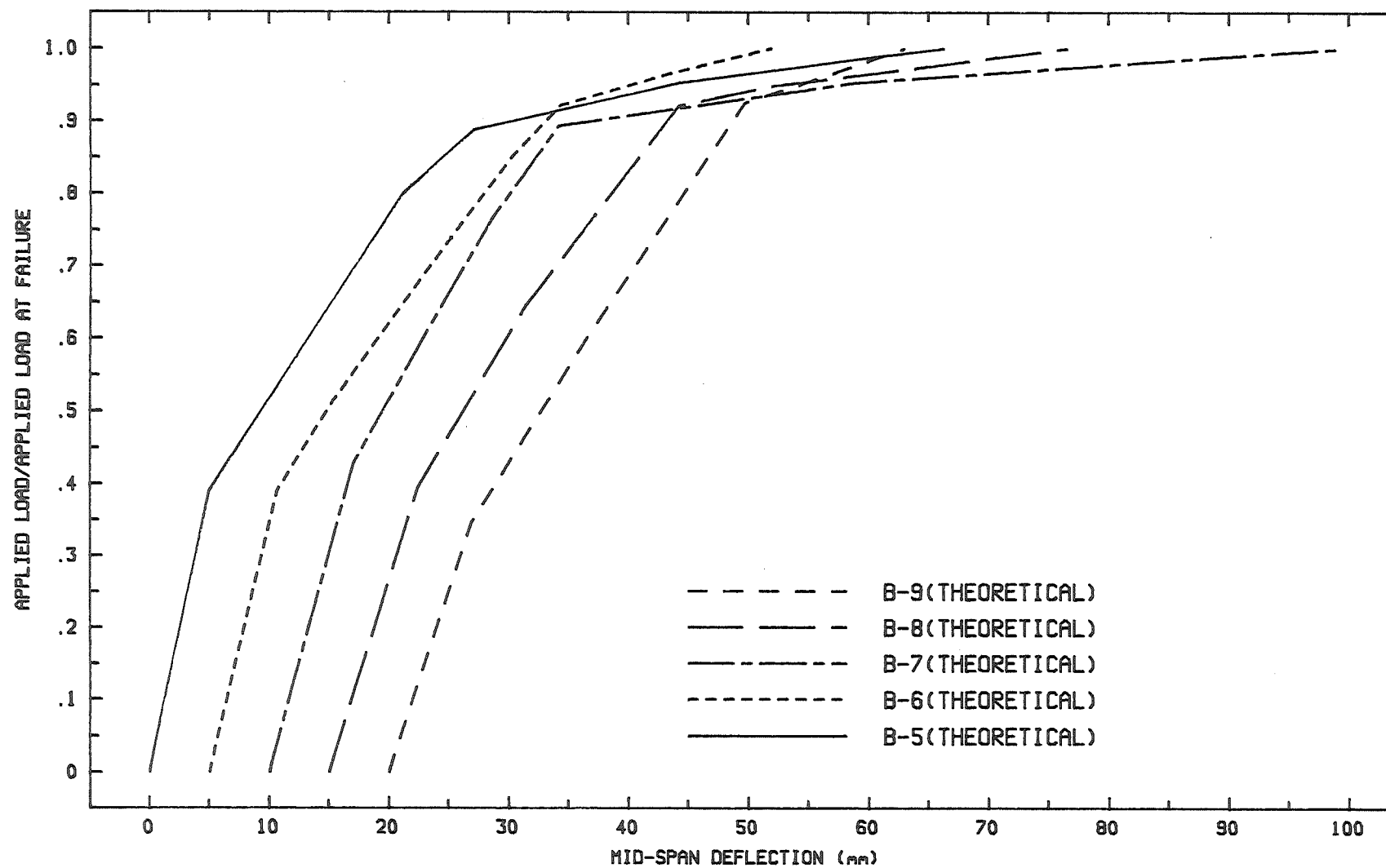


FIGURE 7.14 : LOAD-DEFLECTION CURVE AT MID-SPAN

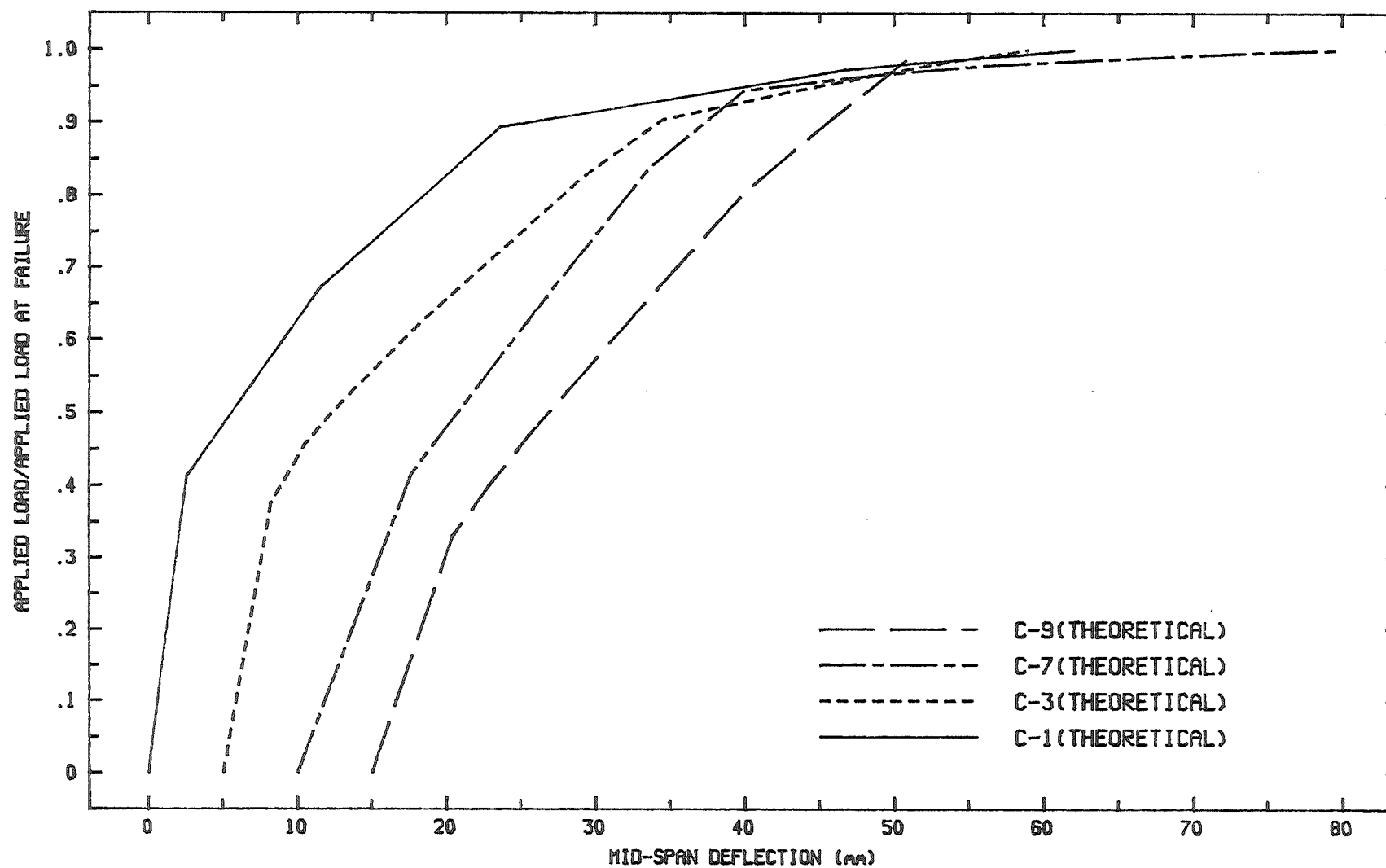


FIGURE 7.15: APPLIED LOAD/FAILURE LOAD VS STRESS INCREASE IN PRESTRESSING STEEL

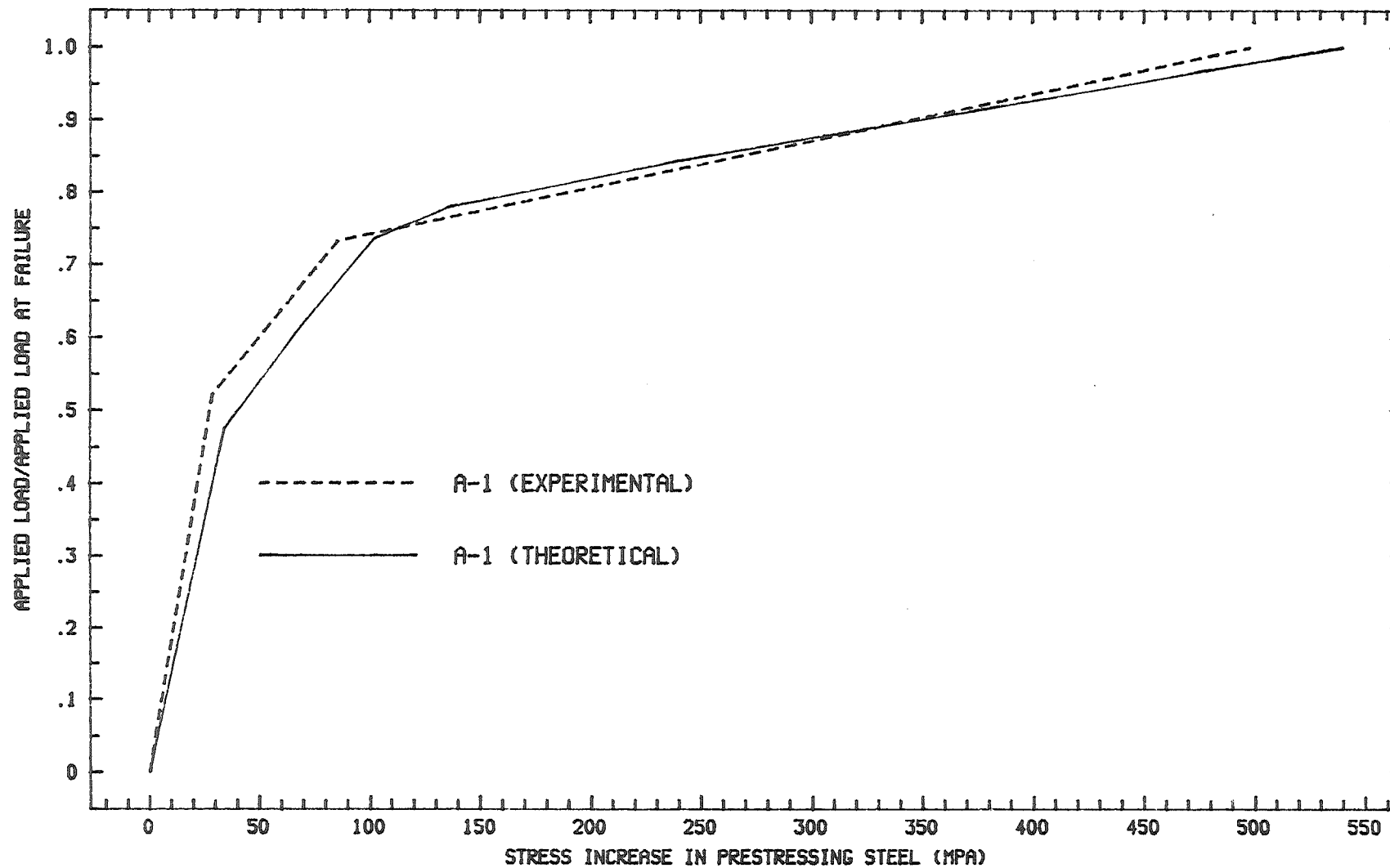


FIGURE 7.16 : APPLIED LOAD/FAILURE LOAD VS STRESS INCREASE IN PRESTRESSING STEEL

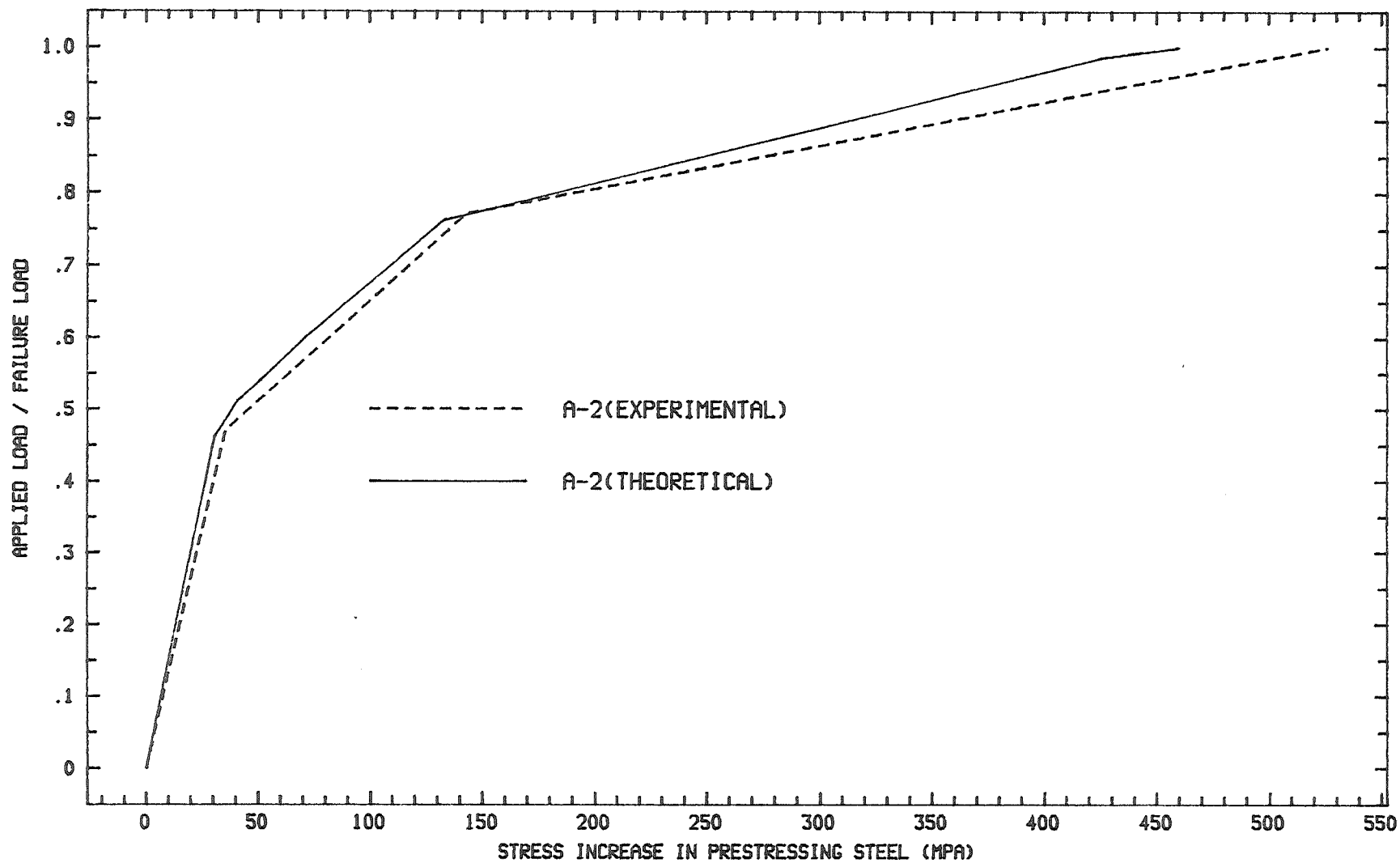


FIGURE 7.17: APPLIED LOAD/FAILURE LOAD VS STRESS INCREASE IN PRESTRESSING STEEL

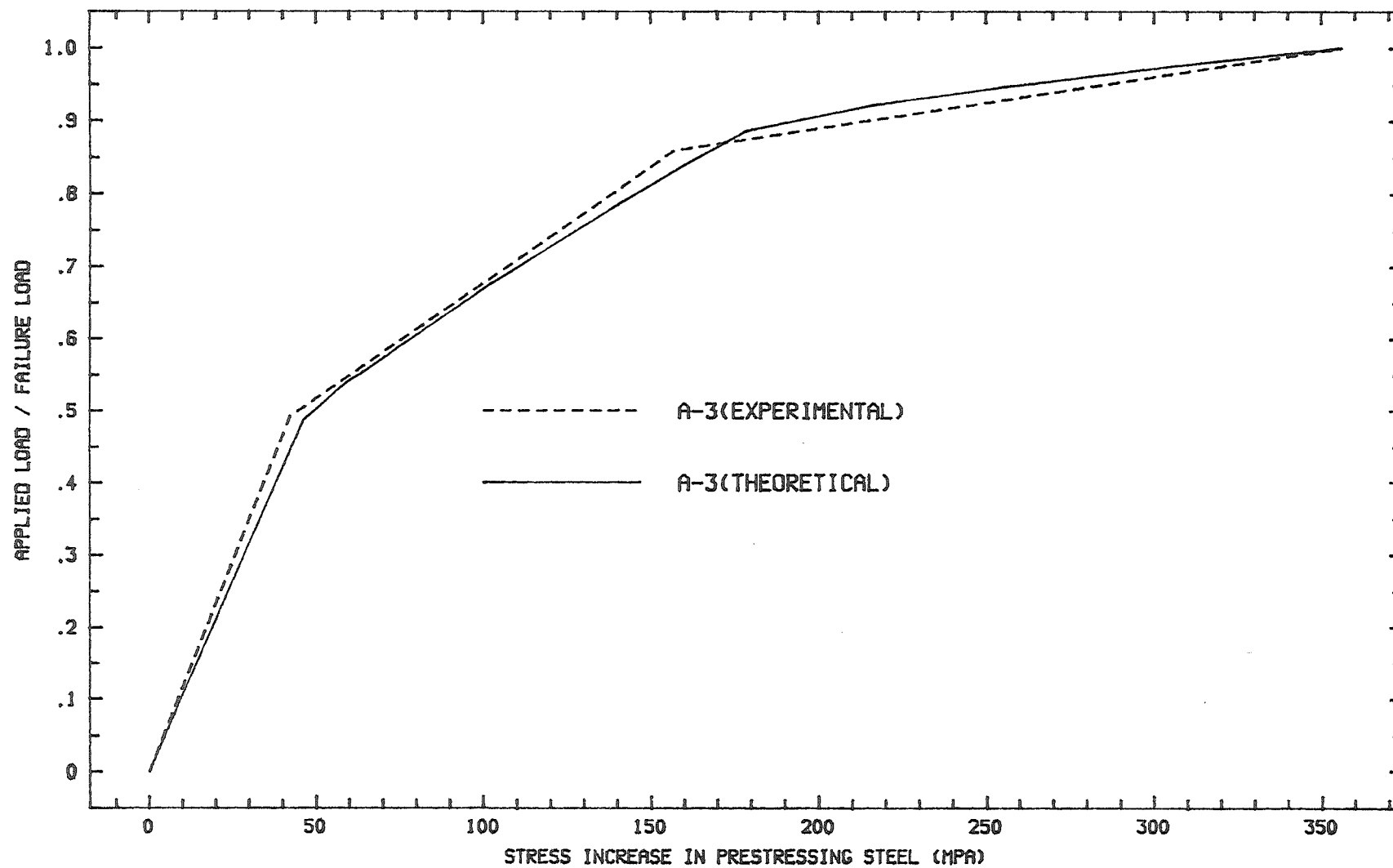


FIGURE 7.18 : APPLIED LOAD/FAILURE LOAD VS STRESS INCREASE IN PRESTRESSING STEEL

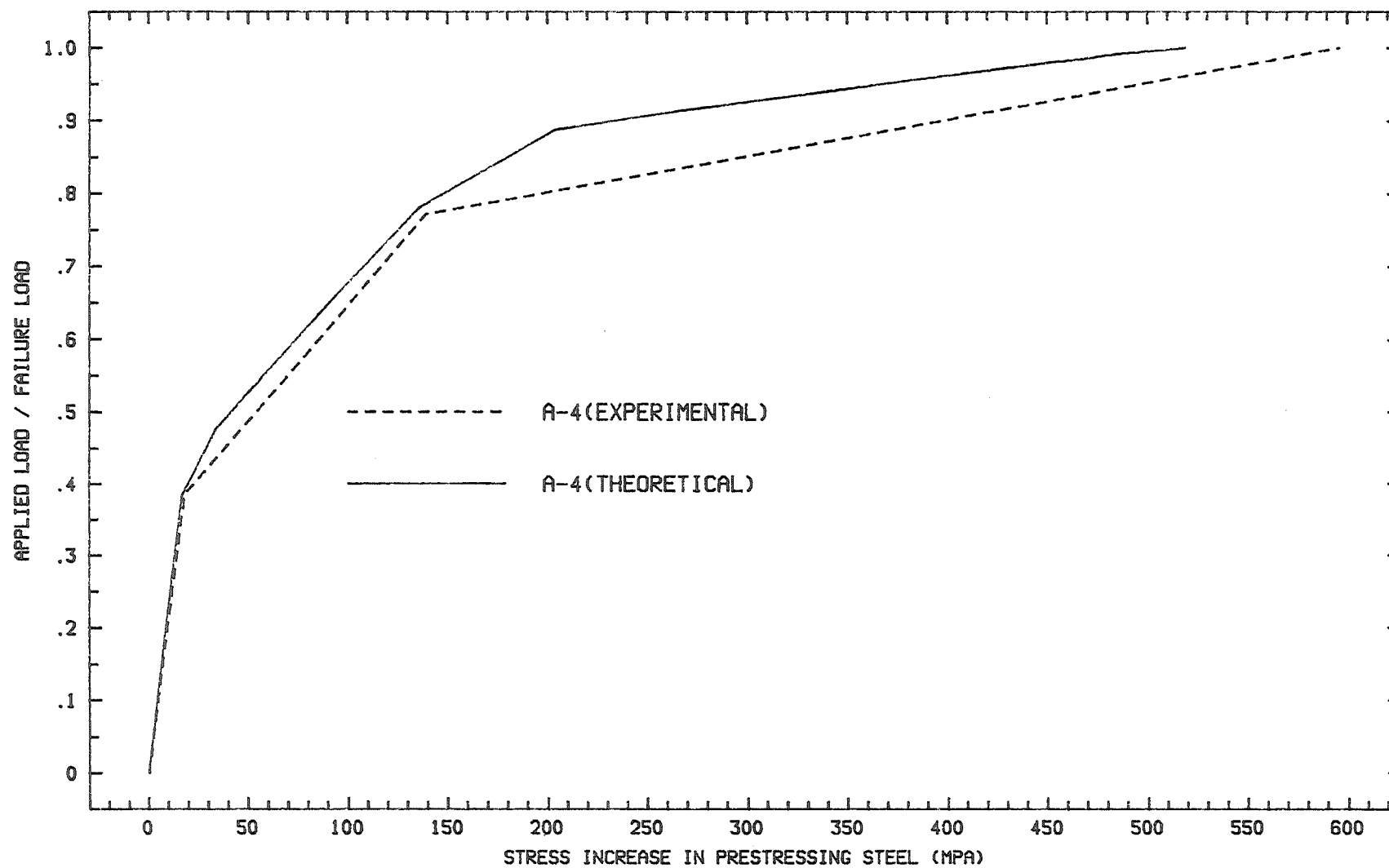


FIGURE 7.19 : APPLIED LOAD/FAILURE LOAD VS STRESS INCREASE IN PRESTRESSING STEEL

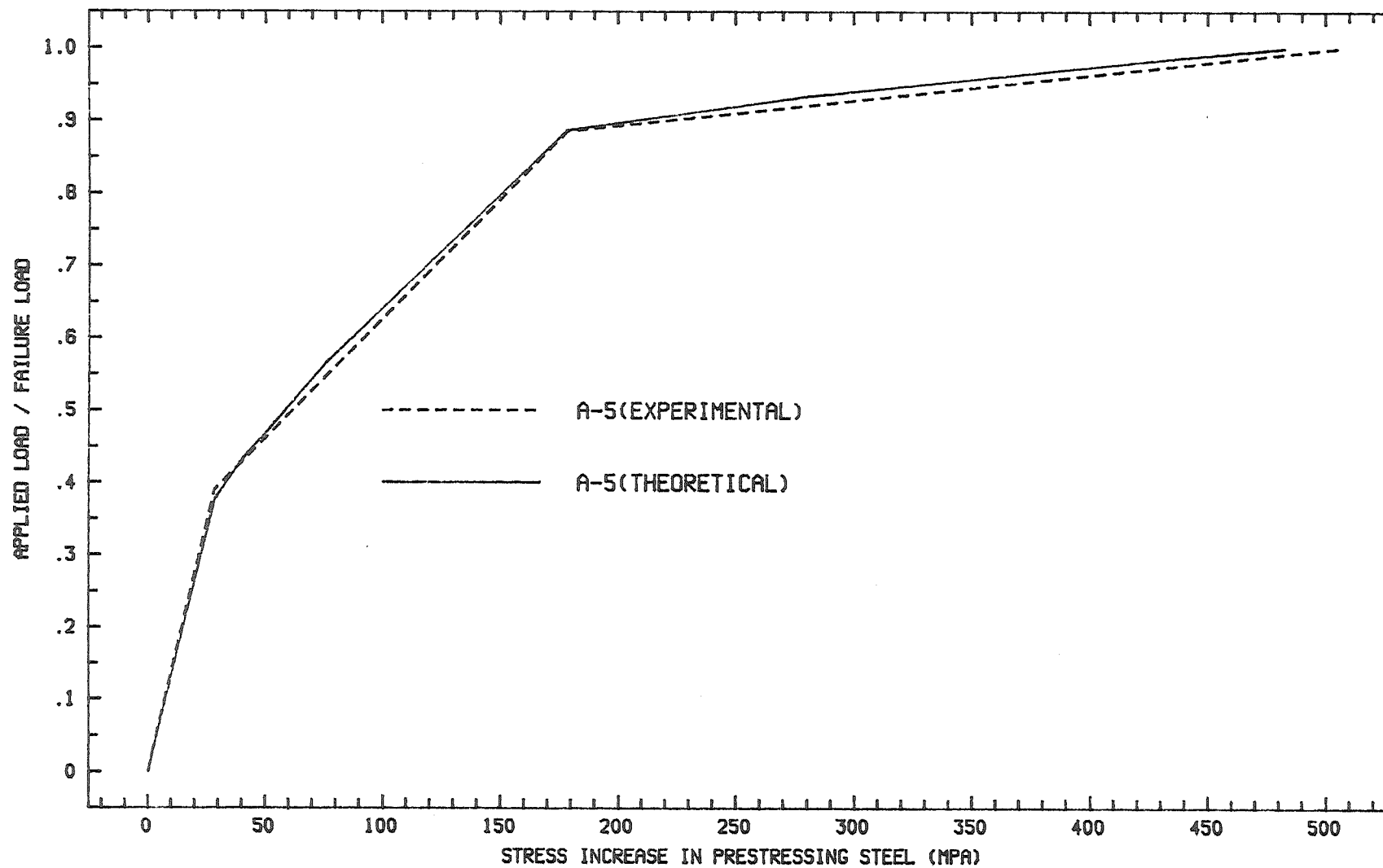


FIGURE 7.20 : APPLIED LOAD/FAILURE LOAD VS STRESS INCREASE IN PRESTRESSING STEEL

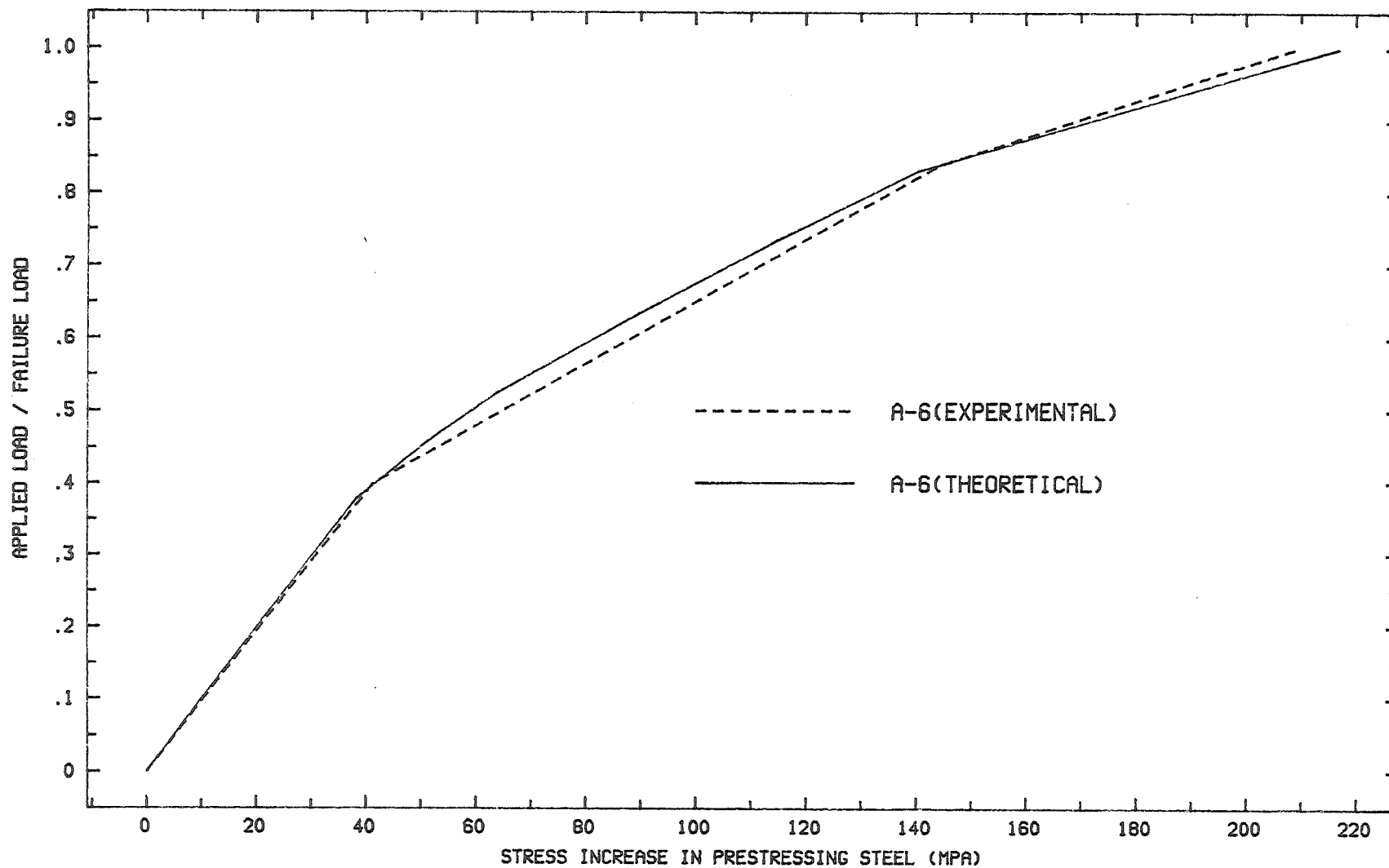


FIGURE 7.21: APPLIED LOAD/FAILURE LOAD VS STRESS INCREASE IN PRESTRESSING STEEL

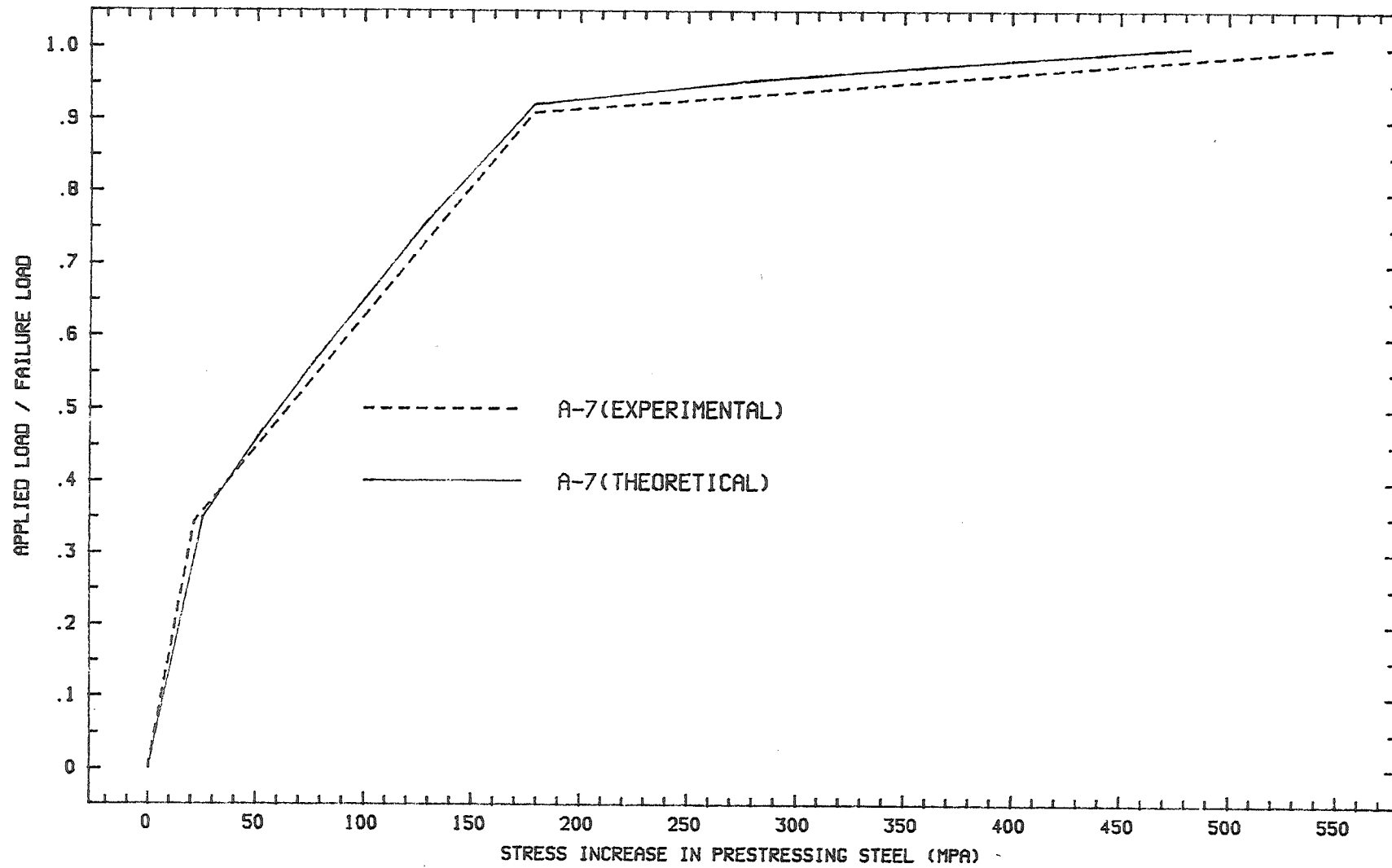


FIGURE 7.22: APPLIED LOAD/FAILURE LOAD VS STRESS INCREASE IN PRESTRESSING STEEL

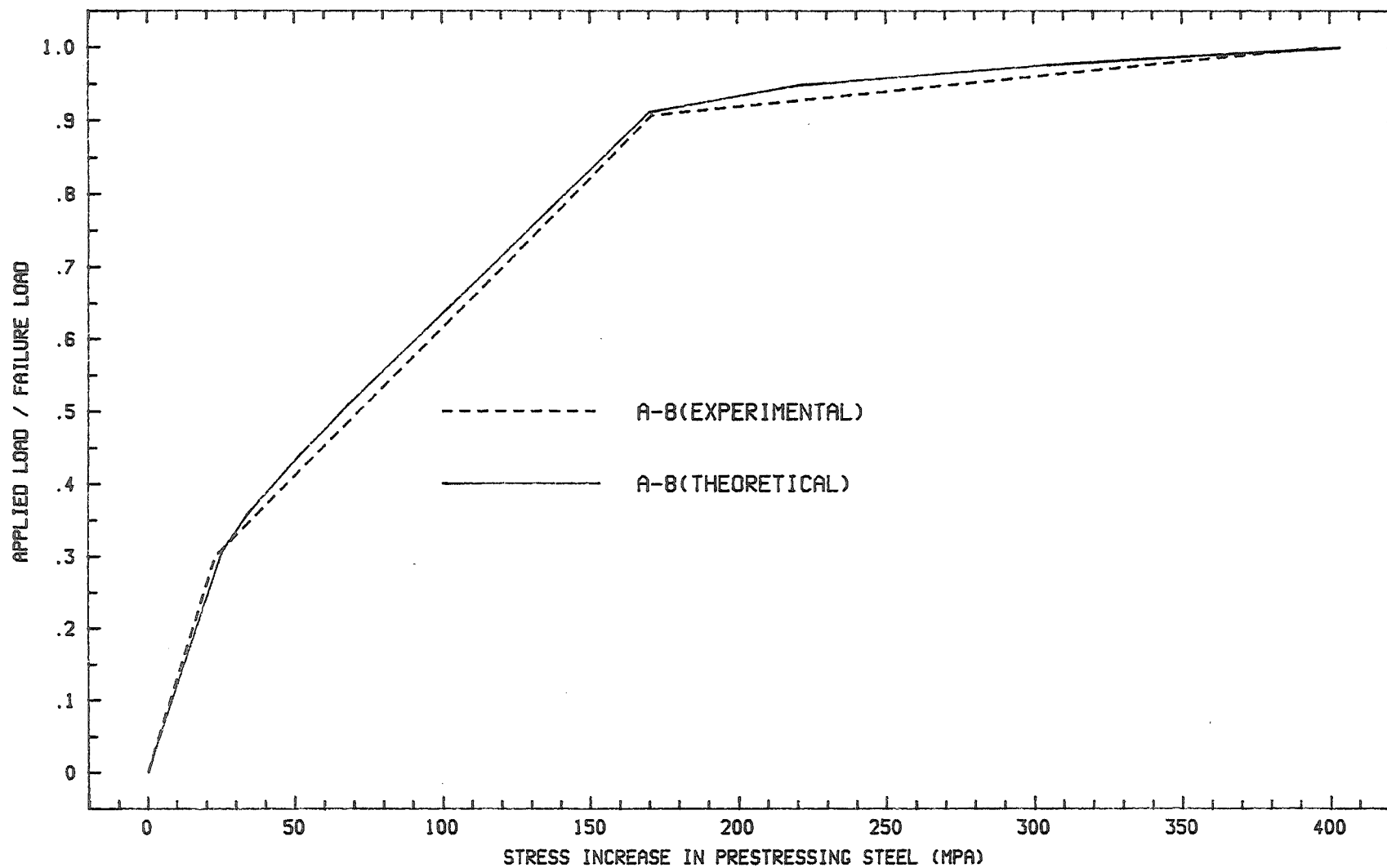


FIGURE 7.23 : APPLIED LOAD/FAILURE LOAD VS STRESS INCREASE IN PRESTRESSING STEEL

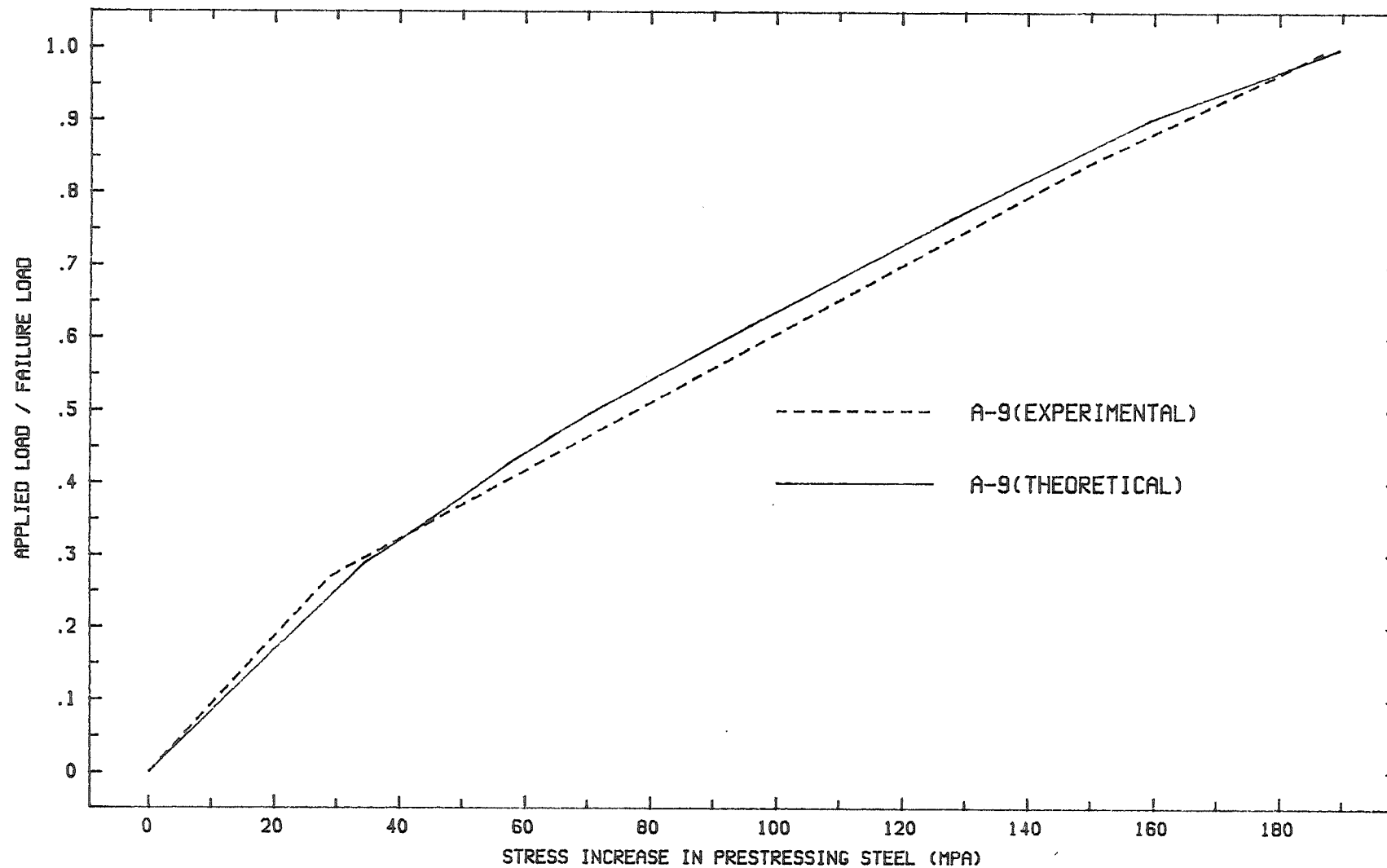


FIGURE 7.24: APPLIED LOAD/FAILURE LOAD VS TENDON STRESS INCREASE

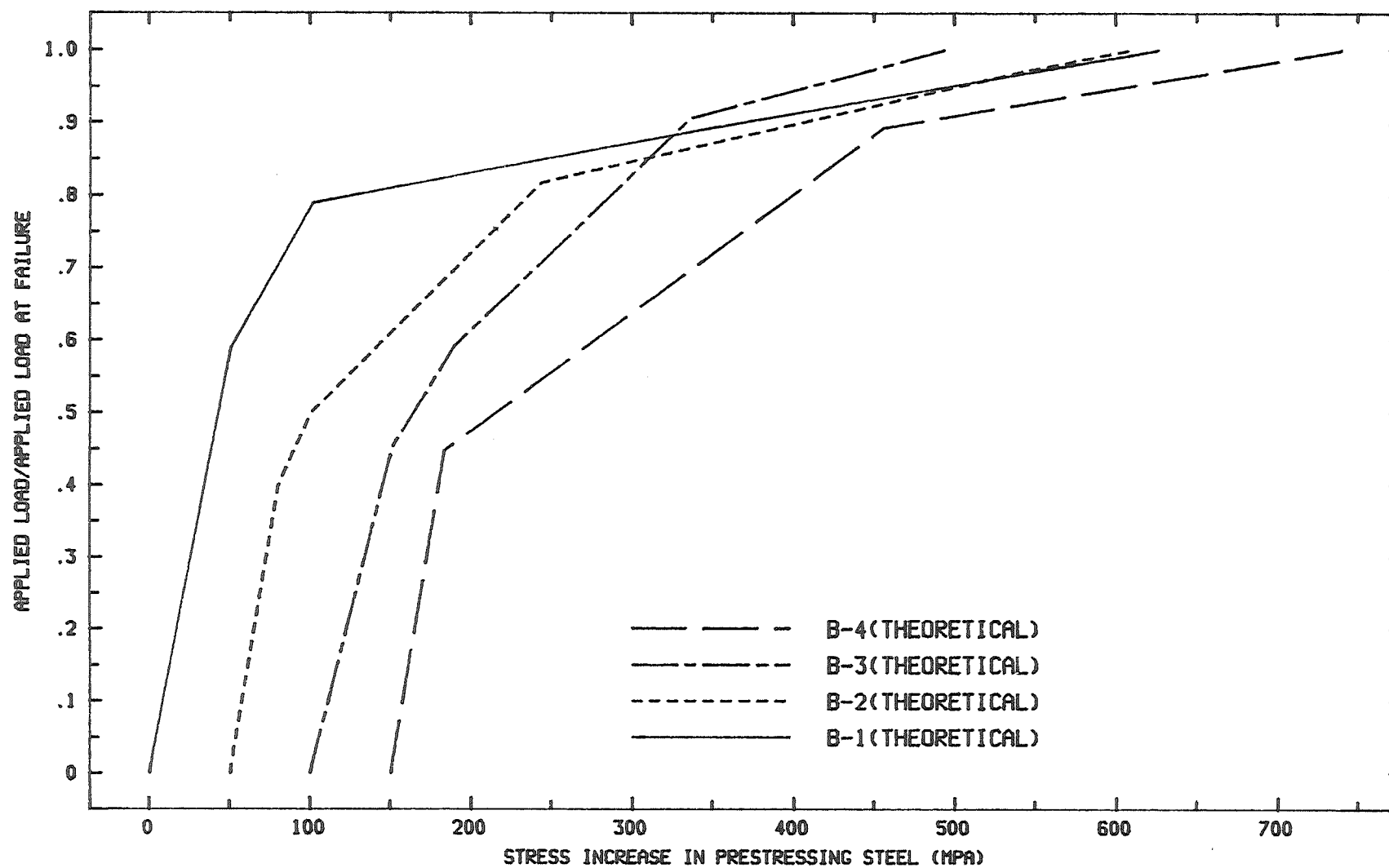


FIGURE 7.25 : APPLIED LOAD/FAILURE LOAD VS TENDON STRESS INCREASE

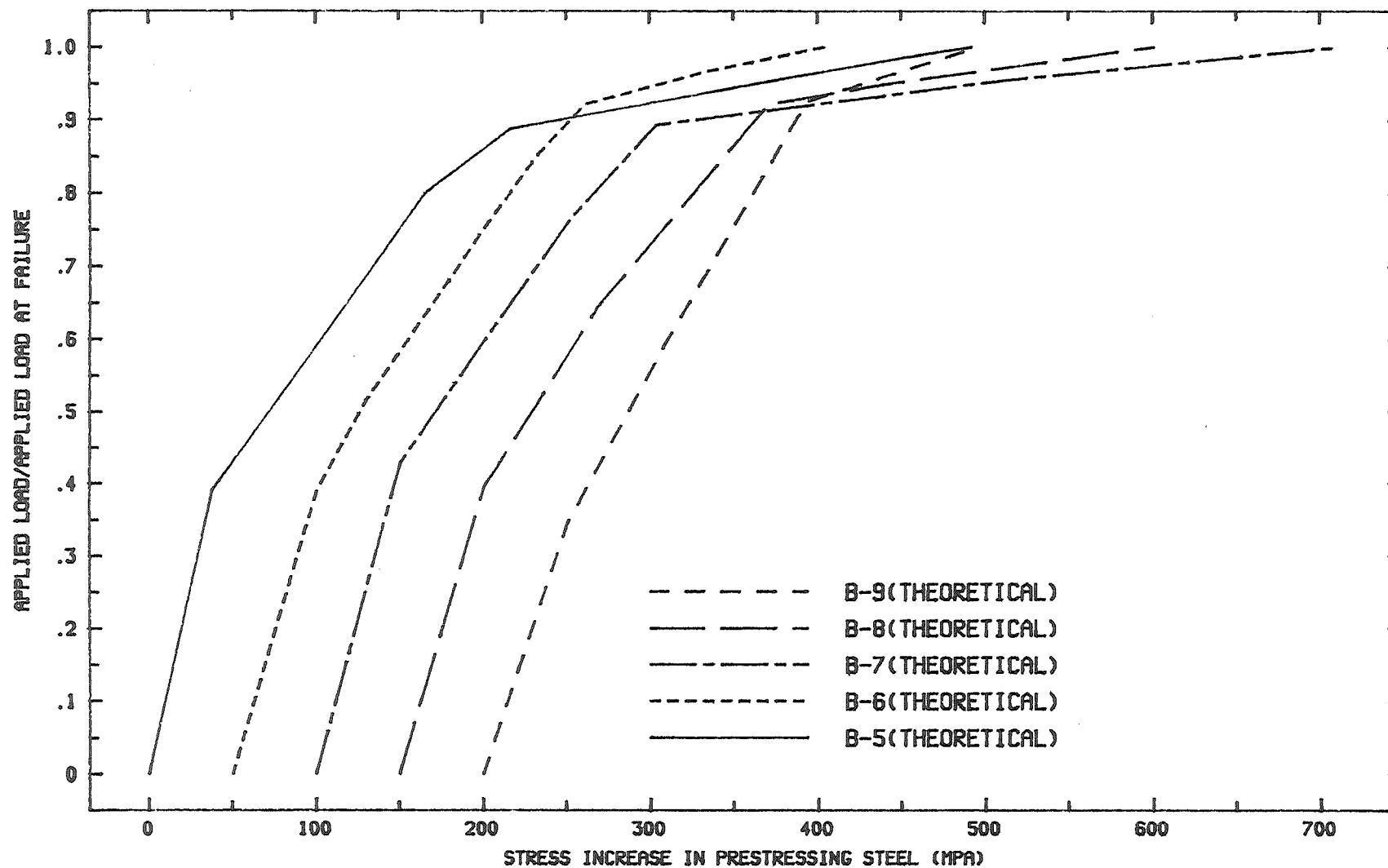


FIGURE 7.26 : APPLIED LOAD/FAILURE LOAD VS TENDON STRESS INCREASE

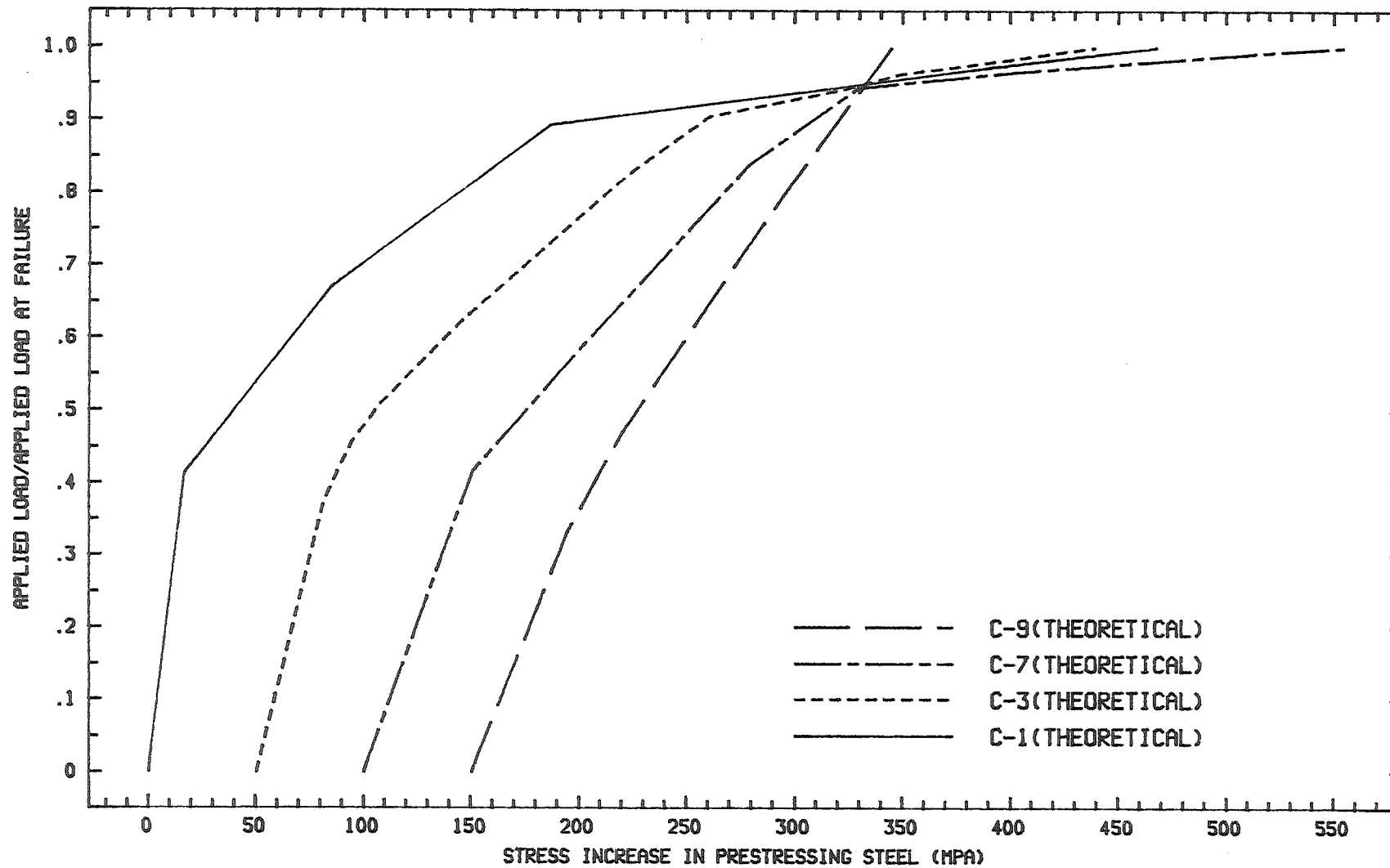


TABLE 7.2

**COMPARISON BETWEEN PREDICTED AND EXPERIMENTAL
TENDON STRESS INCREASE AND MOMENT AT ULTIMATE.**

beam	fsu ACI318-83 (Mpa)	fsu NZS3101 (Mpa)	fsu expt (Mpa)	fsu analytical (Mpa)	Mu expt (KNm)	Mu analytical (KNm)
A1	1212	1060	1458	1500	31.1	28.5
A2	1083	1004	1430	1363.5	46.8	44.07
A3	958	920	1176	1175.14	63.6	59.15
A4	1121	969	1465	1417	38.3	34.49
A5	1016	910	1315	1272.25	51.2	49.81
A6	992	954	1063	1070.84	72.4	70.85
A7	1230	985	1436	1367.05	41.5	41.37
A8	1181	994	1290	1283.79	59.4	58.28
A9	1065	1020	1108	1109.51	102.5	94.61
B1	1351.2	1108	1645	1634.13	30.3	30.24
B2	1220.6	1087	1564	1538.6	50.4	48.05
B3	1127.4	1063	1361	1366.66	61.0	60.3
B4	1363.4	1140	1645	1636.2	38.4	37.55
B5	1248.5	1089	1520	1478.7	53.4	52.99
B6	1179.8	1102	1402	1355.58	75.8	75.7
B7	1272.3	1102	1603	1588.73	42.5	42.39
B8	1331.64	1102	1490	1452.68	63.1	60.35
B9	1294.4	1150	1346	1345.92	89.7	89.51
C1	1176.9	1005	1465	1463.1	33.6	33.22
C3	969.8	925	1231	1056	67.3	62.6
C7	1322.1	1055	1411	1409.08	44.6	43.52
C9	1047.8	1003	1109	1098.51	101.0	99.56

where : expt = experimental

FIGURE 7.27: TENDON STRESS INCREASE AT FAILURE VS COMBINED REINFORCEMENT INDEX

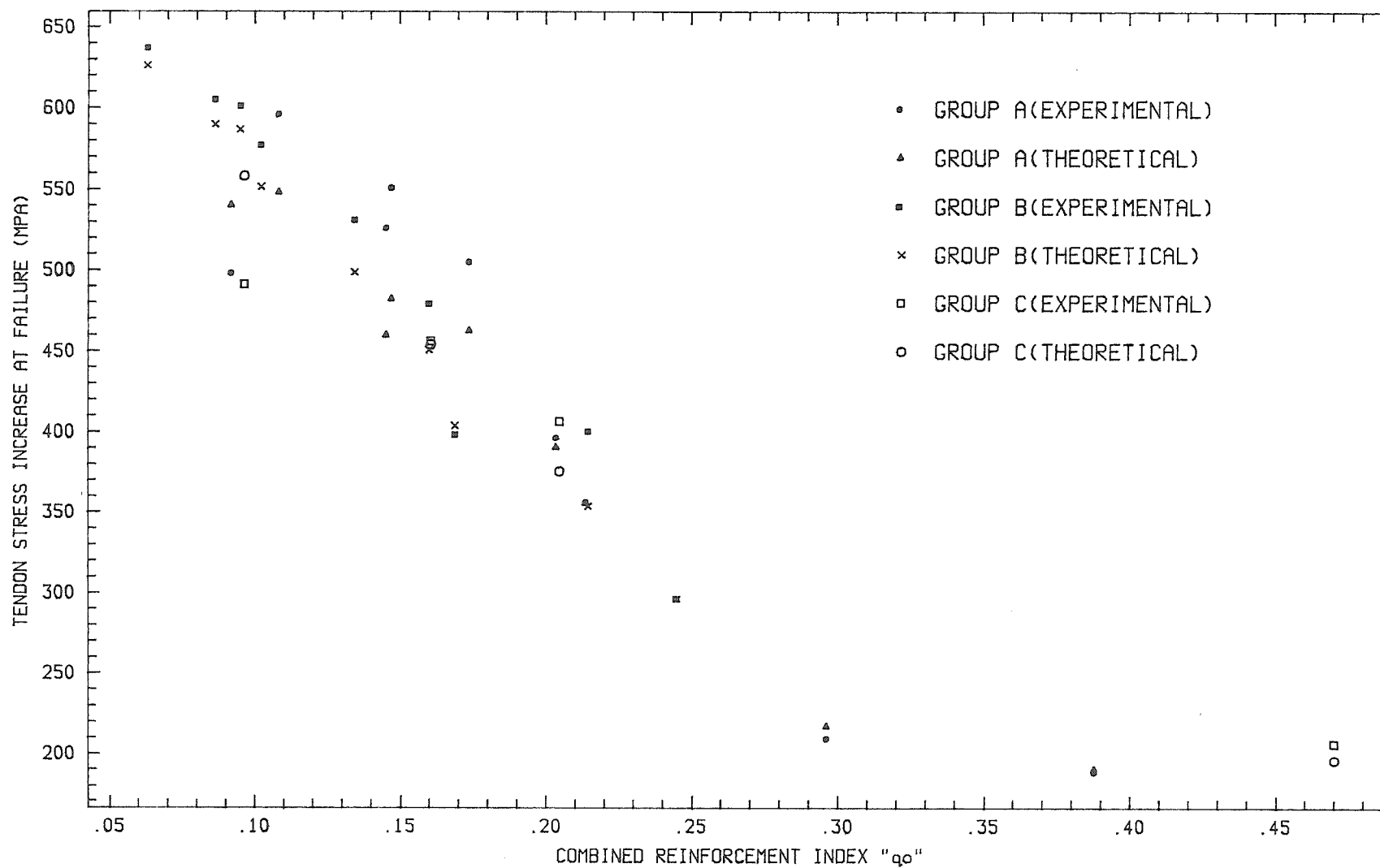
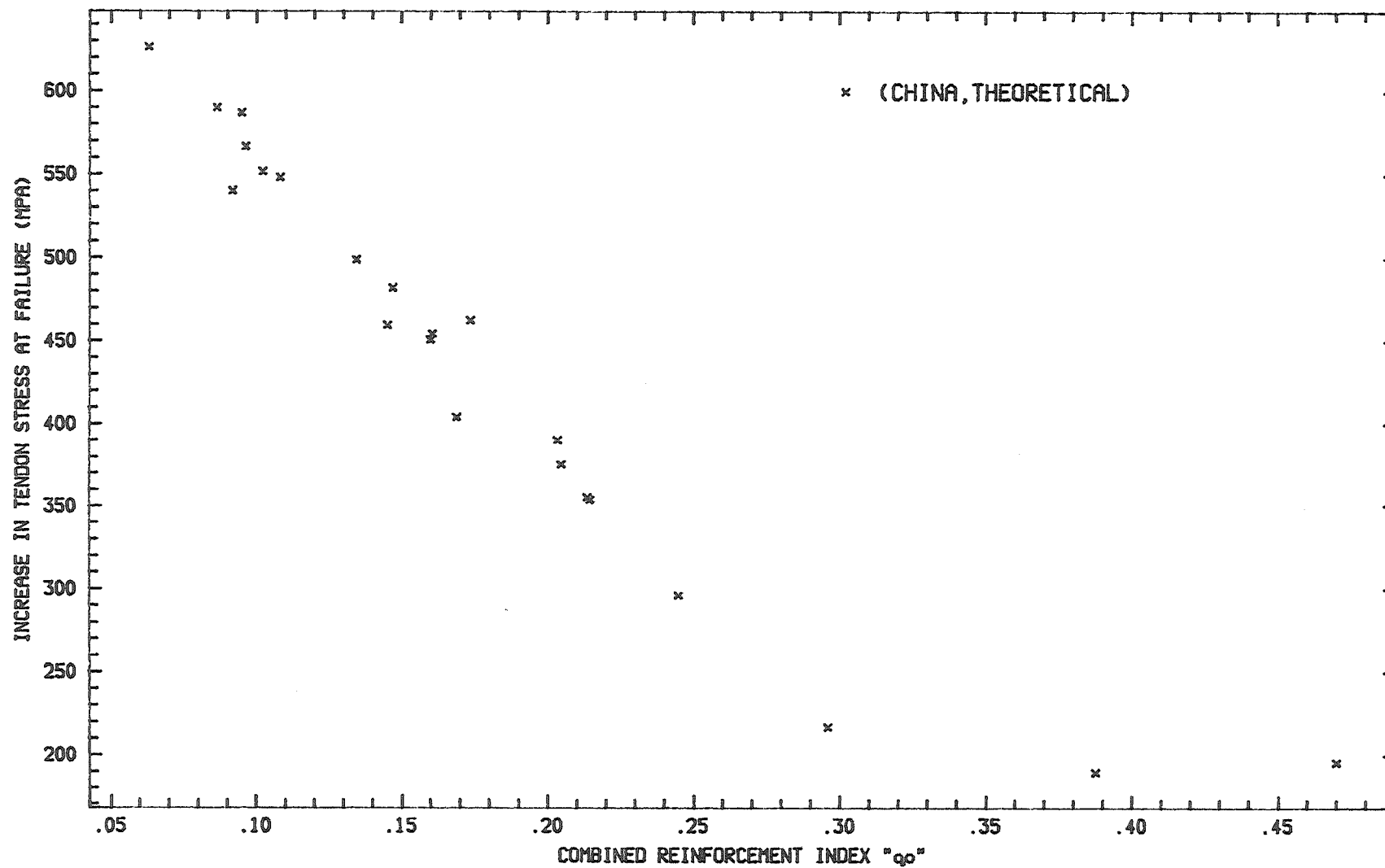
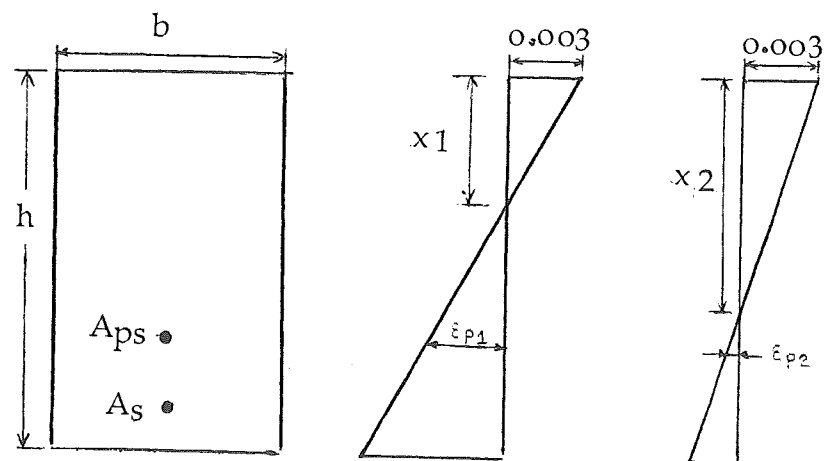


FIGURE 7.28 : INCREASE IN TENDON STRESS AT FAILURE VS COMBINED REINFORCEMENT INDEX



q_0 value will have a lower strain value at the level of prestressing steel at failure where the top strain reaches 0.003. Hence the increase in strain, (and also stress) at the level of prestressing steel will be less for member with higher q_0 value. The increase in strain will be insignificant for a beam having very depth neutral axis where the beams fail by crushing of the concrete in compression . Experimental results show that the increase in strain value at the level of prestressing steel starts to become insignificant at q_0 equal to 0.2959.



(a) section

(b) strain diagram for
beam with low q_0

(c) strain diagram for
beam with high q_0

Figure 7.29 : Strain diagrams of unbonded beams with different q_0 values.

CHAPTER 8

DISCUSSION AND COMPARISON BETWEEN ANALYTICAL AND EXPERIMENTAL RESULTS FOR TESTS DONE AT THE UNIVERSITY OF CANTERBURY.

8.1 GENERAL

Twenty-five slabs with unbonded prestressing strands have been tested in the University of Canterbury. Nine slabs without reinforcing bar were tested by Philip Yong (1980). Savariar (1984) tested eight unbonded slabs with mild steel bars of specified yield strength 275 MPa as bonded reinforcement. Perumal (1986) tested eight unbonded slabs exactly the same as those tested by Savariar (1984) except that in this case high yield strength steel bars of specified yield strength equal to 380 Mpa as bonded reinforcement. Computer analyses have been carried out for six slabs tested by Yong (1980) which do not exhibit flexural instability and twelve slabs tested by Savariar (1984) and Perumal (1986) which are all single span slabs. The appropriate experimental prestressing stress-strain curves and assumed E_c values of $4200 \times (f'_c)^{1/2}$ were used in the analysis.

8.2 UNBONDED SLABS TESTED BY YONG (1980) .

Nine unbonded slabs, all without bonded reinforcement were tested by Yong (1980) . The properties of each beam are as shown in table 8.1.

Table 8.1 : Detail of slabs tested by Yong et al.

slab	q_0 (= q_e)	f_{se} (MPa)	A_{ps} (mm ²)	l_e/d	f'_c (MPa)
UB1	0.254	1162.5	278.7	40	30.1
UB2	0.125	1145.3	278.7	40	30.1
UB3	0.033	1196.5	116.3	40	30.1
UB4	0.222	1162.5	278.7	30	34.4
UB5	0.111	1153.9	278.7	30	34.4
UB6	0.029	1219.7	116.3	30	34.4
UB7	0.249	1163.6	278.7	20	30.8
UB8	0.125	1167.9	278.7	20	30.8
UB9	0.032	1204.2	116.3	20	30.8

Slabs UB3, UB6 and UB9 have extremely low combined reinforcement indices and flexural instability was observed for all these three slabs during the test. Flexural instability describes the state when the flexural resistance of the slab in the elastic range after cracking is less than that immediately before cracking. The total applied load will drop immediately after cracking and will not reach the load level again. Immediately after cracking the deflection will still gradually increase while the applied load drops. Later when the total load starts to increase again the increase in mid-span deflection is very great with only small increase in applied load until failure occurs. Flexural instability is caused by the propagation of a crack from bottom to the top of concrete section as long as the maximum tensile stress at the tip of the crack is greater than the modulus of rupture.

In the computer analysis only slabs which don't show flexural instability were analysed because slabs with too low a value of q_0 will not be recommended in the practical design. Flexural instability is disastrous and should be prevented and not controlled.

The comparison between experimental and analytical results are as shown in Figures 8.1 to 8.6. Figures 8.1 to 8.3 show the comparison between load-deflection curves. All analytical curves follow quite closely to the

FIGURE 8.1: LOAD DEFLECTION CURVE AT MID-SPAN

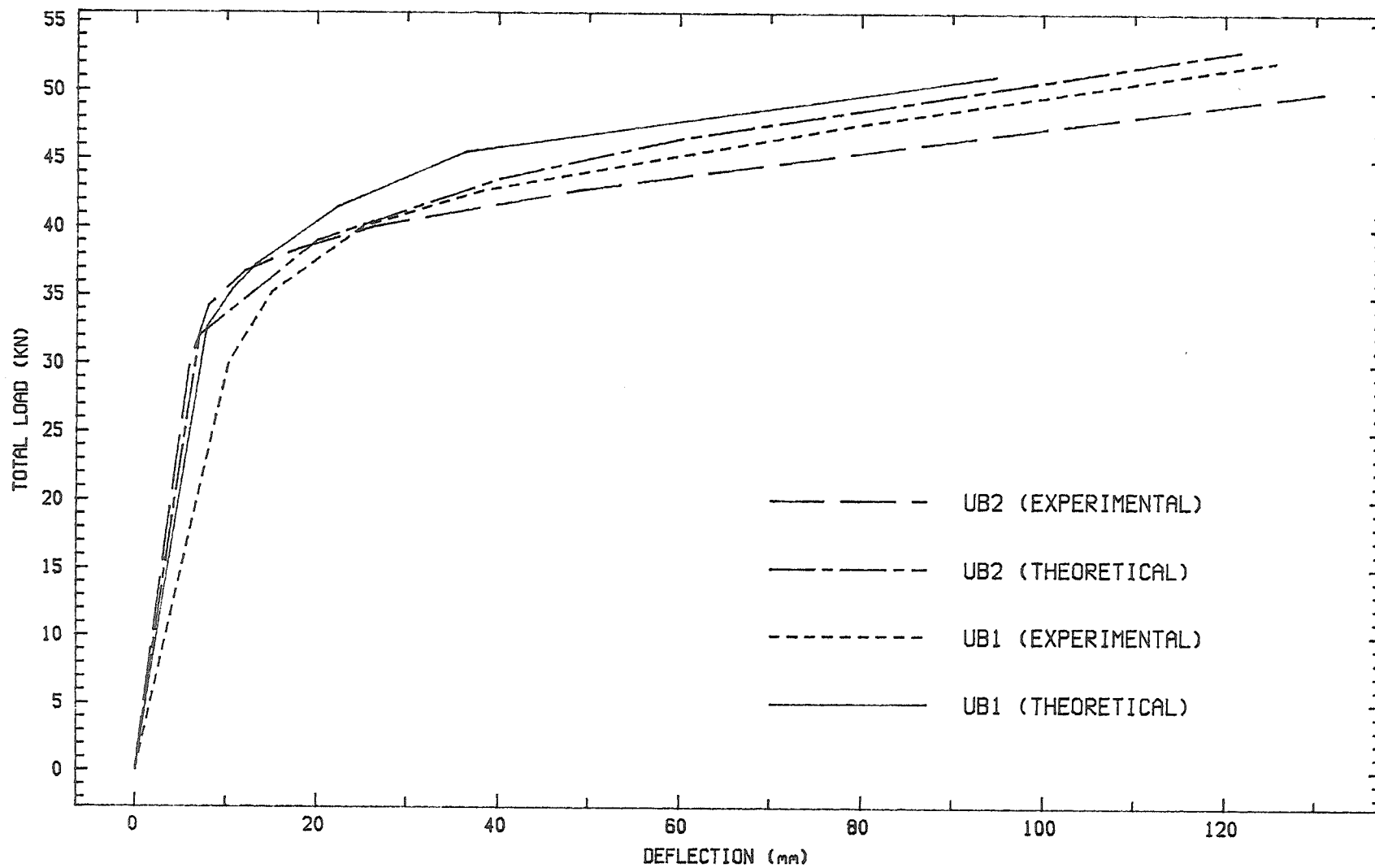


FIGURE 8.2 : LOAD-DEFLECTION CURVE AT MID-SPAN

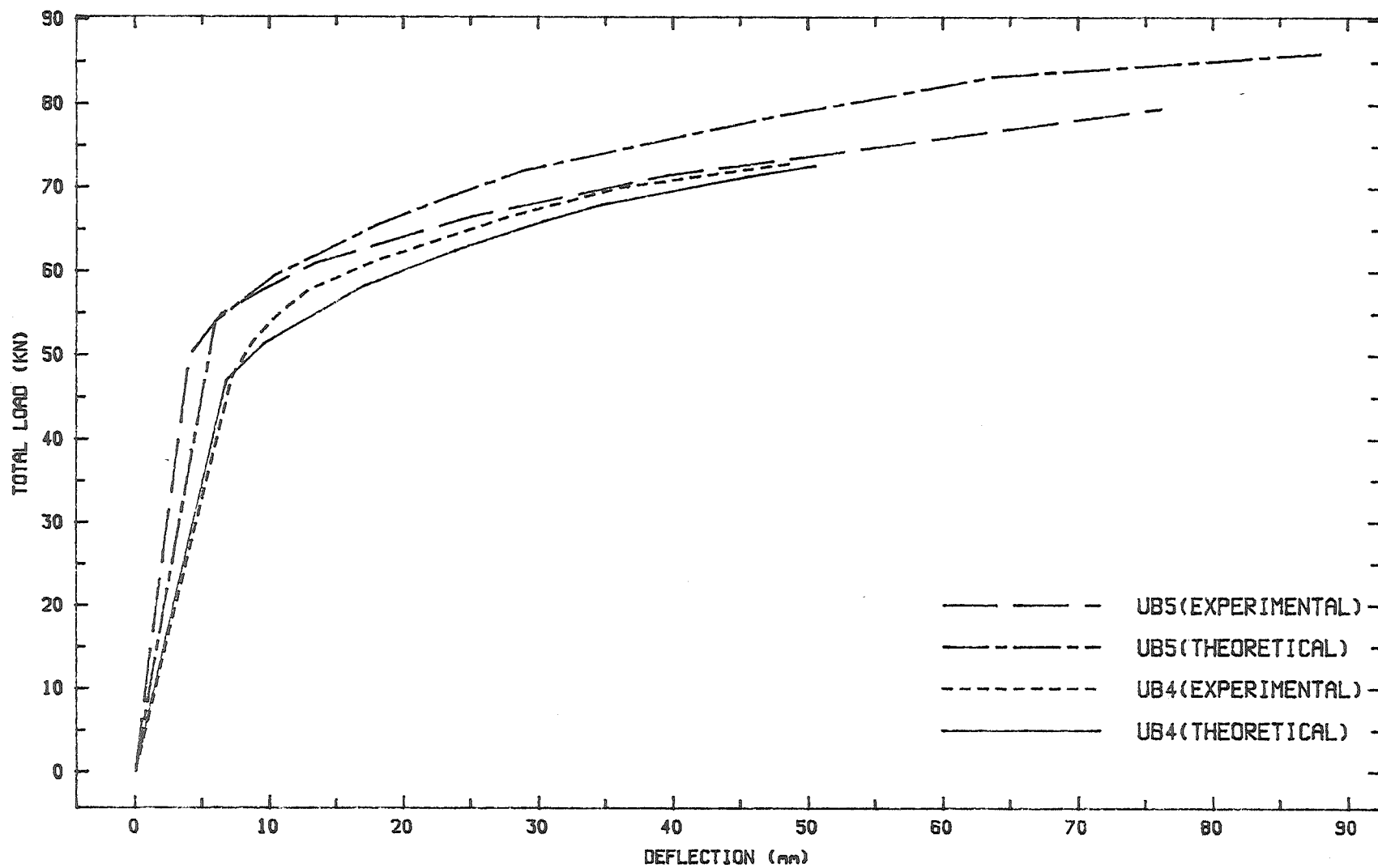


FIGURE 8.3 : LOAD DEFLECTION CURVE AT MID-SPAN

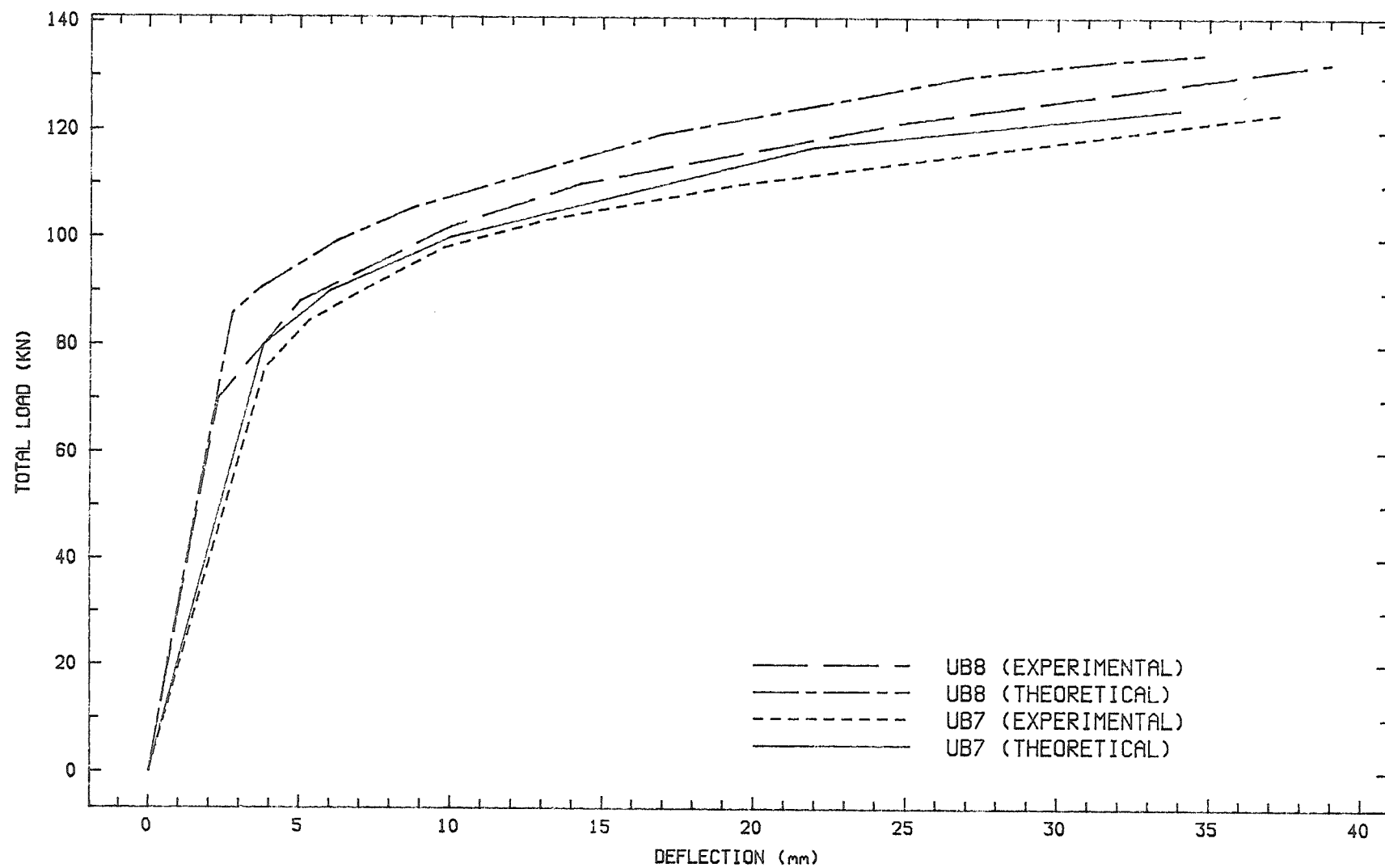


FIGURE 8.4: LOAD-TENDON STRESS CURVES

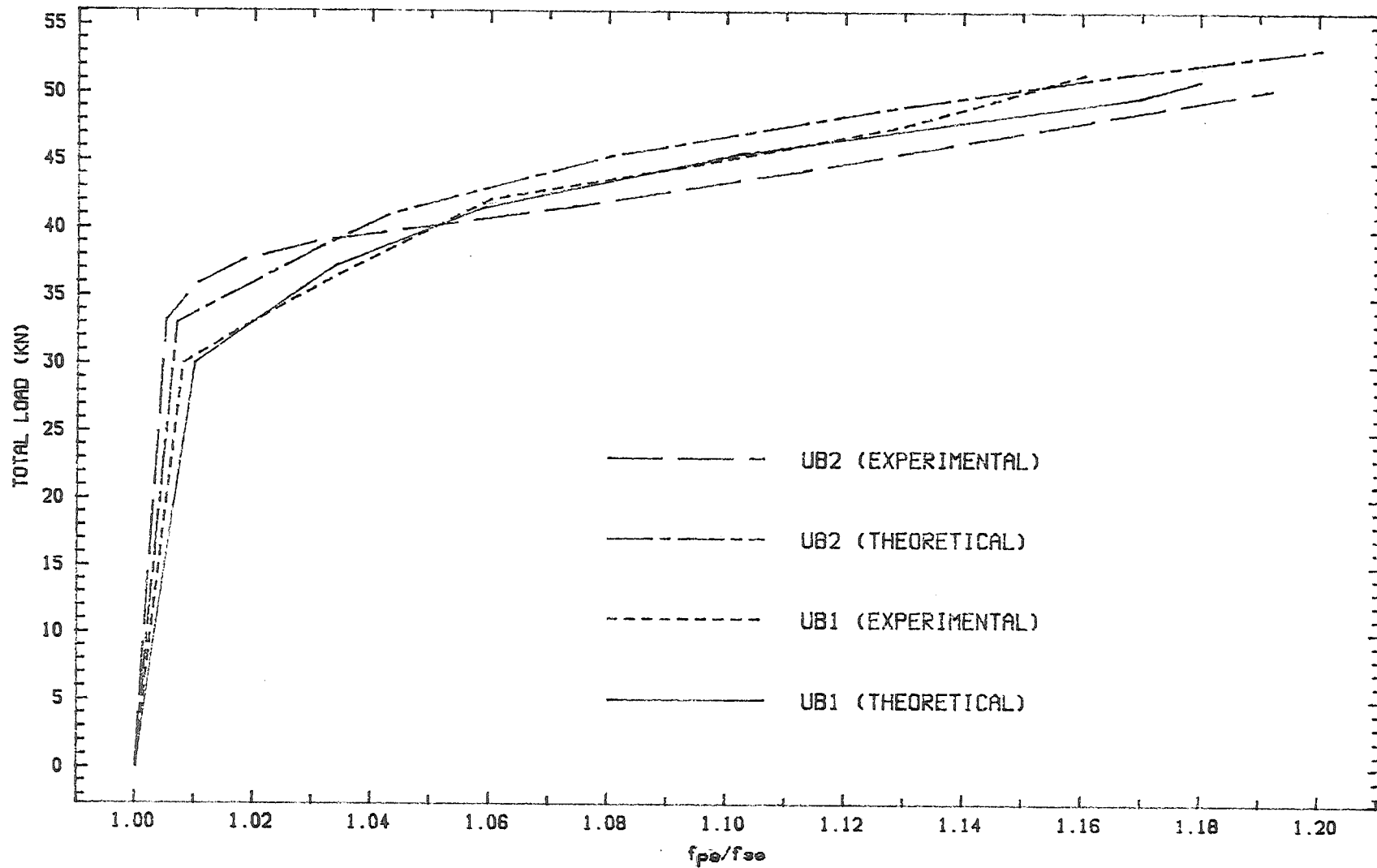


FIGURE 8.5: LOAD-TENDON STRESS CURVES

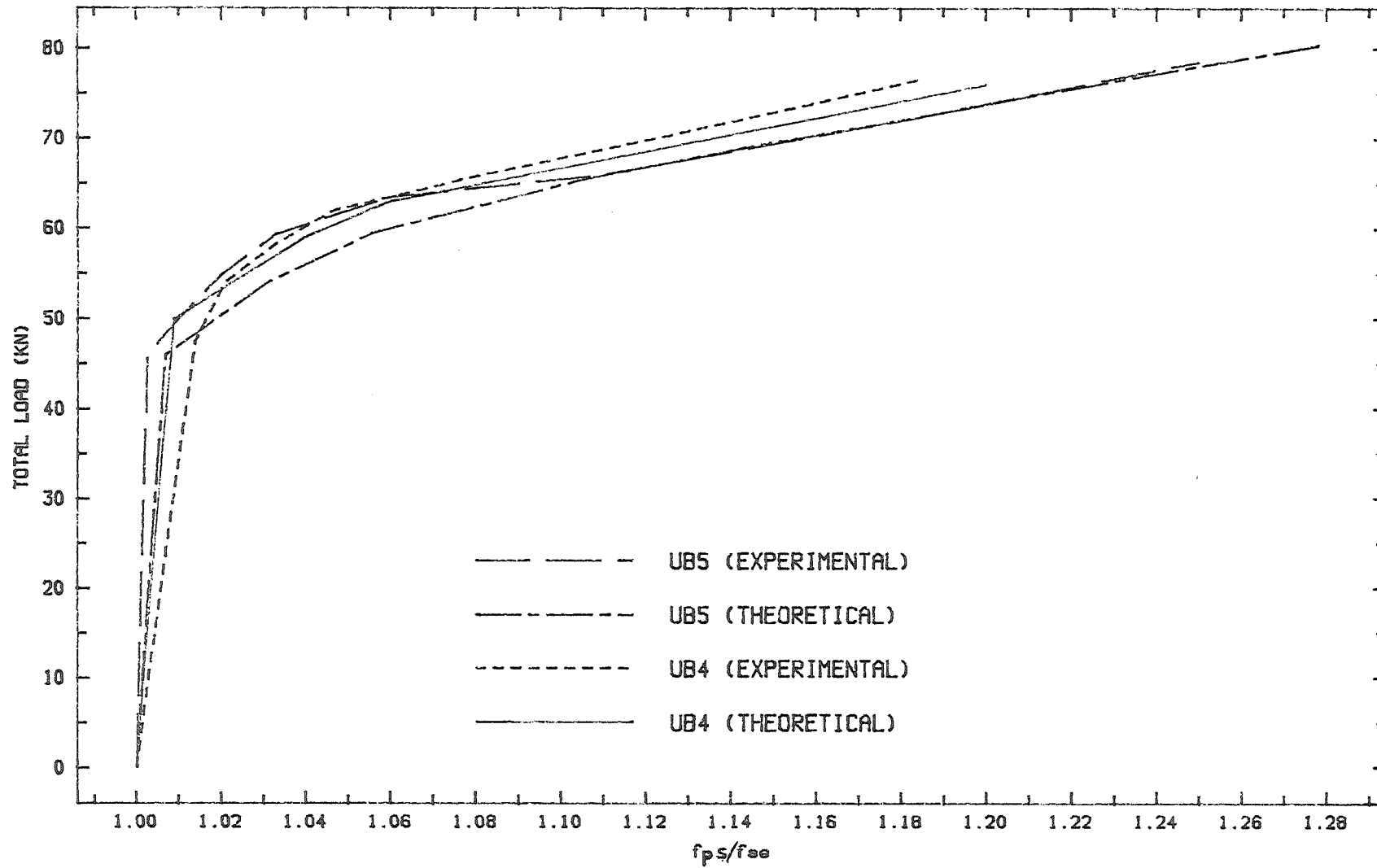


FIGURE 8.6: LOAD-TENDON STRESS CURVES

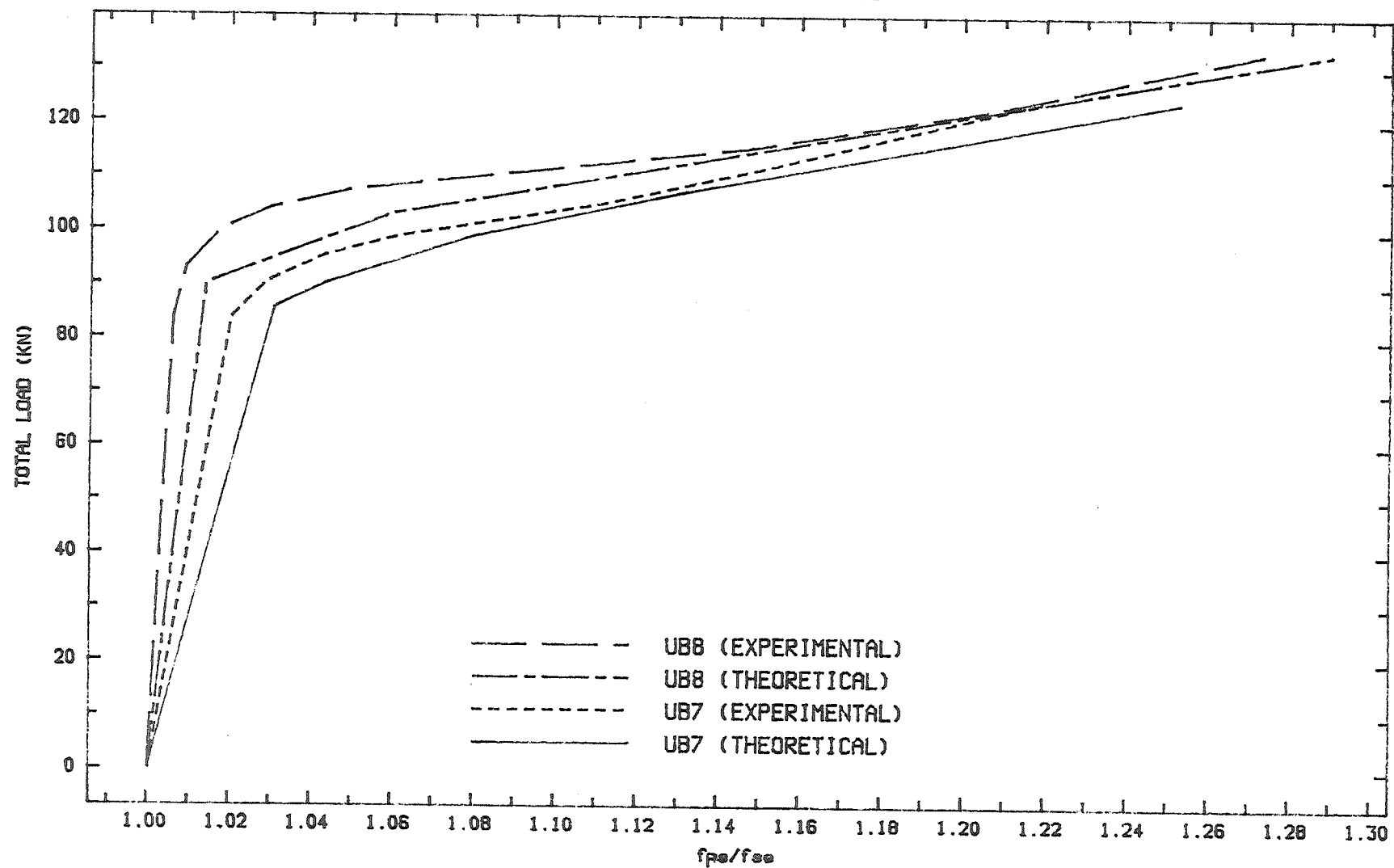


FIGURE 8.7 : TENDON STRESS INCREASE AT FAILURE VS COMBINED REINFORCEMENT INDEX

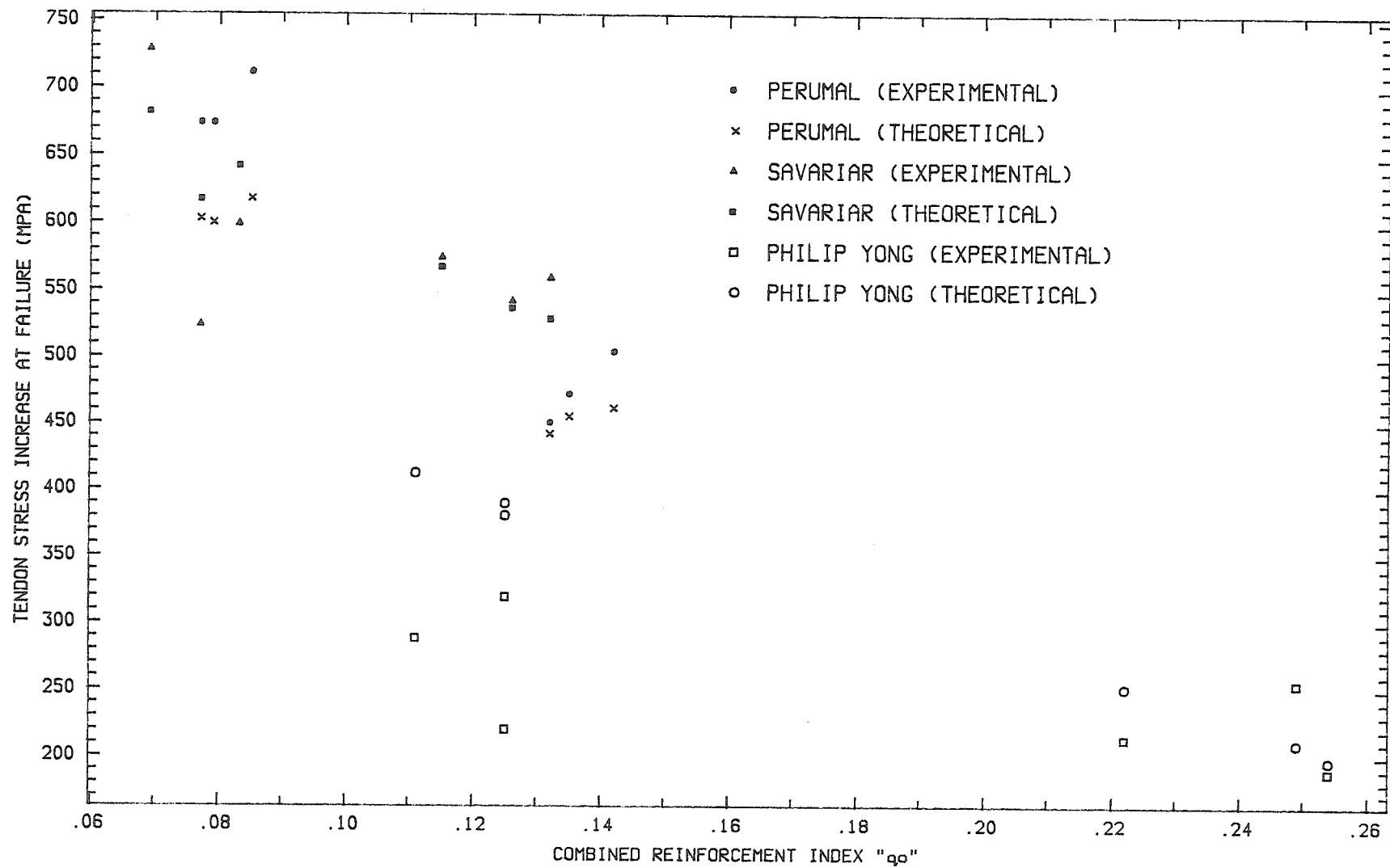


FIGURE 8.8 : TENDON STRESS INCREASE AT FAILURE VS COMBINED REINFORCEMENT INDEX

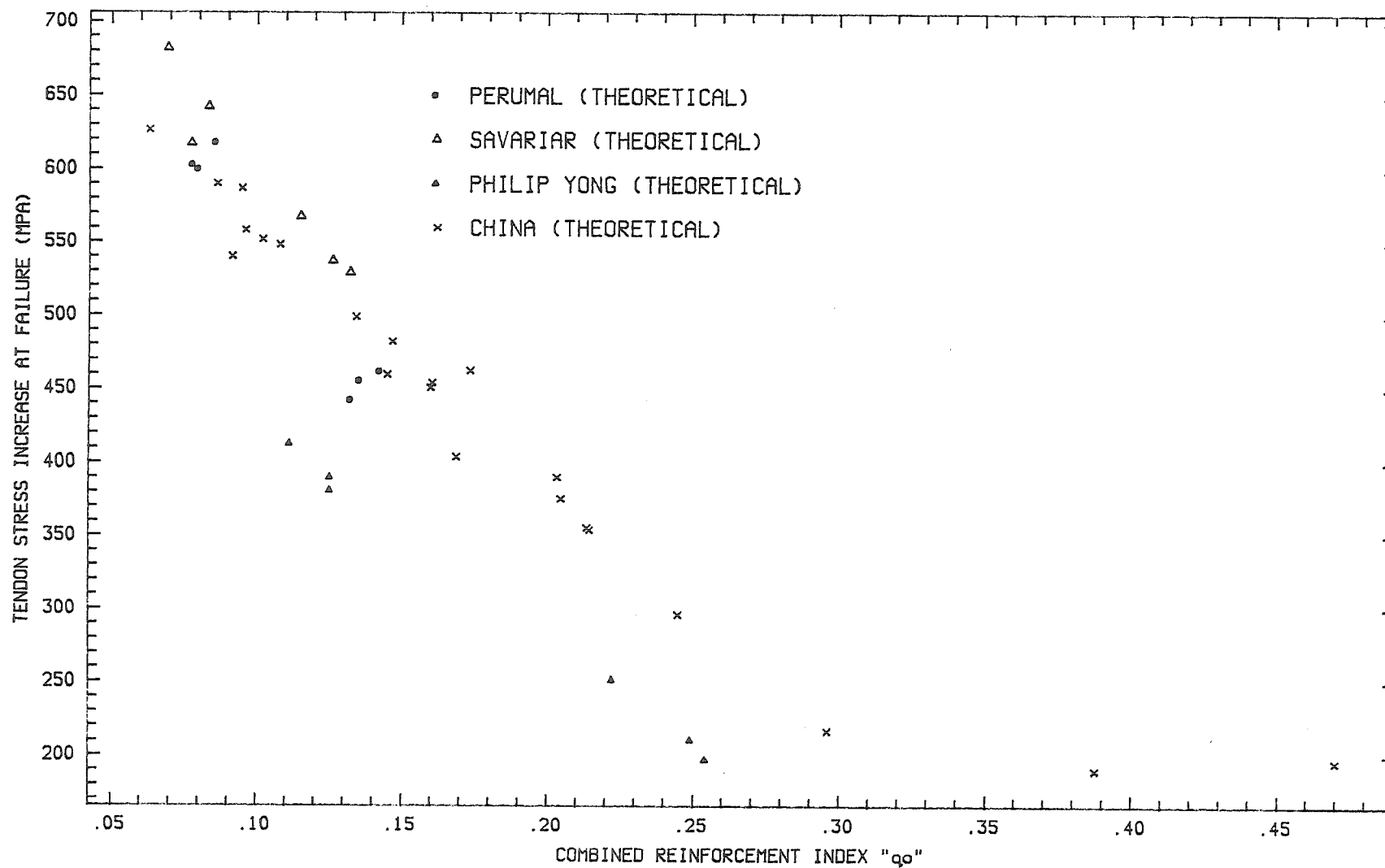


FIGURE 8.9: INCREASE IN TENDON STRESS AT FAILURE VERSUS SPAN-DEPTH RATIO

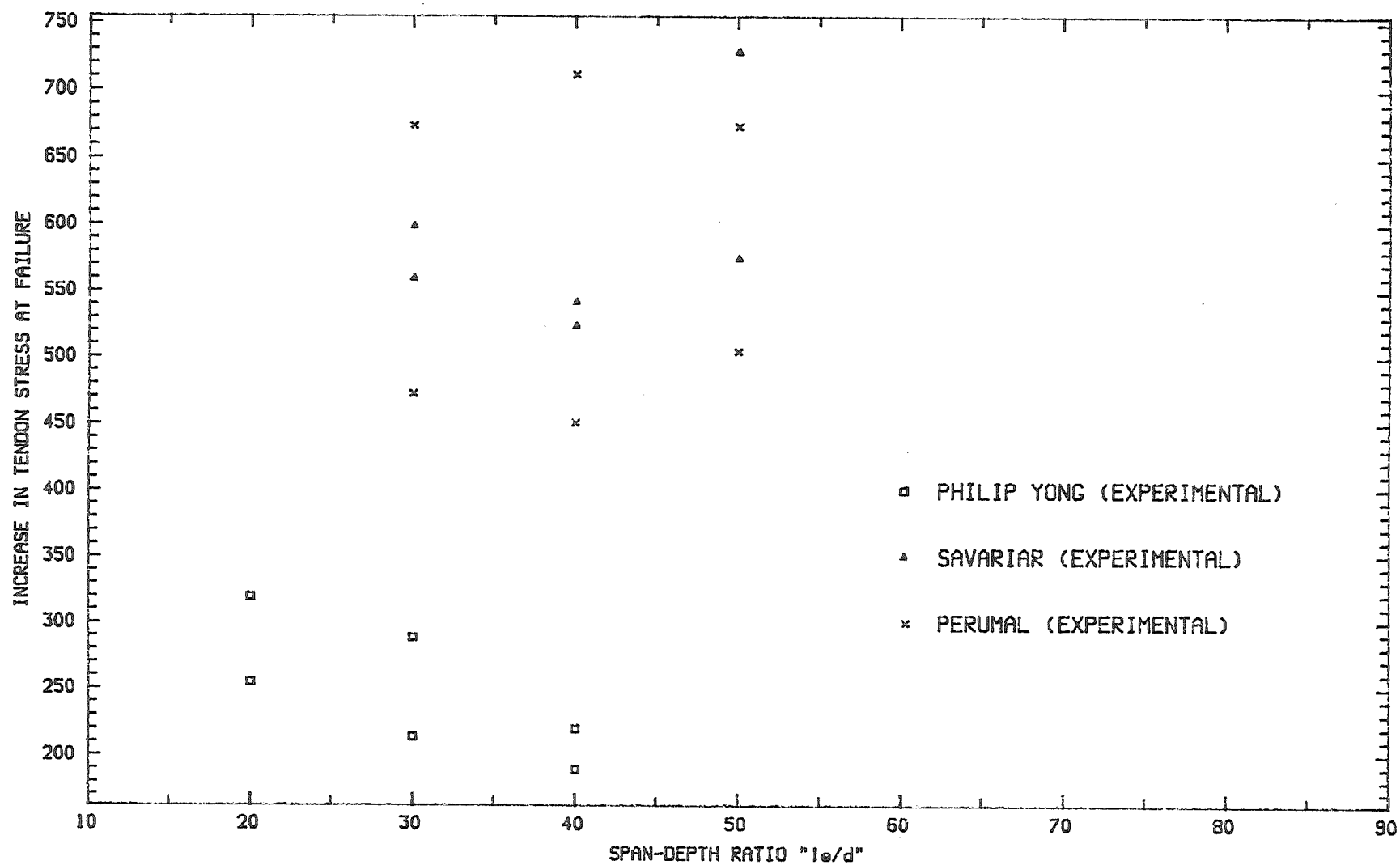


FIGURE 8.10: INCREASE IN TENDON STRESS AT FAILURE VERSUS SPAN-DEPTH RATIO

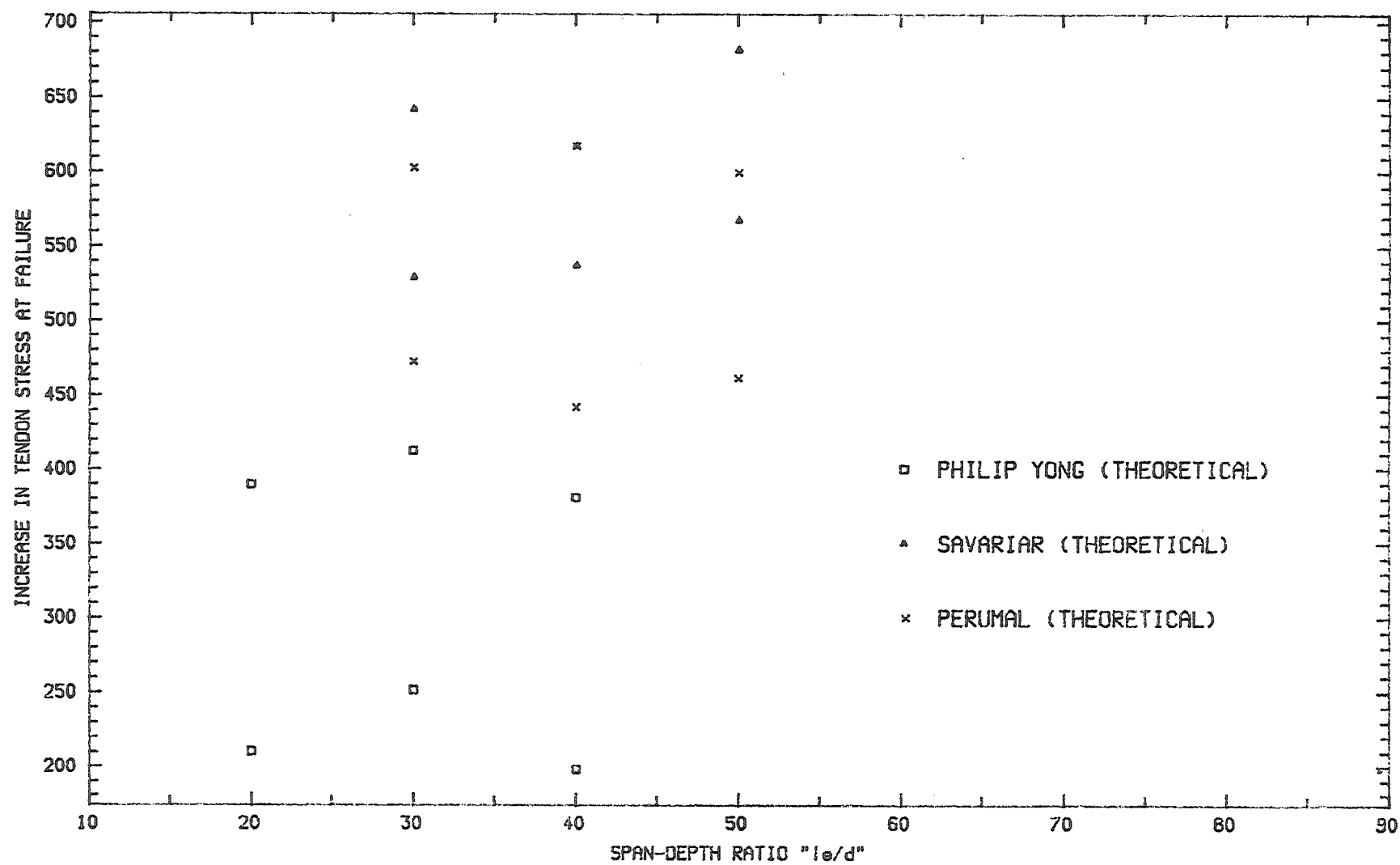


TABLE 8.2

**COMPARISON BETWEEN EXPERIMENTAL, ANALYTICAL AND
PREDICTED TENDON STRESS AND MOMENT AT
ULTIMATE.**

	fsu	fsu	fsu	fsu	fsu	fsu	Mu	Mu
slab	expt	analytical	ACI318-83	Pannell	NZS-3101	Warwaruk	expt	analytical
	(MPa)	(MPa)	(MPa)	(MPa)	(MPa)	(MPa)	(KNm)	(KNm)
HUB3	1912.9	1839	1731.38	1693.5	286.2	1384.7	52.75	44.5
HUB4	1609.4	1566.7	1280.6	1536.8	1205.2	1285.4	73.59	67.1
HUB5	1931.8	1838.1	1546.51	1794.9	1268.1	1365.5	52.78	44.44
HUB6	1588	1579.02	1324	1681.5	1237.3	1320.4	78.47	8.34
HUB7	1886	1842	1587.36	2009.9	1260.4	1359.0	53.47	45.23
HUB8	1609.4	1592.5	1321.18	1846.8	1237.3	1319.7	80.46	68.32
YUB3	1806.3	1759.77	1413.6	1676.3	1178.3	1270.4	42.3	38.97
YUB4	1520.5	1513.6	1126	1469.6	1046.2	1113.2	66.08	59.7
YUB5	1663.5	1757.4	1457.5	1870.8	1240.1	1330.3	42.42	38.28
YUB6	1498.8	1493.8	1129.3	1581.4	1057	1121	68.33	59.29
YUB7	1742.4	1785.8	1444.2	2091.1	1244	1333.4	41.87	38.8
YUB8	1490.5	1460.1	1096.4	1730.4	1031.3	1091.8	63.67	57.39
UB1	1351	1360.0	1246.65	1237	1257	1268.46	42.83	40.0
UB2	1365	1525.8	1244.66	1262	1245	1303.21	45.73	45.69
UB4	1376	1413.6	1283.69	1273	1262	1272.86	44.0	39.23
UB5	1442	1566.0	1327.23	1311	1254	1313.0	47.71	47.64
UB7	1418	1373.7	1279.32	1306	1264	1307.54	44.11	43.28
UB8	1487	1557.29	1330.3	1393	1268	1327.0	47.38	46.78

where : expt = experimental

experimental curves and most analytical curves show smaller mid-span deflections. Figures 8.4 to 8.6 show curves of total load versus prestress-initial prestress ratio, f_{ps}/f_{se} . Similarly the analytical curves follow quite closely to the experimental curves and most analytical curves show higher f_{ps}/f_{se} ratios which also mean that most slabs show higher tendon stress at failure in the analytical results. This over-estimate is also shown in Figure 8.17 where analytical and experimental results are compared in the graph of tendon stress increase versus combined reinforcement index. Analytical results show a much higher increase in tendon prestress especially at lower q_0 values. However they conform more closely to a linear relationship between decrease in tendon stress increase and increasing q_0 value. Experimental data also shows a very slight decrease in tendon stress with increasing q_0 values. The tendon stress increase of UB2 with q_0 value equal to 0.125 is even smaller to that of UB7 with q_0 value equal to 0.249 which is the reverse of the normal relationship or trend as shown in the analytical results plotted in figure 8.8. It is clear that the unbonded slabs without bonded steel show approximately the same tendon stress increase for q_0 values greater than 0.1.

Table 8.2 shows the comparison between experimental, predicted and analytical results. It should be noted that the analytical values of ultimate moments agree very well with the experimental values despite the fact that some analytical ultimate tendon stress increase values are larger than experimental values. All analytical tendon stresses at ultimate for unbonded slabs tested by Yong (1980) show higher values than that predicted by ACI 318-83 (1980), Pannell (1969), NZS 3101(1982) and Warwaruk (1962).

Figures 8.9 and 8.10 attempt to show the effect of span-depth ratio on the increase in tendon stress at failure. In Figure 8.9, the experimental data obtained by Yong (1980) appear to show the trend of decrease in the values of tendon stress increase at failure with decreasing span-depth ratio. This trend is not observed for analytical data plotted in Figure 8.10.

8.3 UNBONDED SLABS TESTED BY SAVARIAR (1984).

Nine unbonded slabs with bonded mild steel, low yield reinforcement were tested by Savariar (1984). Slabs YUB1 and YUB2 were two-span continuous slabs and the other slabs YUB3 to YUB8 were single span slabs. All bonded steel bars have a specific yield strength of 275 MPa. The average yield strength and ultimate tensile strength of the reinforcing bars obtained from testing in an Avery Universal Testing machine were 302 and 414 MPa respectively. The details of all unbonded slabs tested by Savariar (1984) are as shown in Table 8.3.

Table 8.3 : Detail of slabs tested by Savariar (1984).

slab	q_0	q_e	q_s	f_{se} (MPa)	A_{ps} (mm ²)	l_e/d	f_c (MPa)	A_s (mm ²)	
YUB1	.045	.029	.016	993.1	121.53	61.7	45.62	314.16	
YUB2	.085	.068	.017	973.8	280.65	61.7	45.62	314.16	
YUB3	.069	.040	.029	1078.3	121.53	50	35.5	314.16	
YUB4	.115	.085	.030	946.3	280.65	50	35.5	314.16	
YUB5	.077	.046	.031	1140.1	121.53	40	33.12	314.16	
YUB6	.126	.093	.033	957.0	280.65	40	33.12	314.16	
YUB7	.083	.049	.034	1144.0	121.53	30	30.82	314.16	
YUB8	.132	.097	.035	931.3	280.65	30	30.82	314.16	

The computer programme only analyses single span slabs under third point loading, hence YUB1 and YUB2, which are double span slabs, were not analysed. The comparison between experimental and analytical data for slabs YUB3 to YUB6 are as shown in Figures 8.11 to 8.16. Good comparison between analytical and experimental results is only obtained for slabs YUB7 and YUB8 as shown in Figures 8.13 and 8.16. The other four slabs doesn't agree that well as shown in figures 8.11, 8.12, 8.14 and 8.15. But analytical results show a good linear relationship between tendon stress increase and combined reinforcement index as shown in Figures 8.7 and 8.8. Figures 9.7 and 9.8 also show that unbonded slabs with bonded reinforcement of yield strength 275 MPa have much higher tendon stress increases at failure than those without bonded reinforcement of approximately same q_0 values. Hence unbonded slabs with bonded reinforcement are theoretically of better design and have a much higher moment capacity.

Table 8.2 shows that analytical values of tendon stress at ultimate are much closer to experimental results than that predicted by ACI 318-83 (1983), Pannell(1969), NZS 3101(1982) and Warwaruk(1962), even though some analytical f_{su} values are slightly higher than the experimental values. The

FIGURE 8.11: LOAD-DEFLECTION CURVE AT MID-SPAN

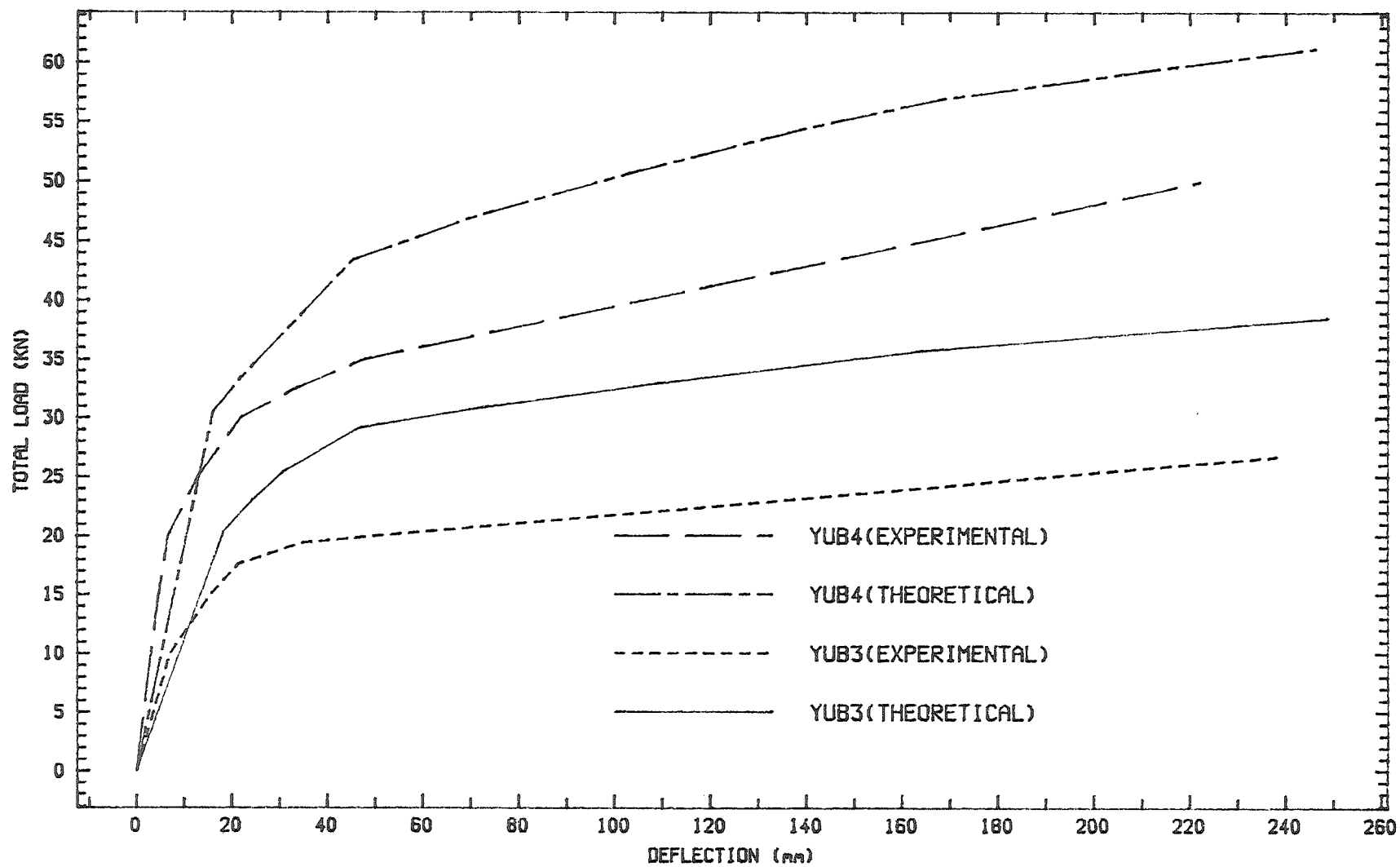


FIGURE 8.12: LOAD-DEFLECTION CURVE AT MID-SPAN

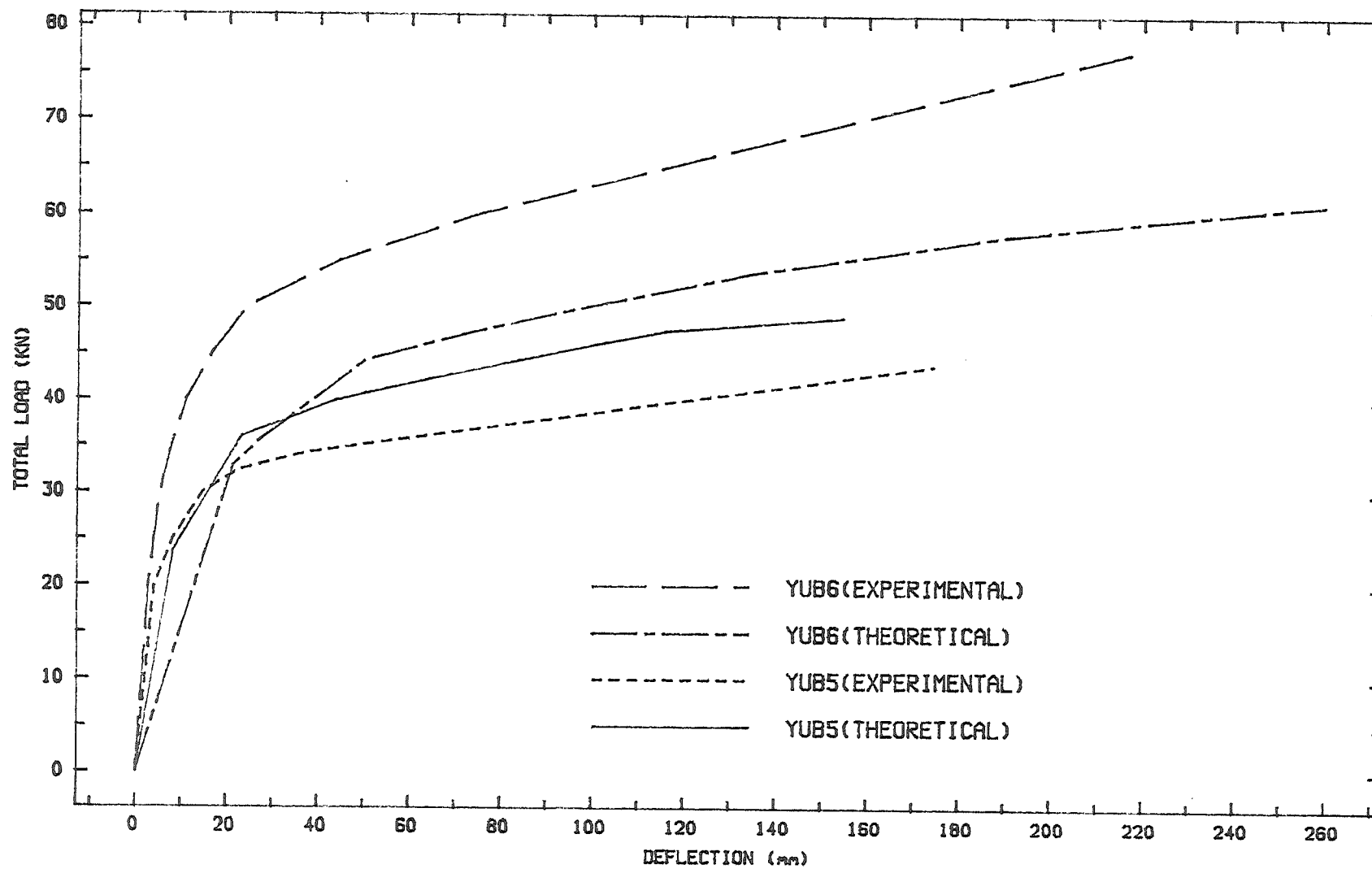


FIGURE 8.13: LOAD-DEFLECTION CURVE AT MID-SPAN

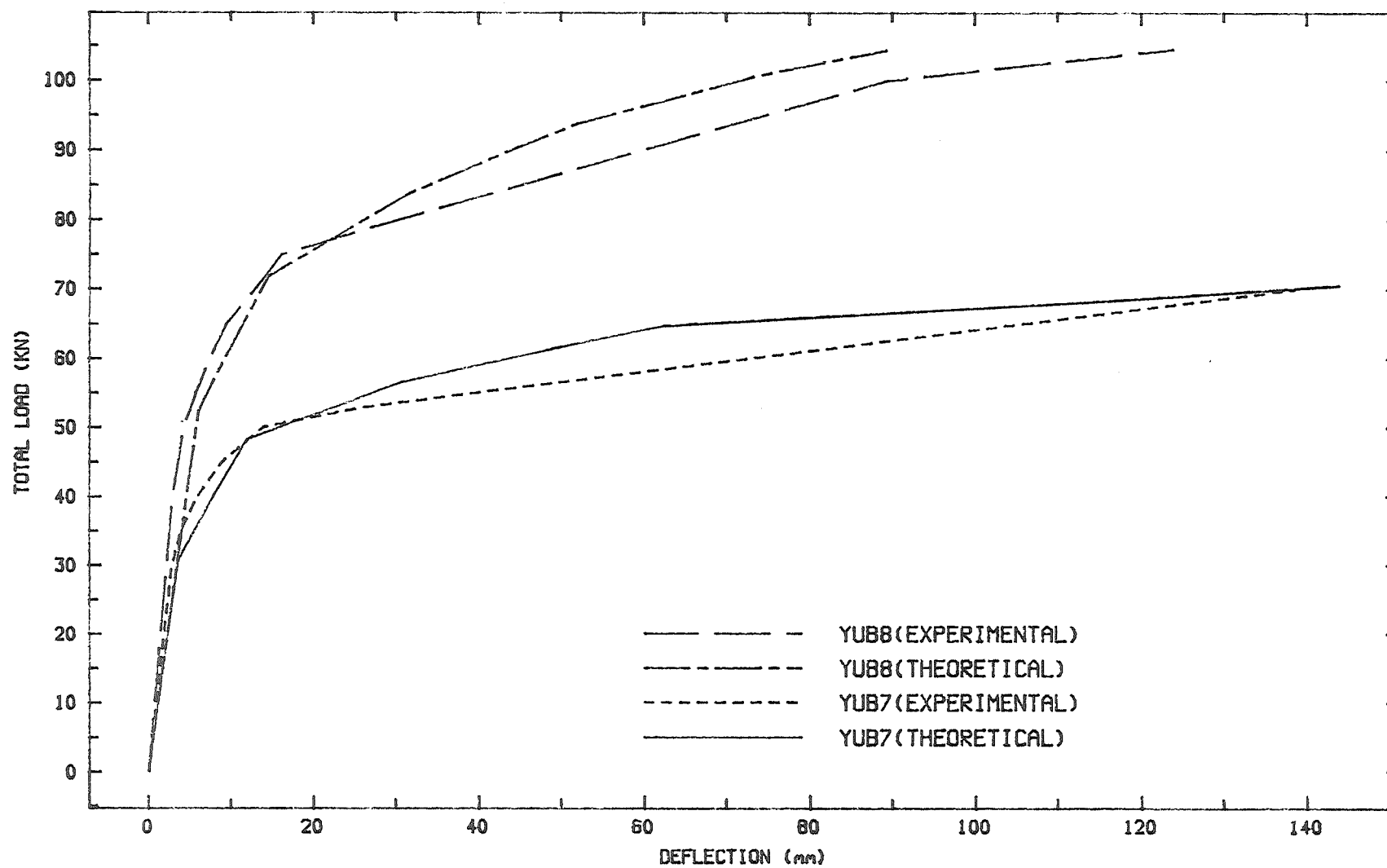


FIGURE 8.14: TOTAL LOAD VS TENDON STRESS INCREASE CURVE

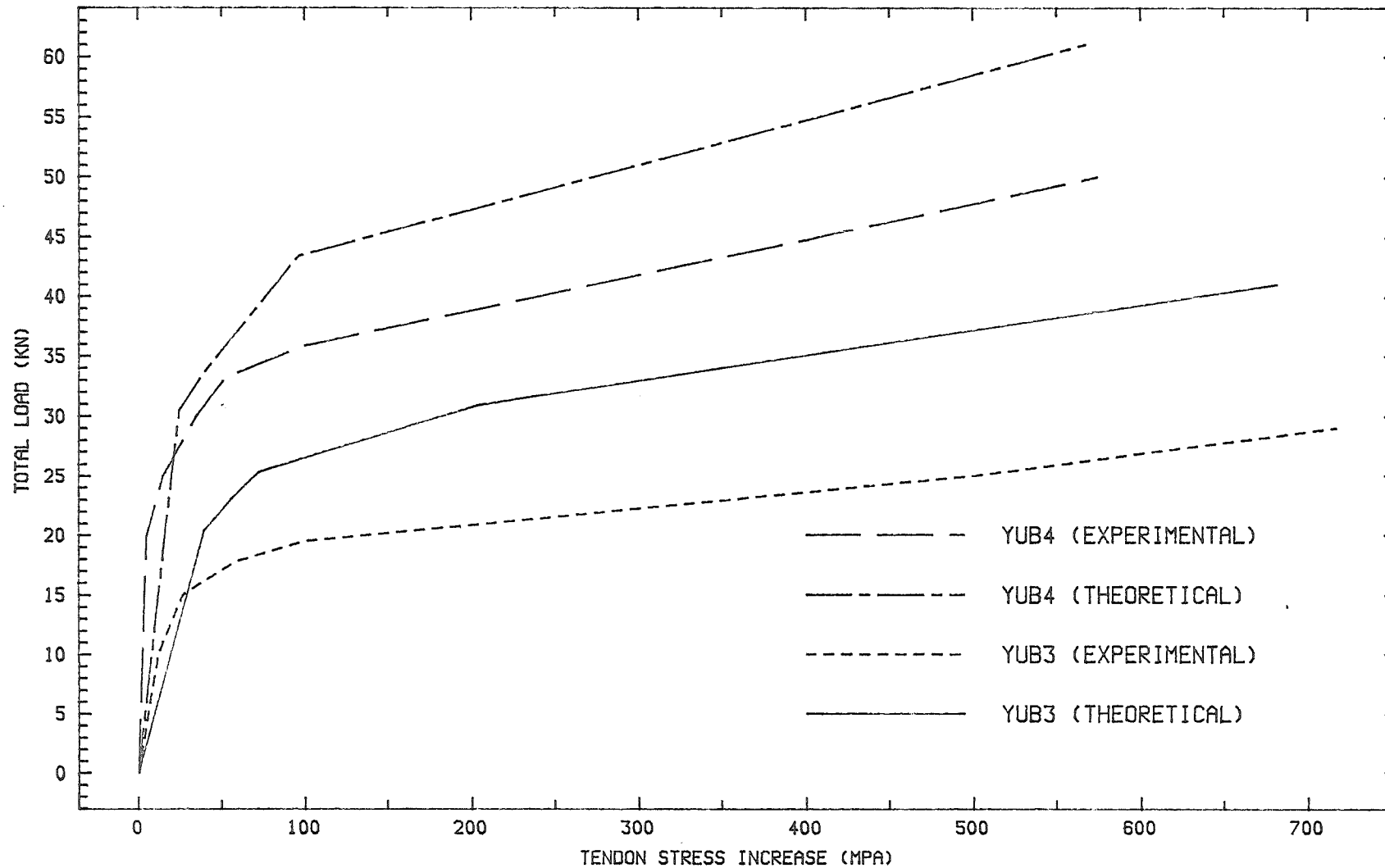


FIGURE 8.15: TOTAL LOAD VS TENDON STRESS INCREASE CURVE

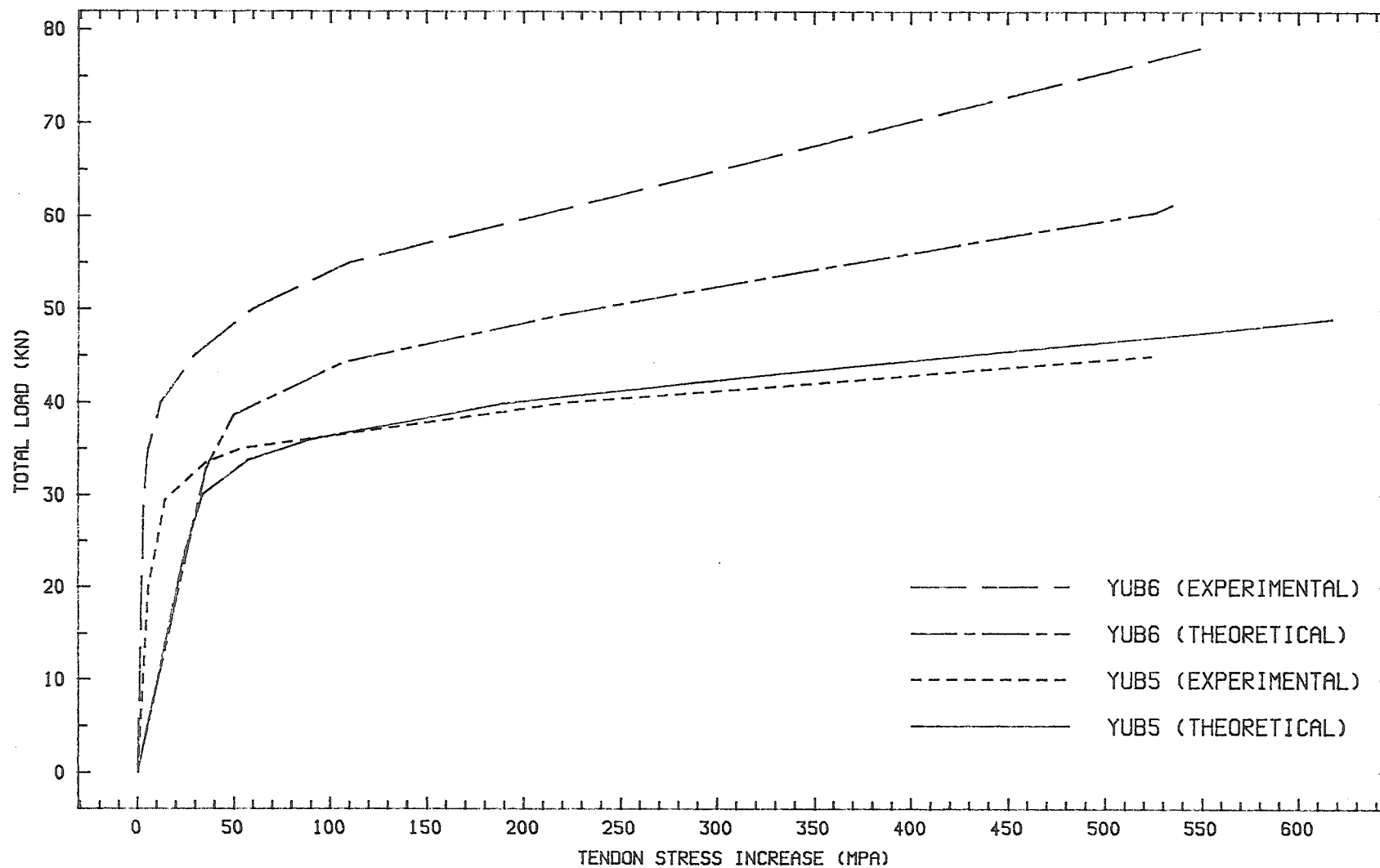
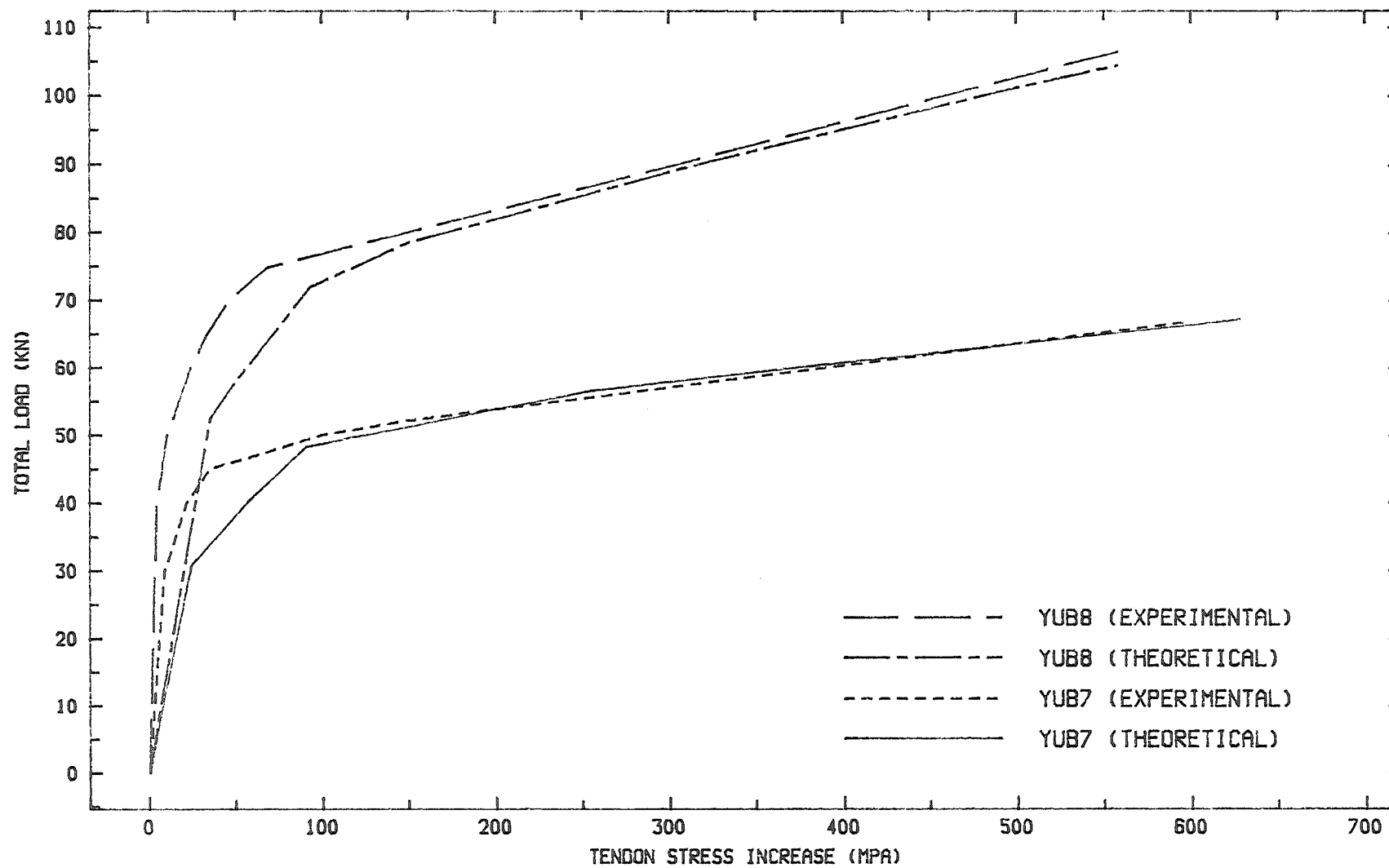


FIGURE 8.16: TOTAL LOAD VS TENDON STRESS INCREASE CURVE



analytical ultimate moment results are all lower and reasonably close to the experimental values obtained for all the slabs tested by Savariar (1984). Figures 8.9 and 8.10 show that the effect of span-depth ratio on tendon stress increase at failure is not significant for both analytical and experimental data of unbonded slabs tested by Savariar (1984), or no trend is apparent .

8.4 UNBONDED SLABS TESTED BY PERUMAL (1986).

Unbonded slabs tested by Perumal (1986) are exactly the same as Savariar (1984) except that reinforcing bars of specific yield strength equal to 380 Mpa were used as bonded reinforcement. The average yield strength and ultimate tensile strength of the reinforcing steel obtained from testing were 521.6 and 693 MPa respectively. The purpose for this difference was to find out the effect of yield strength of bonded reinforcing bars on the flexural behaviour of the unbonded partially prestressed slabs.

Only slabs HUB3 to HUB8, being single span slabs, were analysed using the modified computer program. Slabs HUB1 and HUB2 which are two span slabs, have not been analysed.

Table 8.4 : Detail of slabs tested by Perumal (1986).

slab	q_o	q_e	q_s	f_{se} (MPa)	A_{ps} (mm ²)	l_e/d	f'_c (MPa)	A_s (mm ²)
HUB1	.071	.043	.028	1293.2	111.35	61.7	36.5	314.16
HUB2	.118	.091	.027	1094.4	279.6	61.7	38.5	314.16
HUB3	.079	.043	.036	1186.2	111.35	50	32.9	314.16
HUB4	.142	.104	.038	1105.2	279.6	50	34.0	314.16
HUB5	.085	.046	.039	1168.1	111.35	40	32.8	314.16
HUB6	.132	.097	.035	1137.3	279.6	40	37.6	314.16
HUB7	.077	.042	.035	1160.4	111.35	30	35.6	314.16
HUB8	.135	.099	.036	1137.3	279.6	30	36.7	314.16

The comparison between experimental and analytical results are plotted in Figures 8.17 to 8.22. Generally the analytical curves show less mid-span deflection and higher applied load at failure than the experimental curves. All slabs show a lower increase in tendon stress increase at failure for analytical results compared to the experimental results. This is also shown in Figure 8.7. Again tendon stress increase at failure decreases as q_0 increases is also true for unbonded slabs with bonded steel of higher yield strength. Figure 8.20 shows that the analytical results of unbonded slabs with bonded steel of lower yield strength tested by Savariar (1984) show a higher increase in tendon stress at failure than the unbonded slabs with bonded steel of higher yield strength tested by Perumal (1986) although the magnitude of the stress at ultimate is less than Perumal's. The probable reason is that the increase in yield strength of the bonded steel increases the neutral axis depth at failure.

Analytical results of both Perumal (1986) and Savariar (1984) agree well with the analytical results of beams tested by Du and Tao (1984) to give good linear relationship between values of q_0 and increase in tendon stress at failure as shown in Figure 8.18. Analytical results of Yong (1980) also show the same relationship but the values of tendon stress increase at failure are much lower than the values of unbonded members with bonded reinforcement of the same q_0 values.

Table 8.2 shows that analytical value of tendon stress at ultimate give better results than that predicted by expressions of ACI 318-83 (1983), Pannell(1969), NZS 3101(1982) and Warwaruk(1962). It also shows that all analytical values of increase in tendon stress and moment at ultimate of unbonded slabs tested by Perumal (1986), are slightly lower and agree well with the experimental data.

There is also no particular relationship between span-depth ratio and increase in tendon stress at failure for unbonded slabs with bonded steel of higher yield strength as shown in Figures 8.9 and 8.10 for both experimental and analytical data. Hence we can conclude that the influence of span-depth ratio on increase in tendon stress at failure is not significant.

FIGURE 8.17: LOAD-DEFLECTION CURVE AT MID-SPAN

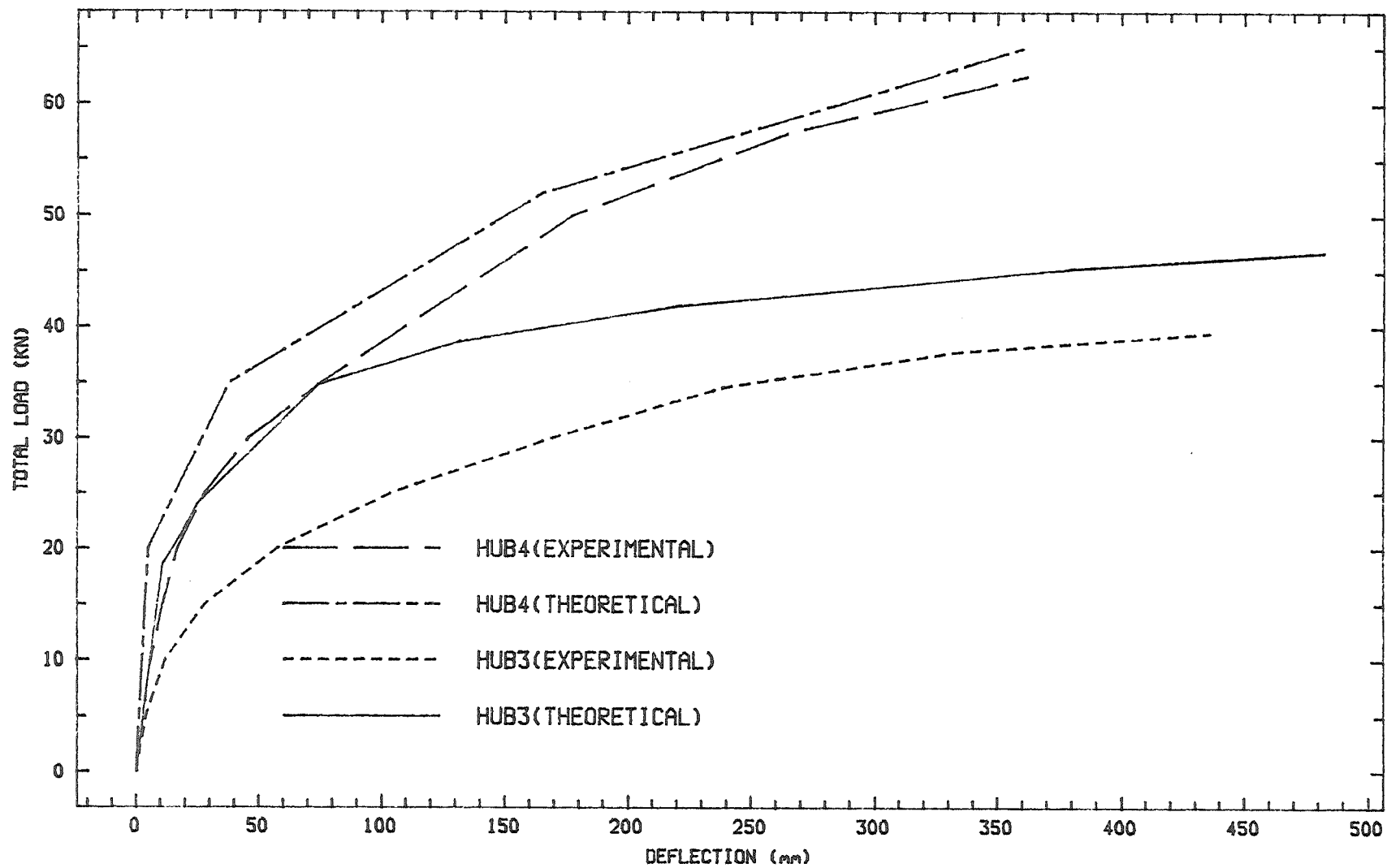


FIGURE 8.18: LOAD-DEFLECTION CURVE AT MID-SPAN

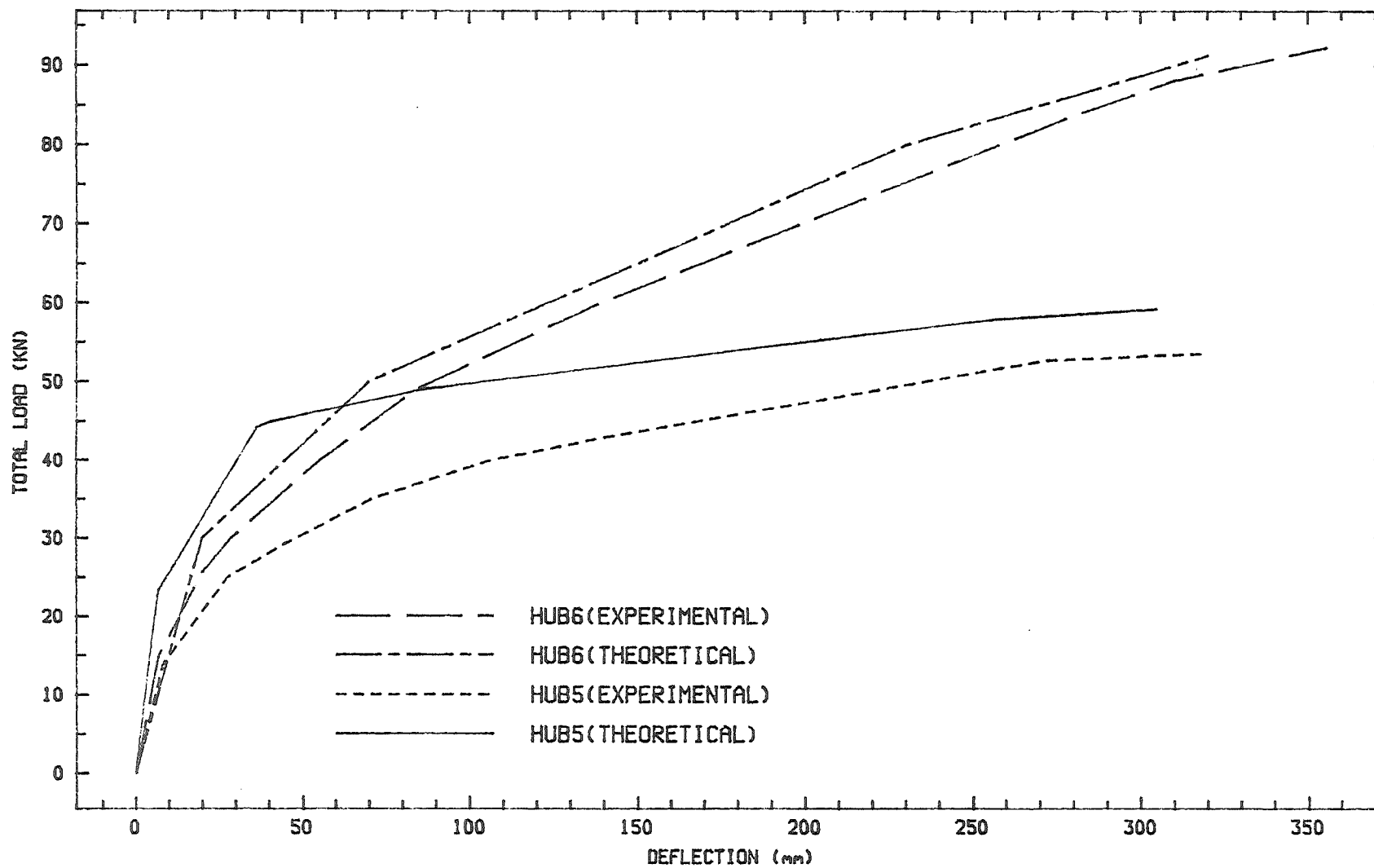


FIGURE 8.19: LOAD-DEFLECTION CURVE AT MID-SPAN

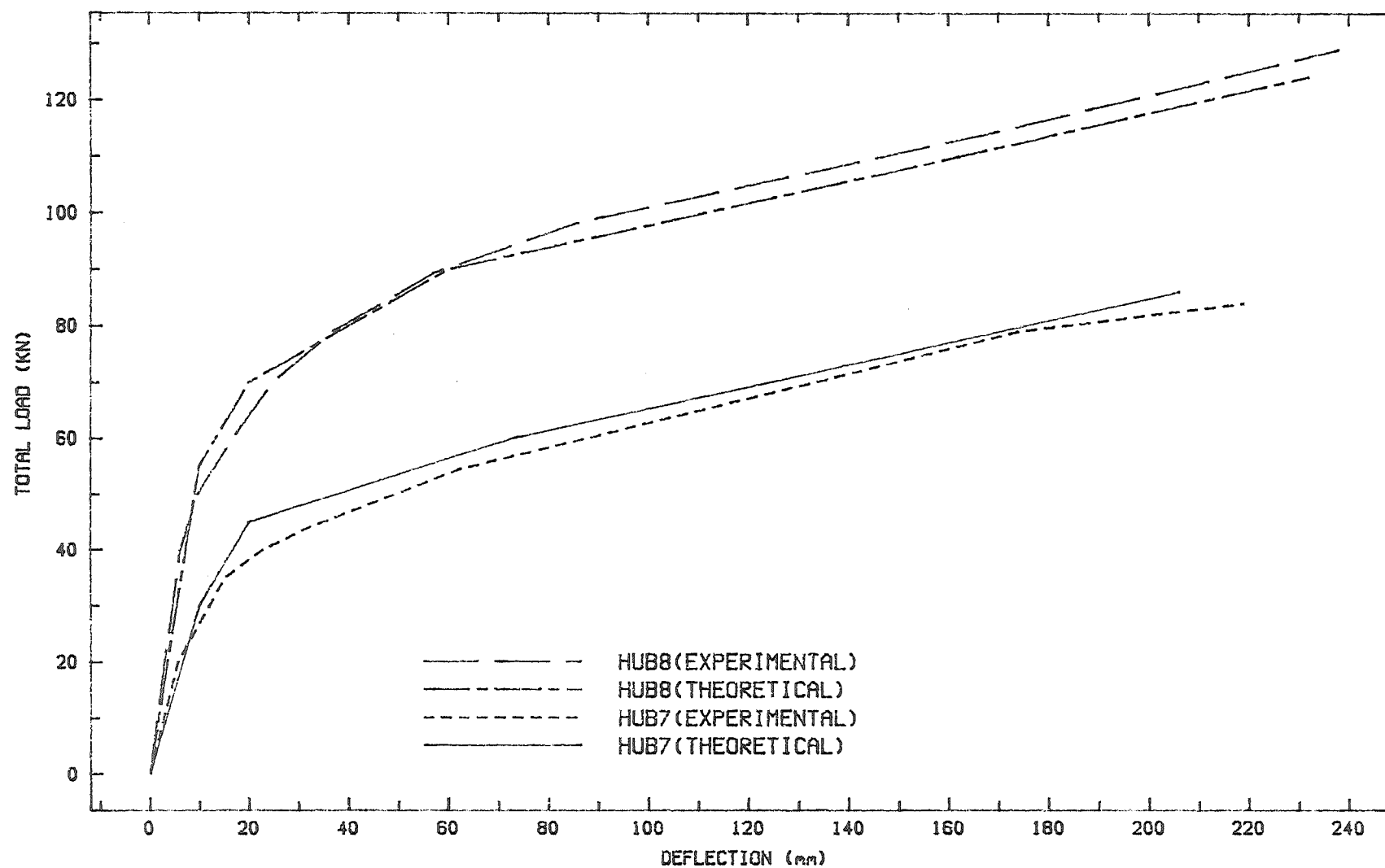


FIGURE 8.20: TOTAL LOAD VS TENDON STRESS INCREASE CURVE

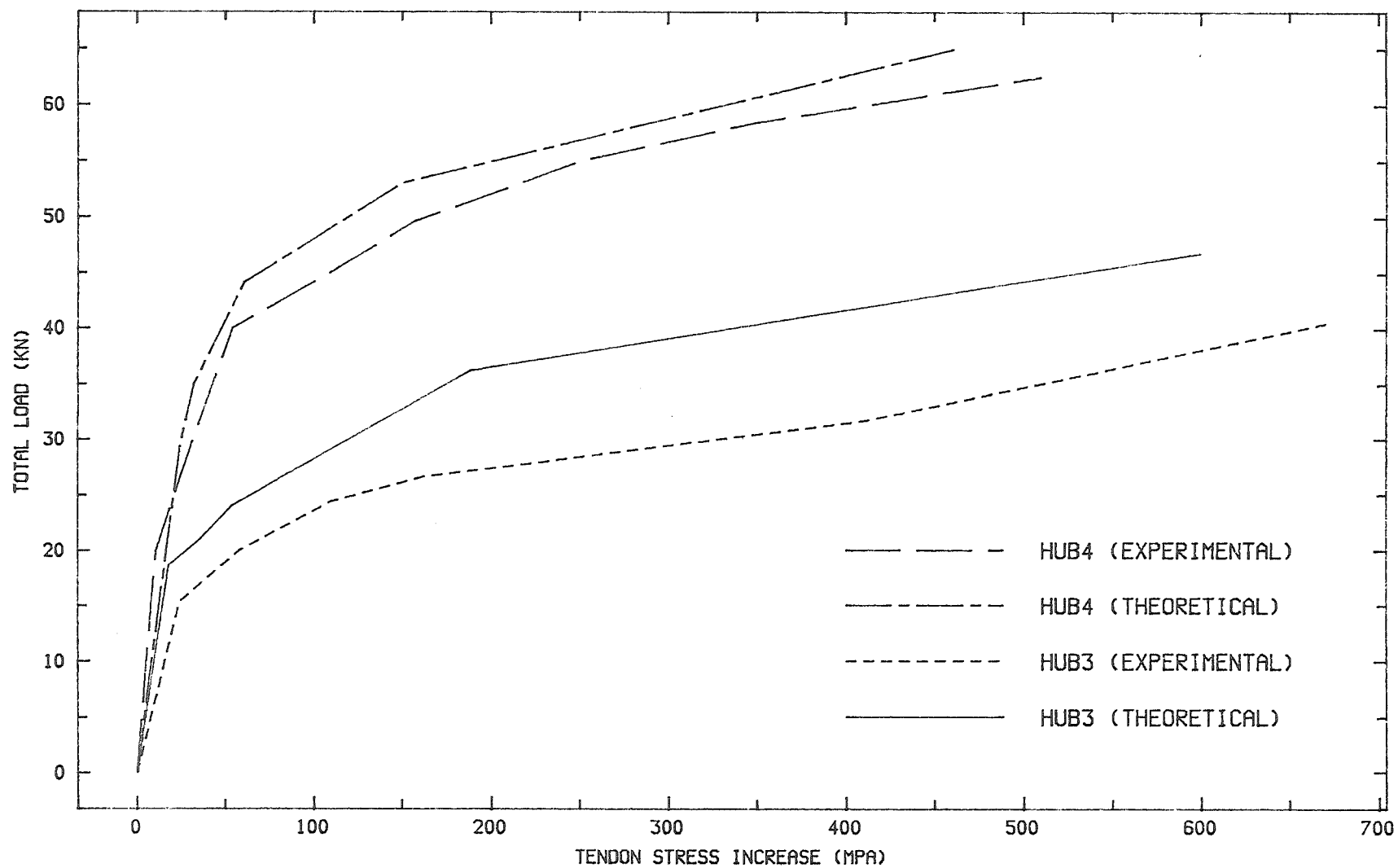


FIGURE 8.21: TOTAL LOAD VS TENDON STRESS INCREASE CURVE

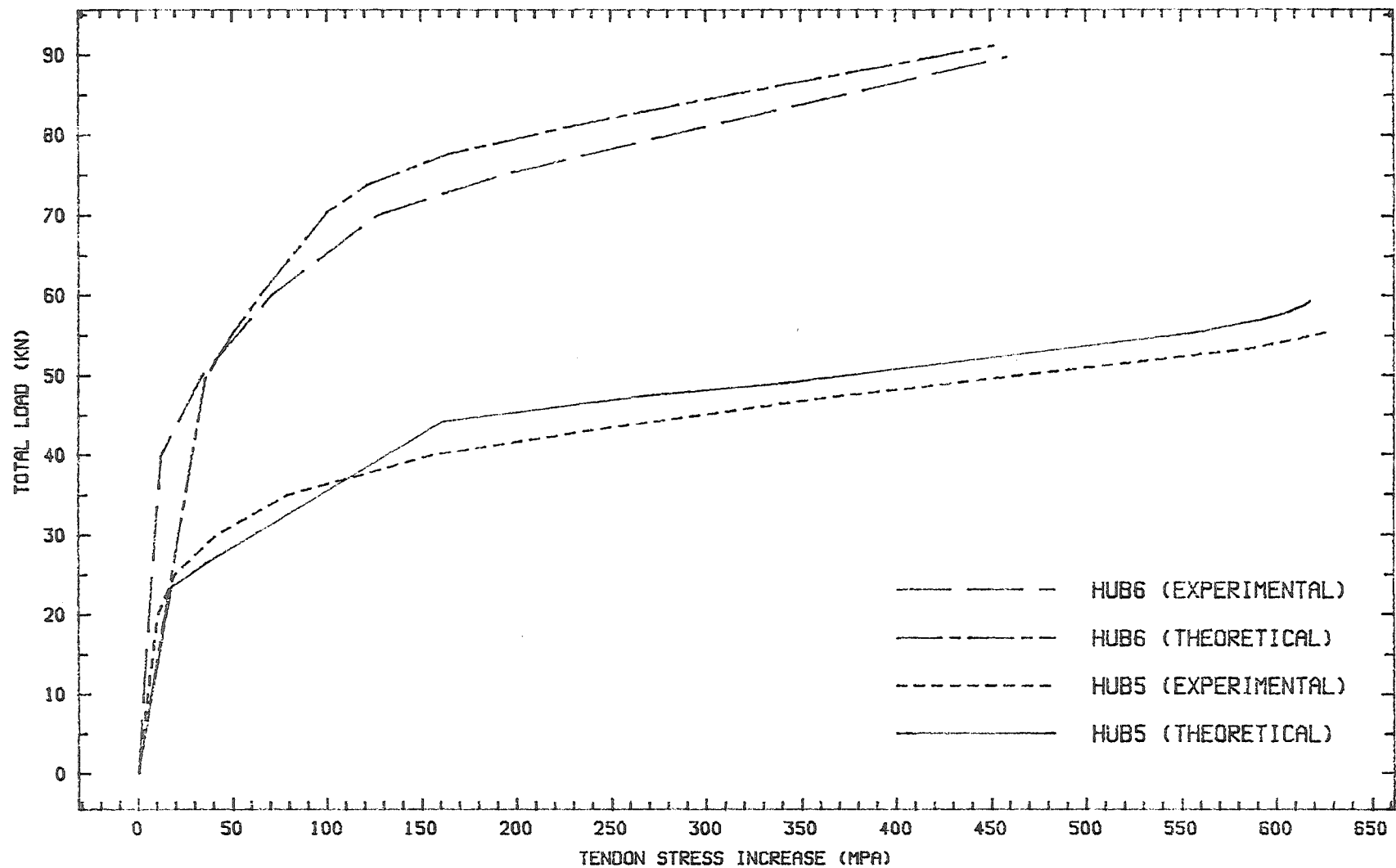
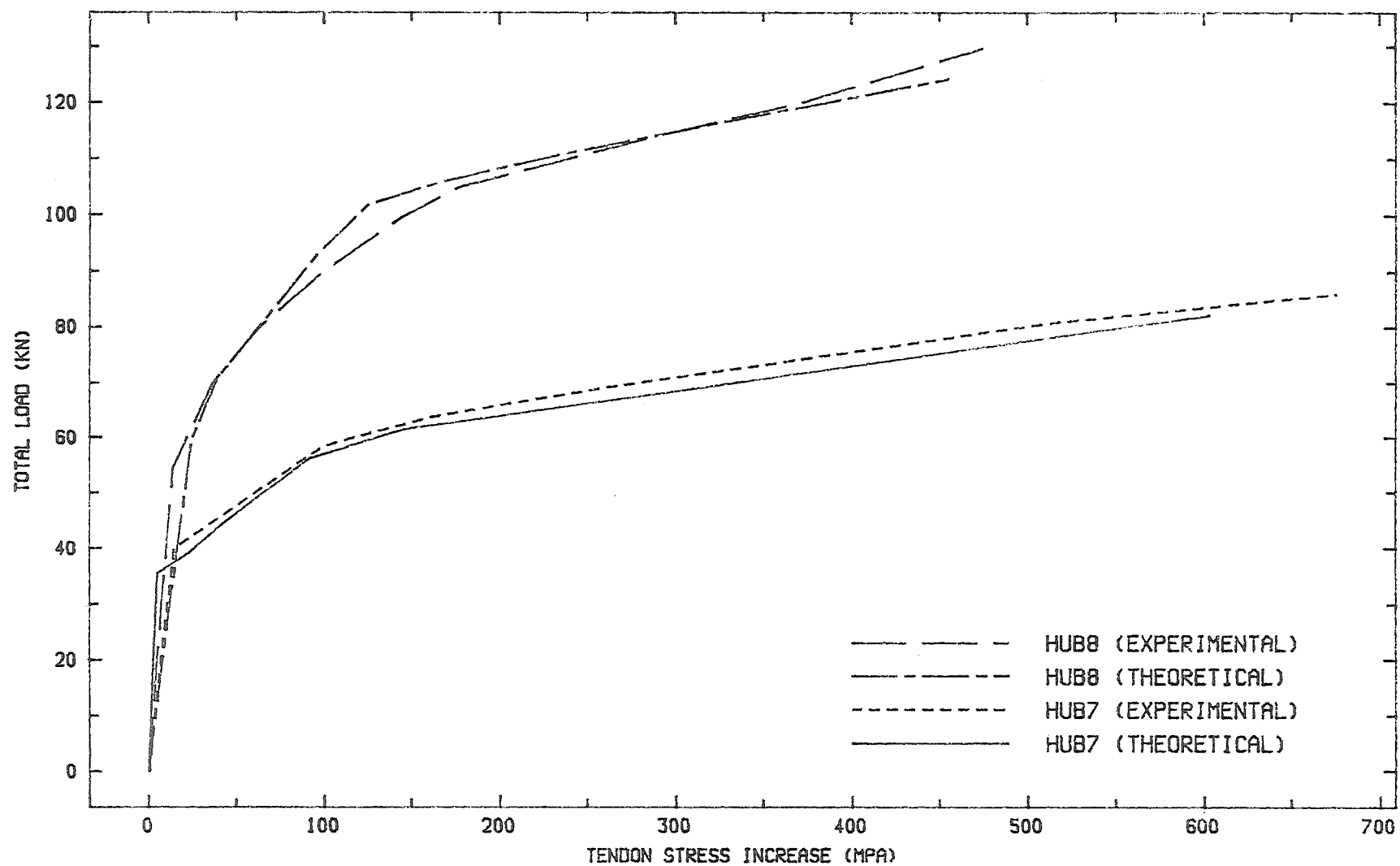


FIGURE 8.22 : TOTAL LOAD VS TENDON STRESS INCREASE CURVE



CHAPTER 9

DESIGN RECOMMENDATION AND DISCUSSION OF RESULTS

Experimental results for unbonded slabs or beams tested by Du and Tao (1984), Savariar(1984), Perumal (1986) and Yong (1980) lead to two proposed design recommendations in this report. It should be noted that the expressions for unbonded slabs or beams without bonded reinforcement are given for comparison only with the expressions for unbonded slabs or beams with bonded reinforcement . This is because, in practice, only unbonded systems with bonded reinforcement are designed and constructed ; systems without bonded steel are not used.

RECOMMENDATION 1

Recommendation 1 is derived from Figure 9.1 where all experimental data obtained from tests in China and at the University of Canterbury are plotted on the graph of tendon stress increase at failure versus combined reinforcement index.

The recommended expressions are as follows : -

(A) Unbonded member with bonded reinforcement.

(a) For value of q_0 between and equal to 0.06 and 0.305

$$f_{su} = f_{se} + 620 - 1430 q_0 \quad (\text{MPa}) \quad (9.1)$$

(b) For value of q_0 greater than 0.305

$$f_{su} = f_{se} + 180 \quad (\text{MPa}) \quad (9.2)$$

(B) Unbonded member without bonded reinforcement.

For value of q_0 between 0.1 and 0.26

$$f_{su} = f_{se} + 180 \text{ (MPa)} \quad (9.2)$$

The proposed design equations are lower bounds to all experimental data plotted. We can find that the experimental tendon stress increase results of all members with bonded reinforcement are much greater than those obtained from members without bonded reinforcement for the same combined reinforcement index values. It is therefore more economical, reliable and efficient to always use bonded reinforcement when designing beams or slabs with unbonded prestressing tendons.

The ultimate moment is expressed by :-

$$M_u = A_{ps} f_{su} (d_p - \beta_1/2) + A_s f_y (d_s - \beta_1 C/2) \quad (9.3)$$

Where

$$\beta_1 C = (A_{ps} f_{su} + A_s f_y) / (\epsilon_1 b f'_c) \quad (9.4)$$

$$\epsilon_1 = [\epsilon_{ct}/\epsilon_{cs} - 1/3 \times (\epsilon_{ct}/\epsilon_{cs})^2] / [(6 - 2 \times \epsilon_{ct}/\epsilon_{cs}) / (4 - \epsilon_{ct}/\epsilon_{cs})] \quad (9.5)$$

$$\epsilon_{cs} = 2 \times f'_c / E_c \quad (9.6)$$

Collins' (1983) expressions 9.3 to 9.6 are proposed instead of equations 3.1c and 3.1d of ACI 318-83 (1983) code expressions because Collins' (1983) expressions give better agreement with results for all unbonded beams and slabs tested as shown in Tables 9.1 and 9.2. Also shown is that the ultimate moment capacity calculated by the proposed equations 9.1 or 9.2 with Collins' equations give less conservative results than that obtained by ACI 318-83 (1983) code expressions for all unbonded beams and slabs tested. Tables 9.3, 9.4 and

9.5 show that the values of mean and standard deviation of $M_u(\text{Recommendation 1}) / M_u(\text{experimental})$ ratios for all beams and slabs are better than $M_u(\text{ACI 318-83})/M_u(\text{experimental})$ ratios .It is shown in Table 9.6 that all ultimate tendon stress values calculated using proposed design equation 9.1 or 9.2 give less conservative results than the values calculated using ACI 318-83 (1983) equations 3.1a and 3.1b. Similarly the values of mean and standard deviation of $f_{su}(\text{proposed equations 9.1 or 9.2})/f_{su}(\text{experimental})$ ratios for all beams and slabs tested are also better than $f_{su}(\text{ACI 318-83})/f_{su}(\text{experimental})$ ratios as shown in Table 9.5, 9.7 and 9.8 . Hence Recommendation 1 give less conservative, but safe, results for all beams and slabs tested than those obtained by ACI 318-83 (1983) code expressions.

RECOMMENDATION 2

The proposed design expression for Recommendation 2 , is obtained from Figure 9.2 where all experimental data are plotted in the graph of $M_u/bd^2f'_c$ versus combined reinforcement index. It should also be noted that the design expression for an unbonded member without bonded reinforcement is included just for comparison and is not recommended for design practice.

The proposed design equations are as follows :-

(A) Unbonded member with bonded reinforcement

(a) For values of q_o between and equal to 0.06 and 0.42

$$M_u = (0.5542 \times q_o + 0.008) \times b d^2 f'_c \quad (9.7)$$

(b) For values of q_o greater than 0.42

$$M_u = 0.24 \times b d^2 f'_c \quad (9.8)$$

(B) Unbonded member without bonded reinforcement

For value of q_0 between 0.1 and 0.26

$$M_u = (0.448 \times q_0 + 0.008) \times b d^2 f_c \quad (9.9)$$

The above design expressions are also lower bounds to all the experimental data plotted. Recommendation 2 is easier and simpler to use in design than Recommendation 1, where the ultimate moment capacity can be obtained directly without going through the calculation for the ultimate tendon stress of prestressing steel. The ultimate moment of any unbonded member with known dimension and any q_0 values greater than 0.06 can be obtained from equations 9.7 to 9.9 or by just reading the graph plotted in Figure 9.2.

The values of ultimate moment capacity of Recommendation 2 are less conservative than those obtained using ACI 318-83 code expressions and Recommendation 1 proposed expressions for slabs tested in the University of Canterbury as shown in Tables 9.2 and 9.4 but more conservative results for beams tested in China, as shown in Tables 9.1 and 9.3. But Table 9.5 shows that the mean value of $M_u(\text{Recommendation 2})/M_u(\text{experimental})$ ratio for all beams and slabs tested is better than $M_u(\text{ACI 318-83})/M_u(\text{experimental})$ ratio. Hence as a whole, Recommendation 2 gives less conservative results than those obtained by ACI 318-83 (1983) code expressions

GENERAL RECOMMENDATION

It is recommend for designers to use q_0 values between 0.06 and 0.3. The reason is if q_0 is too small, flexural instability will set in and if the q_0 values are too large a compression failure will occur which means the increase in tendon stress is too small for efficient and economical unbonded system design. It is also recommended that the minimum amount of non-tensioned bonded reinforcement should be provided to eliminate flexural instability and at the same time increase the flexural strength to 1.2 times the cracking moment as required by ACI 318-77 (1977). Unbonded members without bonded steel do not perform well as shown in Figures 9.1 and 9.2 and hence is not recommended as a practical design.

FIGURE 9.1: TENDON STRESS INCREASE AT FAILURE VS COMBINED REINFORCEMENT INDEX

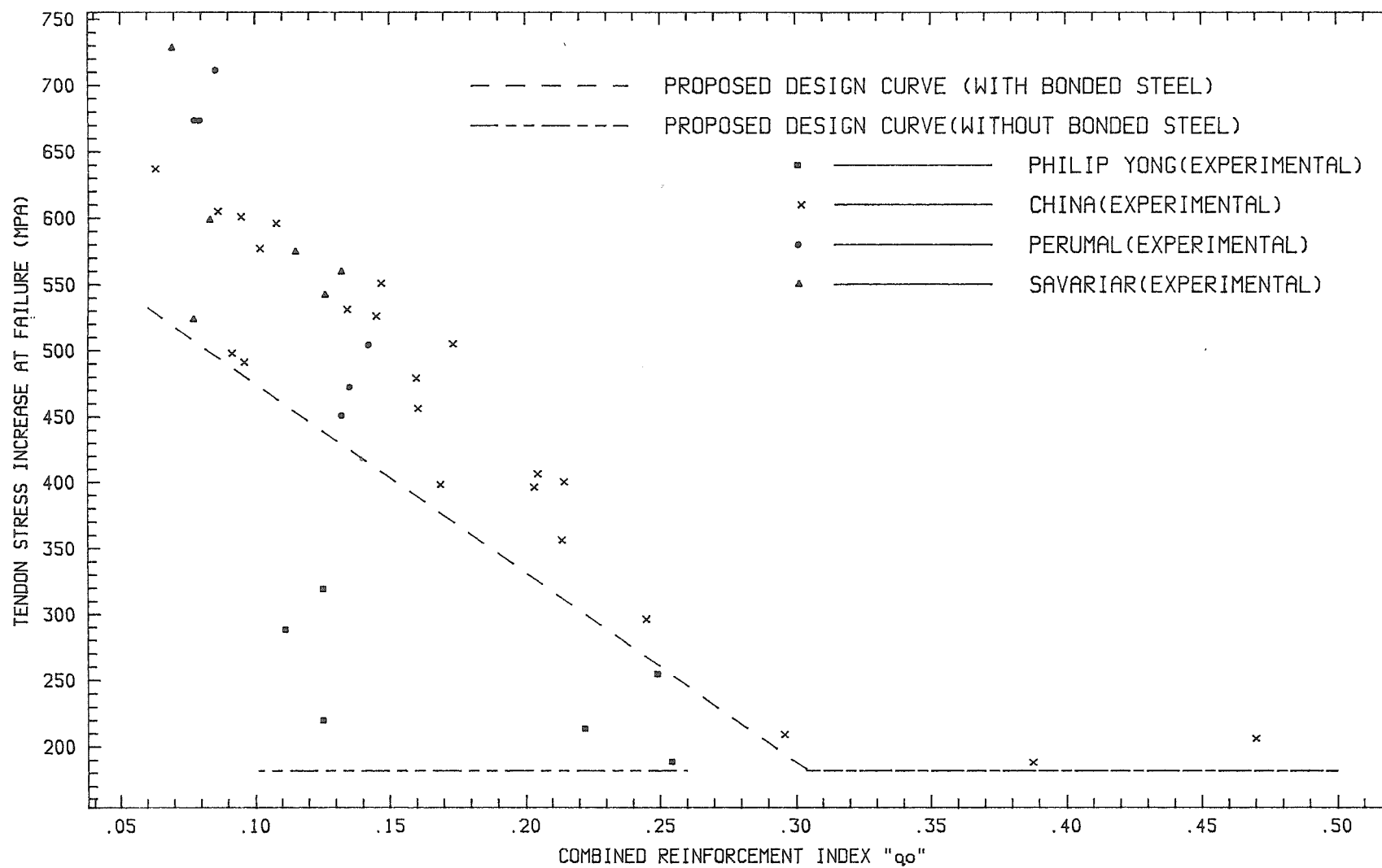


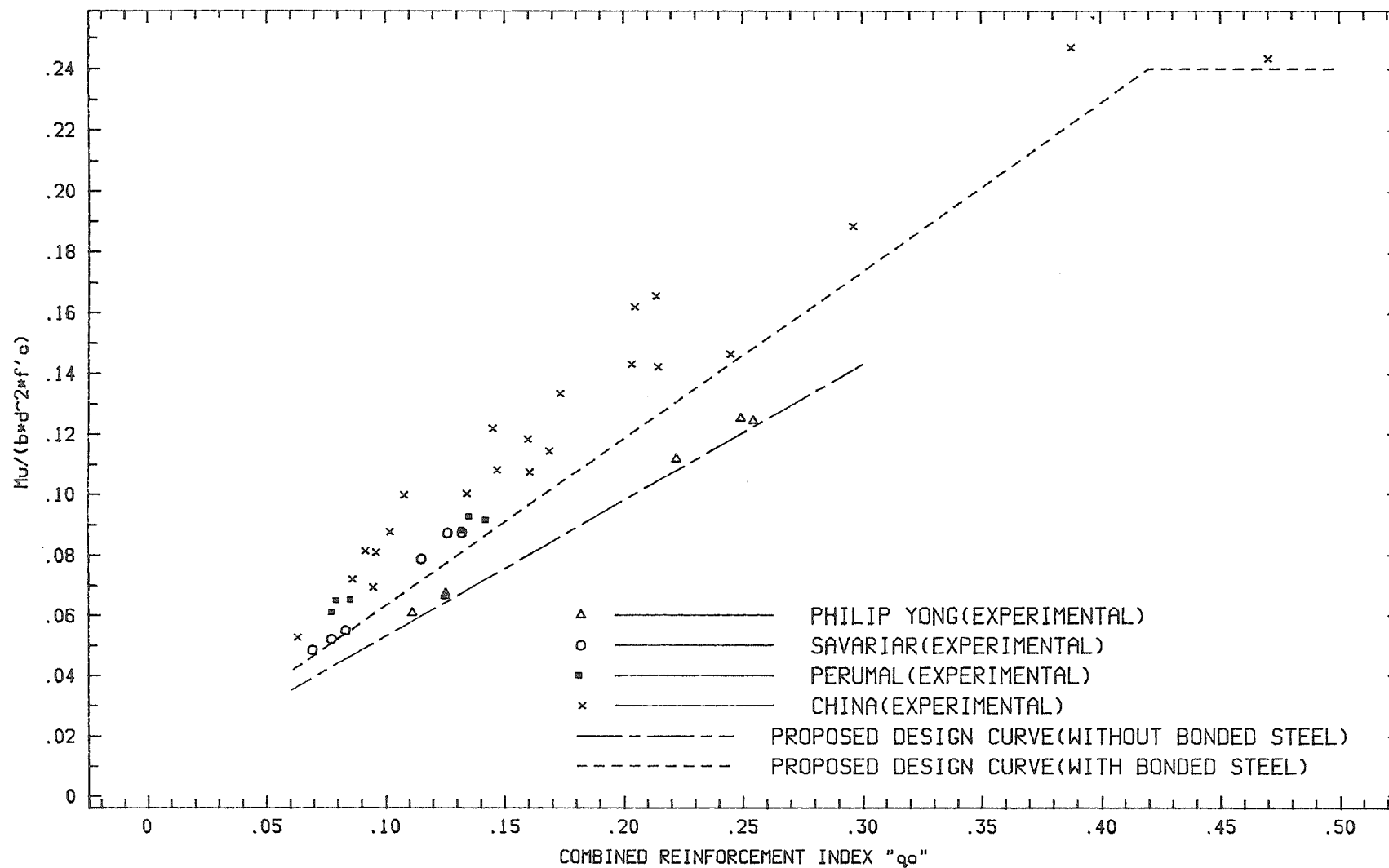
FIGURE 9.2: THE GRAPH OF $M_u/(b*d^2*f'_c)$ VS COMBINED REINFORCEMENT INDEX

TABLE 9.1

**COMPARISON BETWEEN EXPERIMENTAL AND PREDICTED
ULLTIMATE MOMENT OF RESISTANCE BY ACI 318-83
AND PROPOSED DESIGN EQUATIONS.**

	Mu	Mu	Mu	Mu	Mu
beam	experimental	ACI318-83	proposed eqns 9.1 or 9.2 with ACI eqns	proposed eqns 9.1 or 9.2 with Collins' eqns (Recom 1)	proposed eqn 9.7 or 9.8 (Recom 2)
	(KNm)	(KNm)	(KNm)	(KNm)	(KNm)
A1	31.1	25.2	27.18	27.4	22.5
A2	46.8	36.61	40.58	40.9	33.82
A3	63.6	50.8	55.07	55.8	48.34
A4	38.3	29.24	31.26	31.75	25.91
A5	51.2	43.38	45.55	45.98	39.84
A6	72.4	66.5	67.71	68.81	65.81
A7	41.5	37.88	38.31	38.59	34.16
A8	59.4	54.3	54.68	55.12	49.95
A9	102.5	90.05	90.68	92.62	92.22
B1	30.3	26.77	28.92	28.97	24.53
B2	50.4	40.38	44.77	44.84	36.94
B3	61.0	57.56	60.17	60.24	53.98
B4	38.4	32.63	34.57	34.65	29.6
B5	53.4	48.12	48.83	48.98	43.79
B6	75.8	71.42	74.31	74.68	67.4
B7	42.5	39.52	41.11	41.14	36.89
B8	63.1	57.44	58.03	58.24	51.33
B9	89.7	89.2	89.34	89.5	87.68
C1	33.6	28.59	30.93	31.07	25.32
C3	67.3	49.8	54.22	54.89	50.25
C7	44.6	44.25	44.39	44.5	40.09
C9	101.0	100.25	100.62	100.8	99.65

where : Recom = recommendation

TABLE 9.2

COMPARISON BETWEEN EXPERIMENTAL AND PREDICTED
ULTIMATE MOMENT OF RESISTANCE BY ACI 318-83
AND PROPOSED DESIGN EQUATIONS.

slab	Mu experimental (KNm)	Mu ACI318-83 (KNm)	Mu proposed eqns 9.1 or 9.2 with ACI eqns (KNm)	Mu proposed eqns 9.1 or 9.2 with M.Collin eqns (Recom 1) (KNm)	Mu proposed eqn 9.7 or 9.9 (Recom 2) (KNm)
HUB3	52.75	37.4	39.34	39.5	41.83
HUB4	73.59	56.07	62.47	62.93	69.51
HUB5	52.78	37.16	39.16	39.32	44.38
HUB6	78.47	57.79	64.31	64.75	71.96
HUB7	53.47	37.81	39.68	39.84	44.3
HUB8	80.46	57.5	64.06	64.5	71.68
YUB3	42.3	32.55	34.94	35.08	40.31
YUB4	66.08	47.64	55.30	55.64	60.06
YUB5	42.42	33.01	35.49	35.63	41.21
YUB6	68.33	47.47	54.79	55.18	60.79
YUB7	41.87	32.73	35.29	35.45	40.87
YUB8	63.67	46.26	53.34	53.79	58.98
UB1	42.83	35.01	38.73	37.76	41.92
UB2	45.73	38.29	40.57	40.86	44.0
UB4	44.0	36.73	38.12	38.6	42.28
UB5	47.71	41.07	41.28	41.5	45.36
UB7	44.11	35.91	37.36	37.94	42.11
UB8	47.38	40.77	41.29	41.6	45.03

where : Recom = Recommendation

TABLE 9.3

COMPARISON BETWEEN EXPERIMENTAL AND PREDICTED
 ULTIMATE MOMENT OF RESISTANCE BY ACI 318-83 (1983)
 , RECOMMENDATION 1 AND 2 .

beam	Mu(ACI)/Mu(expt)	Mu(Recom1)/Mu(expt)	Mu(Recom2)/Mu(expt)
A1	0.810	0.881	0.723
A2	0.782	0.874	0.723
A3	0.799	0.877	0.760
A4	0.763	0.829	0.677
A5	0.847	0.898	0.778
A6	0.918	0.950	0.909
A7	0.913	0.930	0.823
A8	0.914	0.928	0.841
A9	0.878	0.904	0.900
B1	0.883	0.956	0.810
B2	0.8021	0.890	0.733
B3	0.944	0.988	0.885
B4	0.849	0.902	0.771
B5	0.901	0.917	0.820
B6	0.942	0.985	0.890
B7	0.929	0.968	0.868
B8	0.910	0.923	0.813
B9	0.944	0.988	0.977
C1	0.851	0.925	0.754
C3	0.740	0.816	0.747
C7	0.992	0.998	0.900
C9	0.992	0.998	0.987
mean	0.880	0.924	0.822
standard deviation	0.074	0.052	0.084

NOTE : Recom = Recommendation , ACI = ACI 318-83 (1983)

TABLE 9.4

COMPARISON BETWEEN EXPERIMENTAL AND PREDICTED
ULTIMATE MOMENT OF RESISTANCE BY ACI 318-83 (1983)
, RECOMMENDATION 1 AND 2

beam	Mu(ACI)/Mu(expt)	Mu(Recom1)/Mu(expt)	Mu(Recom2)/Mu(expt)	
HUB3	0.709	0.749	0.793	
HUB4	0.762	0.855	0.944	
HUB5	0.704	0.745	0.841	
HUB6	0.736	0.825	0.917	
HUB7	0.707	0.745	0.829	
HUB8	0.715	0.802	0.891	
YUB3	0.770	0.829	0.953	
YUB4	0.721	0.842	0.909	
YUB5	0.778	0.840	0.971	
YUB6	0.695	0.808	0.890	
YUB7	0.782	0.847	0.976	
YUB8	0.726	0.845	0.926	
UB1	0.817	0.882	0.979	
UB2	0.837	0.894	0.962	
UB4	0.835	0.877	0.961	
UB5	0.861	0.870	0.951	
UB7	0.814	0.860	0.955	
UB8	0.860	0.878	0.950	
mean	0.768	0.883	0.922	
standard				
deviation	0.057	0.046	0.054	

NOTE : Recom = Recommendation , ACI = ACI 318-83 (1983)

TABLE 9.5

COMPARISON BETWEEN EXPERIMENTAL AND PREDICTED
MEAN AND STANDARD DEVIATION FOR ALL
UNBONDED BEAMS AND SLABS

	Mean	Standard Deviation
Mu(ACI 318-83)/Mu(expt)	0.829	0.87
Mu(Recommendation 1)/Mu(expt)	0.883	0.067
Mu(Recommendation 2)/Mu(expt)	0.867	0.087
$f_{su}(ACI\ 318-83)/f_{su}(expt)$	0.844	0.065
$f_{su}(\text{proposed Eqn 9.1 or 9.2})/f_{su}(expt)$	0.940	0.036

where : expt = experimental , Eqn = Equation

TABLE 9.6

COMPARISON BETWEEN EXPERIMENTAL AND PREDICTD
INCREASE IN TENDON STRESS AT FAILURE .

beam or slab	f_{su} (experimental) (Mpa)	f_{su} (ACI 318-83) (Mpa)	f_{su} (proposed equation 9.1 or 9.2) (Mpa)
A1	1458	1212	1447.2
A2	1430	1083	1314.36
A3	1176	958	1132.27
A4	1465	1121	1332.77
A5	1315	1016	1179.69
A6	1063	992	1048.3
A7	1436	1230	1293.1
A8	1290	1181	1220.87
A9	1108	1065	1101
B1	1645	1351.2	1536.07
B2	1564	1220.6	1459.08
B3	1361	1127.4	1339.3
B4	1645	1363.4	1534.85
B5	1520	1248.5	1299.98
B6	1402	1179.8	1312.98
B7	1603	1272.3	1484.53
B8	1490	1331.64	1391.17
B9	1346	1294.4	1317.45
C1	1465	1176.9	1385.67
C3	1231	969.8	1150
C7	1411	1322.1	1343.45
C9	1109	1047.8	1084
UB1	1351	1246.65	1343.5
UB2	1365	1244.66	1326.3
UB4	1376	1283.69	1343.5
UB5	1442	1327.23	1334.9
UB7	1418	1279.32	1344.6
UB8	1487	1330.3	1348.9
YUB3	1806.3	1413.6	1597.49
YUB4	1520.5	1126	1399.62
YUB5	1663.5	1457.5	1647.84
YUB6	1498.8	1129.3	1394.57
YUB7	1742.4	1444.2	1643.14
YUB8	1490.5	1096.4	1355.98
HUB3	1912.9	1566	1731.38
HUB4	1609.4	1280.6	1519.86
HUB5	1931.8	1546.51	1716.78
HUB6	1588	1324	1566.3
HUB7	1886	1587.36	1747.14
HUB8	1609.4	1321.18	1561.98

TABLE 9.7

**COMPARISON BETWEEN EXPERIMENTAL AND PREDICTED
INCREASE IN TENDON STRESS AT FAILURE**

beam	$f_{su}(ACI\ 318-83)/f_{su}(expt)$	$f_{su}\ (proposed\ eqn\ 9.1\ or\ 9.2)/f_{su}(expt)$	
A1	0.831	0.993	
A2	0.757	0.919	
A3	0.815	0.963	
A4	0.765	0.910	
A5	0.773	0.897	
A6	0.933	0.986	
A7	0.857	0.900	
A8	0.915	0.946	
A9	0.961	0.994	
B1	0.821	0.934	
B2	0.780	0.933	
B3	0.828	0.984	
B4	0.829	0.933	
B5	0.821	0.855	
B6	0.841	0.936	
B7	0.794	0.926	
B8	0.894	0.885	
B9	0.962	0.979	
C1	0.803	0.946	
C3	0.788	0.934	
C7	0.937	0.952	
C9	0.945	0.977	
mean	0.848	0.940	
standard			
deviation	0.067	0.038	

where : expt = experimental eqn = equation

TABLE 9.8

COMPARISON BETWEEN EXPERIMENTAL AND PREDICTED
INCREASE IN TENDON STRESS AT FAILURE

beam	$f_{su}(ACI\ 318-83)/f_{su}(expt)$	$f_{su} (proposed\ eqn\ 9.1\ or\ 9.2)/f_{su}(expt)$	
UB1	0.923	0.994	
UB2	0.912	0.972	
UB3	0.933	0.976	
UB5	0.920	0.926	
UB7	0.902	0.948	
UB8	0.895	0.907	
YUB3	0.783	0.884	
YUB4	0.740	0.920	
YUB5	0.876	0.991	
YUB6	0.753	0.930	
YUB7	0.829	0.943	
YUB8	0.736	0.910	
HUB3	0.819	0.896	
HUB4	0.796	0.944	
HUB5	0.801	0.889	
HUB6	0.834	0.986	
HUB7	0.842	0.926	
HUB8	0.821	0.971	
mean	0.840	0.940	
standard			
deviation	0.064	0.035	

where : expt = experimental eqn = equation

SUMMARY, CONCLUSIONS AND SUGGESTIONS FOR FUTURE RESEARCH

10.1 SUMMARY

A computer programme written by Chan (1986) was modified in order to carry out the analysis more efficiently and effectively while still maintaining the required accuracy. The computer analysis was used to carry out an analysis of the behaviour of twenty-two unbonded partially prestressed concrete beams tested by Du and Tao (1986) in China and eighteen unbonded slabs tested by Savariar (1984), Perumal (1986) and Yong (1980) at the University of Canterbury. Of these, only six of them tested by Yong (1980) were constructed without bonded reinforcement.

The modified program maintains the basic assumptions made by Chan (1986) whilst Collins' flexural theory is used to give a first estimation of neutral axis depth at a section. The beam or slab is divided span-wise. External moments from load calculated for each section are matched with internal moments tabulated in the order of increasing moment for a particular level of prestressing force. Interpolation between values in the table is used to obtain the values required for equilibrium. Appropriate prestressing stress-strain curves were used in the computer analysis and are represented by a series of straight lines giving a best fit to the prestressing curves. Prestressing stress-strain curves obtained for Perumal (1986), Savariar (1984) and Yong (1980) were typical curves obtained from testing. Typical experimental prestressing stress-strain curves for unbonded beams tested by Du and Tao (1984) were not given. Hence prestressing curves for the Chinese, groups A or C and B were obtained by adjusting either typical stress-strain curve for 6.35mm diameter wire or Savariar's (1984) prestressing curve for 12.5mm diameter strand respectively according to the values of 0.2 % proof stress and ultimate prestressing strength given.

All analytical results were compared with experimental results and those predicted by different code expressions. Experimental data from the University of Canterbury and China which consist of a wide range of combined reinforcement index values and span-depth ratios were plotted together in graphical form in order to find new design equations which give less conservative, although safe results compared to results using the existing code expressions.

Two recommendations have been proposed based on the lower bounds of the experimental data . Recommendation 1 is based on the graph of tendon stress increase at ultimate versus combined reinforcement index and the ultimate moment is calculated using Collins' (1983) flexural expressions. Recommendation 2 was obtained from the graph of $M_u / bd^2f'_c$ versus combined reinforcement index and the ultimate moment is obtained directly in this case.

10.2 CONCLUSIONS

From a study of the results of the computer analyses and experimental results carried out in this project, the following conclusions can be drawn :-

- (1) It was found that the combination of some important parameters have a very significant effect on the tendon stress increase at ultimate and ultimate moment capacity of unbonded concrete members with or without bonded reinforcement. The separate parameters are the initial effective prestress , the quantity of prestressing reinforcement, the quantity of non-prestressing reinforcement, and the material characteristics . These are combined to form the combined reinforcement index.
- (2) All experimental results obtained from the University of Canterbury and the Chinese tests cover a wide range of span-depth ratios. These results agree well together in the graph of tendon stress increase at ultimate versus combined reinforcement index. A reasonable linear relationship is obtained. This indicates that the effect of span-depth ratio on tendon stress increase at ultimate is not significant. This is further shown by the graphs of increase in tendon stress at ultimate versus span-depth ratio which do not show specific trends or relationships.
- (3) It was found that Collins' expressions give better results for ultimate moment than those obtained by the ACI 318-83 (1983) code expressions after obtaining the ultimate tendon stress from the proposed equation 9.1 or 9.2 .
- (4) All analytical curves for the Chinese unbonded beams of group A, B, and C exhibit two or three distinctive stages for value of q_0 greater than and less than 0.305 respectively agreeing with the experimental data. This indicates that the computer analysis gives a good representation of actual flexural behaviour for all unbonded partially prestressed beams tested by Du and

Tao (1984). It also shows that compression failure might have occurred which causes the increase in tendon stress at failure to remain roughly constant for values of q_0 greater than 0.305 .

- (5) The modified computer program has been successful in carrying out all the analysis more effectively and efficiently than the program of Chan (1986) and still give as good or better results.
- (6) From the good comparison between analytical and experimental data especially for unbonded partially prestressed beams, we can deduce that the computer program can be further developed to analyse the flexural behaviour of unbonded systems under different forms of loading and unbonded partially prestressed multi-span concrete members.
- (7) From Table 9.5 we can conclude that both Recommendation 1 and 2 give less conservative results than ACI 318-83 (1983) code expressions for unbonded beams or slabs . Hence recommendation 1 and 2 are proposed for the design of unbonded partially prestressed concrete members.
- (8) The value of q_0 used should be between 0.06 and 0.305 for effective design and for preventing the occurrence of flexural instability or compression failure.
- (9) Unbonded concrete members with bonded reinforcement give much better results than the members without bonded reinforcement.

10.3 SUGGESTIONS FOR FUTURE RESEARCH

In view of the recommendations proposed, it would be worth while studying the various factors affecting the proposed design expressions such as :-

- (1) The effect of breadth to depth ratio on the proposed expressions recommended.
- (2) The safe value of combined reinforcement index to be used without causing flexural instability. More tests might have to be done for unbonded member with q_0 values less than 0.06.

- (3) The largest value of q_0 which can be used to avoid a compression failure and inefficient design.
- (4) The earthquake resistant behaviour of unbonded systems.
- (5) The influence of the form of loading on the behaviour of unbonded system.
- (6) The flexural behaviour of unbonded partially prestressed multi-span concrete members.

REFERENCES

- ACI-COMMITTEE 318 (1963). Building Code Requirements for Reinforce Concrete, American Concrete Institute, Detroit, Michigan.
- ACI Standard 318-77 (1977). Building Code Requirements for Reinforced concrete, American Concrete Institute, Detroit, Michigan.
- ACI 318-83 (1983). Proposed Revisions to Building Code Requirements for Reinforced Concrete (ACI 318-77) and Commentary to Building Code Requirements for Reinforced Concrete (ACI 318-77), Concrete International, Nov. 83, Vol. 4, No. 11 .
- ARTHUR E.ANDREW (1987). "Unbonded tendons in post-tensioned construction. "
- AS 1431- 1378 (1978). SSA Concrete Structure code, Australia, Standard 1481-1978.
- British Standard Code of Practice for the Structural Use of Concrete (1972). Part 1. Design, Materials and Workmanship, CP 110 .
- CEP -FIP Model Code for Concrete Structures (1978). Third Edition, CEB, Paris.
- CHAN YAN KIT, N. COOKE, R. PARK (1986). "Theoretical Analysis of flexural strength and behaviour of unbonded partially prestressed concrete slabs with and without bonded reinforcement. " M.E. Research Report 86. Department of Civil Engineering , University of Canterbury, Christchurch, New Zealand.
- COLLINS, M.P. (1983). " Prestressed Concrete Structures", A Post-graduate course at the University of Canterbury, May- August 1983 . pp 3-40 - 3.47.
- Design of Post-tensioned slabs (1977) . Post-Tensioning Institute, First Edition.
- DU GONG, TAO XUEKANG (1987). "Research and application of unbonded tendon for partially prestressed concrete structures in China" FIP NOTES, Quarterly Journal of the Federation Internationale de la Precontrainte 1987/3 , pp 10 - 14 .
- DU GONG, TAO XUEKANG (1984). " Ultimate Stress in Unbonded Tendons of Partially Prestressed Concrete Beams". Institute of Building Structures, China Academy of Building Research Beijing, China.
- ESI ENGINEERING SERVICES INC (1971) . A post-earthquake survey of structures post-tensioned with the Atlas unbonded strand system, Los Angeles .
- FIP (1980) Recommendations for the design of flat slabs in post-tensioned concrete (using bonded and unbonded tendons). May 1980.
- G. IVANYI W.BUSCHMEYER AND R.A. MULLER (1985). "Additional strains in unbonded tendons during loading". Magazine of Concrete Research Volume 37, No. 130, March 1985, pp 39 - 43 .

- NZS 3101 (1982). Part 1 and 2, " Code of Practice for the Design of Concrete Structures ", Standard Association of New Zealand , Wellington .
- PANNELL, F.N. (1969). " The Ultimate Moment of resistance of Unbonded Prestressed Concrete Beams ", Magazine of Concrete Research , Vol. 21, No. 6 March 1969.
- PCI MANUAL (1973) on design of connections for precast prestressed concrete. First Edition.
- PERUMAL , V. , COOKE, N. , PARK, R. , "Flexural Strength and Behaviour of Unbonded Prestressed Concrete Slabs With Bonded Reinforcement" M.E. Research Report, Department of Civil Engineering, University of Canterbury, Christchurch, New Zealand.
- SAVARIAR, V.J. , COOKE, N. , PARK, R. (1984). " Flexural Behaviour and Strength of Unbonded Prestressed Concrete Slabs with Bonded Reinforcement ". M.E. Research Report, Department of Civil Engineering, University of Canterbury, Christchurch, New Zealand.
- TAM , A. PANNELL, F.N. (1976). " The Ultimate Moment of Resistance of Unbonded Partially Prestressed Reinforced Concrete Beam ", Magazine of Concrete Research, Vol. 28, No. 97, December 1976.
- The Design of Post-tensioned Concrete flat slabs in building (1974).
Recommendations of the Concrete Society Working Party on Post-tensioned flat slabs, Technical Report.
- WARWARUK, J. , SOZEN, M.A. , AND SEISS, C.P. (1962). "Strength and Behaviour in Flexure of Prestressed Concrete Beams ", Bulletin 464, Engineering Experimental Station, University of Illinois, Urbana, Aug. 1962.
- W. WUTHRICH (1982) . "Post-tensioned concrete flat slabs in building design and construction - the support-strip method " The Ninth International Congress of the FIP , Stockholm , June 6-10 1982.
- YONG MIN FUI, P. , COOKE, N. , PARK, R. (1980). " The Use of Unbonded Tendons in Design of Prestressed Concrete Beams and Slabs ". M.E. Research Report 80-15, Department of Civil Engineering, University of Canterbury, Christchurch, New Zealand.

APPENDIX

A

NOTATION

AR	= Cross sectional area (mm ²)
AMD	= Average dead load moment (N. mm)
APS	= Area of unbonded prestressing steel (mm ²)
B	= Overall width (mm)
BECP	= Augmented concrete strain
BEZ	= Width of effective embedment zone (mm)
C	= Concrete compression force (N)
CCT	= Top fibre concrete strain
D	= Interval between each section (mm)
DIS	= Half span length (mm)
DPS	= Effective depth of prestressing steel (mm)
DRS	= Effective depth of bonded reinforcement (mm)
DTEZ	= Depth to the top of effective embedment zone (mm)
DBEZ	= Depth to bottom of effective embedment zone (mm)
DECP	= Initial concrete strain due to prestress alone
EB	= Bottom fibre concrete strain
EC	= Concrete modulus of elasticity (MPa)
ECC	= Eccentricity (mm)
ECT	= Top fibre of concrete strain
ECB	= Bottom fibre concrete strain
ECP	= Average concrete strain at prestressing steel level
ESH	= Strain hardening modulus (MPa)
EST	= Prestressing strain
ESP	= Modulus of elasticity for prestressing steel (MPa)
ETH	= Internal concrete top strain
ET	= Top fibre concrete strain
ETMAX	= Maximum specified concrete top strain
ETMIN	= Minimum specified concrete top strain
FC	= 28 Days concrete cylinder strength (MPa)
FY	= Philip Yong (1980)
FP1	= Prestressing stress
FCR	= Cracking strain
FSU	= Ultimate tensile strength of steel
FPI1	= Initial prestressing steel
H	= Overall depth
INC	= Increment for bottom strain
IEST	= Initial prestressing strain
IDEF	= Deflection due to initial prestress
L	= Overhang length (mm)

LA	= Line of action (mm)
LAA	= Length of applied load from support (mm)
LBB	= Length of applied load from support (mm)
LPS	= Specified limit for the average concrete strain
MH(JJ)	= Internal moment (N. mm)
MP	= Specified maximum prestressing force (N)
M(I)	= External moment (N.mm)
MLIM	= Specified limit for moment equilibrium (N.mm)
NINT	= No of specified top strain internal
NS	= Number of section to be analysed
PT	= Total Strain over the length
P(R)	= Prestressing force (N)
PHI	= Curvature
PH(JJ)	= Curvature
PIN	= Initial prestressing force (N)
PINC	= Prestressing force increment (N)
Q	= Concrete strain at the level of prestressing steel
RT	= Resultant of curvature at support for half span
S	= Span (mm)
SM	= Section of modulus (mm ³)
SV	= Savariar (1984)
SSH	= Steel strain at commencement of strain hardening
SSU	= Steel strain corresponding to FSU
T1	= Concrete tensile force (N)
T2	= Embedment tensile force
T3	= Reinforcing steel tensile force (N)
TEN	= Total tensile force (N)
TDEL	= Total deflection at mid-span (mm)
TINC	= Top fibre strain increment
VM	= Perumal (1986)
W	= External applied load (N)
WINC	= Load increment (N)
X	= Depth to crack (mm)
X1	= Neutral axis depth (mm)
XB	= Centroid for the section
YRS	= Yield stress of reinforcing steel (MPa)
ZM	= Section of modulus (MPa)

APPENDIX

B

```

100 REM %%%%%%%%%%
110 REM %%%%%%%%%%
120 REM ##### THEORETICAL ANALYSIS FOR UNBONDED #####
130 REM ##### PRESTRESSED CONCRETE SLAB #####
140 REM ##### WITH AND WITHOUT BONDED REINFORCEMENT #####
150 REM ##### (THIRD POINT LOADING ONLY) #####
160 REM %%%%%%%%%%
170 REM %%%%%%%%%%
180 DIM XB(150),P(150),TDEL(150),CCT(150),PHI(150),Q(150),ETH(150)
190 DIM MH(150),GH(150),W(150),RA(150),MW(150),PH(150)
200 OPEN "UNBOND.LIS" FOR OUTPUT AS FILE #1
210 OPEN "UNBOND.DAT" FOR INPUT AS FILE #2
220 INPUT #2,N$
230 INPUT #2,PIN
240 INPUT #2,W(O)
250 INPUT #2,WIN
260 INPUT #2,STP
270 INPUT #2,MP
280 INPUT #2,PINC
290 INPUT #2,LAA
300 INPUT #2,LBB
310 INPUT #2,L
320 INPUT #2,B
330 INPUT #2,H
340 INPUT #2,BEZ
350 INPUT #2,DTEZ
360 INPUT #2,DBEZ
370 INPUT #2,DRS
380 INPUT #2,ARS
390 INPUT #2,APS
400 INPUT #2,YRS
410 INPUT #2,Z$
420 INPUT #2,FC
430 INPUT #2,NS
440 INPUT #2,DPS
450 INPUT #2,ETMAX
460 INPUT #2,ETMIN
470 INPUT #2,NINT
480 S=LAA+LBB \ R=0
490 P(R)=STP \ N=0
500 PRINT #1," *****"
510 PRINT #1," *****"
520 PRINT #1," ***** THEORETICAL ANALYSIS FOR UNBONDED *****"
530 PRINT #1," ***** PRESTRESSED CONCRETE SLAB *****"
540 PRINT #1," ***** WITH AND WITHOUT BONDED REINFORCEMENT *****"
550 PRINT #1," *****"
560 PRINT #1," *****"
570 PRINT #1,"UNBONDED SLAB",N$
580 PRINT #1
590 IF Z$="N" THEN PRINT #1, "LONG TERM LOADING"
600 IF Z$="Y" THEN PRINT #1, "SHORT TERM LOADING"
610 PRINT #1
620 PRINT #1, "THIRD POINT LOADING"
630 PRINT #1
640 PRINT #1,"Overall width & height (mm) =" ;B,H
650 PRINT #1,"Applied load from support (mm) =" ;LAA,LBB
660 PRINT #1,"Span length (mm) =" ;S

```

```

580 PRINT #1,"Overhang length                      (mm) =" ;L
590 PRINT #1,"Embedment width & depths (mm)=" ;BEZ,DTEZ,OBEZ
600 PRINT #1,"                ,,              ,,,      Bonded             ,,   (mm)=" ;DRS
610 PRINT #1,"Area of re-bars                         (mm^2)=" ;ARS
620 PRINT #1,"Area of prestressing steel               (mm^2)=" ;APS
630 PRINT #1,"28 day cylinder strength fc'            (MPa)=" ;FC
640 PRINT #1,"Yield stress of re-bars                 (MPa)=" ;YRS
650 PRINT #1
660 PRINT #1,"Initial prestressing force=" ;PIN
670 PRINT #1
680 PRINT #1,"@@@@@@@@@@@@@@@@@@@@@@@@@@@@@@@@@@@@@@@@@@@@@@@@@@@@@@@@@@@@@@@@@@@@@@@@@@@@@
@"
690 REM *****
700 REM **** AUGMENTED VALUE OF ECP ****
710 REM **** ALONG LENGTH=BECP ****
720 REM *****
730 AR=B*H \ SM=B*(H^2)/6
740 DL=24.OE-6*AR \ REA=(DL*S)/2
750 ZM=(B*(H^3))/(12*H*.5)
760 AMD=(2/3)*(DL*(S^2))/8
770 IF Z$="Y" THEN EC=4200*(FC^.5) ELSE EC=1500*(FC^.5)
780 IF Z$="Y" THEN ECR=7.27E-5 ELSE ECR=2.67E-5
790 ECS=(2*FC)/EC
800 REM *****
810 REM ***** PRESTRESSING STRESS AND *****
820 REM ***** PRESTRESSING STRAIN *****
830 REM *****
840 REM ***** ECCENTRICITY OF PRESTRESS*****
850 PINCCC=PINC
860 PINCC=PINC
870 ECC=DPS-H/2
880 WINC=WIN
890 WINCC=WIN
900 FP1=P(R)/APS \ FPI1=PIN/APS \ ESP=205000
910 IF FPI1>1307.3 THEN GO TO 940
920 IEST=FP1/186757.14
930 GO TO 1100
940 IF FPI1>1400 THEN GO TO 970
950 IEST=(FPI1-658.4)/92700
960 GO TO 1100
970 IF FPI1>1493.6 THEN GO TO 1000
980 IEST=(FPI1-1025.6)/46800
990 GO TO 1100
1000 IF FPI1>1620.9 THEN GO TO 1030
1010 IEST=(FPI1-1366.3)/12730
1020 GO TO 1100
1030 IF FPI1>1695.9 THEN GO TO 1060
1040 IEST=(FPI1-1470.9)/7500
1050 GO TO 1100
1060 IF FPI1>1745.9 THEN GO TO 1090
1070 IEST=(FPI1-1545.9)/5000
1080 GO TO 1100
1090 IEST=(FPI1-1657.7)/2205
1100 IF FPI1>1307.3 THEN GO TO 1130
1110 EST=FP1/186757.14
1120 GO TO 1410
1130 IF FP1>1400 THEN GO TO 1160
1140 EST=(FP1-658.4)/92700

```

```

1150 GO TO 1410
1160 IF FP1>1493.6 THEN GO TO 1190
1170 EST=(FP1-1025.6)/46800
1180 GO TO 1410
1190 IF FP1>1620.9 THEN GO TO 1220
1200 EST=(FP1-1366.3)/12730
1210 GO TO 1410
1220 IF FP1>1695.9 THEN GO TO 1250
1230 EST=(FP1-1470.9)/7500
1240 GO TO 1410
1250 IF FP1>1745.9 THEN GO TO 1280
1260 EST=(FP1-1545.9)/5000
1270 GO TO 1410
1280 EST=(FP1-1657.7)/2205
1290 REM *****
1390 REM ***** TO DETERMINE AUGMENTED CONCRETE STRAIN *****
1400 REM *****
1410 ECB=-((PIN/(AR*EC))-((PIN*ECC)/(SM*EC))+AMD/(SM*EC)
1420 ECT=-((PIN/(AR*EC))+((PIN*ECC)/(SM*EC))-AMD/(SM*EC)
1430 IF (ECT*ECB)<0 THEN 1460
1440 IF ABS(ECT)>ABS(ECB) THEN IECP=((H-DPS)*(ECT-ECB))/H)+ECB ELSE IECP=(DPS*E
CB/H)+ECT
1450 GO TO 1480
1460 XNX=(H*ECT)/(ECT+ECB)
1470 IECP=((XNX-DPS)*ECT)/XNX
1480 DECP=ABS(IECP)+IEST
1490 BECP=EST-DECP
1500 IF BECP>.001 THEN LPS=9.E-6 ELSE LPS=3.E-6
1510 NU=0
1520 REM *****
1530 REM ***** CALCULATE MOMENT AT EACH SECTION *****
1540 REM ***** MOMENT FOR THIRD POINT LOADING *****
1550 REM *****
1560 IF BECP<0 THEN WINC=5000
1570 D=(S*.5)/NS
1580 FOR I=0 TO NS
1590 V=(I-1)*D
1600 IF V<LAA THEN 1630
1610 MW(I)=.5*W(R)*LAA
1620 GO TO 1640
1630 MW(I)=.5*W(R)*V
1640 IF I<2 THEN MW(I)=0
1650 NEXT I
1660 REM *****
1670 REM ***** DEFLECTION DUE TO INITIAL PRESTRESS *****
1680 REM *****
1690 IDEF=(PIN*ECC(NS)*((S*.5)2*6)/(EC*B*(H3))
1700 REM @*****@
1710 REM @***** ANALYSIS STARTS FROM HERE *****@
1720 REM @*****@
1730 REM @*****@
1740 K=0 \ N=0
1750 TINC=1.25E-5 \ N=N+1 \ N1=0
1760 DLIM=3.5E-4*P(R) \ MLIM=3.5E-4*MW(K)
1770 ERAN=-(ETMAX-ETMIN)/NINT
1780 FOR JJ=0 TO NINT
1790 ESTR=ETMAX+JJ*ERAN
2000 ERAT=ESTR/ECS \ ERAT=ABS(ERAT)

```



```

2010 AB1=ERAT-(ERAT^2)/3
2020 IF AB1=0 THEN CZ=.95*H
2030 IF AB1=0 THEN 2050
2040 CZ=P(R)/(AB1*FC*B)
2050 PHI=-ESTR/CZ \ EB=ESTR+PHI*H \ ET=ESTR
2060 IF CZ>H THEN EB=-P(R)/(AR*EC)-(P(R)*ECC(K))/(SM*EC)+AMD/(SM*EC)
2070 INC=.001
2080 IF ET=0 THEN EB=-.5E-4
2090 REM *****CALCULATE THE LEVEL OF Ecr AND E=0 *****
2100 IF EB>ET THEN 2130
2110 PHI=- (EB-ET)/H \ X=(ECR-EB)/PHI \ X1=-EB/PHI
2120 GO TO 2140
2130 PHI=(EB-ET)/H \ X=(ECR-ET)/PHI \ X1=-ET/PHI
2140 IF X>H THEN 2150
2150 FCR=EC*ECR
2160 T1=.5*FCR*B*(X-X1)
2170 DT1=X1+(2*(X-X1)/3)
2180 IF DTEZ=0 THEN 2320
2190 IF X>DTEZ THEN 2260
2200 E3=ET+(PHI*DTEZ) \ E5=ET+(PHI*DBEZ)
2210 IF E3<0 THEN F3=FCR/(1+((-E3/5.0E-3)^.5)) ELSE F3=FCR/(1+((E3/5.0E-3)^.5))
2220 IF E5<0 THEN F5=FCR/(1+((-E5/5.0E-3)^.5)) ELSE F5=FCR/(1+((E5/5.0E-3)^.5))
2230 T2=.5*(F3+F5)*BEZ*(DBEZ-DTEZ)
2240 D4=DTEZ+((F3+2*F5)*(DBEZ-DTEZ)/(3*(F3+F5)))
2250 GO TO 2320
2260 D8=DBEZ-X
2270 E3=(DBEZ-X1)*EB/(H-X1)
2280 IF E3<0 THEN F3=FCR/(1+((-E3/5.0E-3)^.5)) ELSE F3=FCR/(1+((E3/5.0E-3)^.5))
2290 T2=.5*(FCR+F3)*BEZ*D8
2300 D4=X+(((FCR+2*F3)*D8)/(3*(FCR+F3)))
2310 REM *****
2320 REM ***** TO DETERMINE THE RE-BAR FORCE *****
2330 REM *****
2340 E5=ET+(PHI*DRS)
2350 IF YRS=0 THEN 2570
2360 IF YRS<320 THEN 2420
2370 IF E5>.1 THEN N=N-1
2380 IF E5>.1 THEN PRINT "FRACTURE STRAIN OF RE-BAR EXCEEDED"
2390 IF E5>.1 THEN 1750
2400 IF E5>.013 THEN 2500
2410 GO TO 2460
2420 IF E5>.2 THEN PRINT "FRACTURE STRESS IN RE-BAR EXCEEDED"
2430 IF E5>.2 THEN N=N-1
2440 IF E5>.2 THEN 1750
2450 IF E5>.02 THEN 2520
2460 F4=2000000*E5
2470 IF F4>YRS THEN F4=YRS
2480 T3=F4*ARS
2490 GO TO 2570
2500 FSU=710 \ ESH=9755.0 \ SSU=.106 \ SSH=.013
2510 GO TO 2530
2520 FSU=414 \ ESH=4921.4 \ SSU=.202 \ SSH=.02
2530 PH=ESH*((SSU-SSH)/(FSU-YRS))
2540 F4=FSU+(YRS-FSU)*(((SSU-E5)/(SSU-SSH))^PH)
2550 T3=F4*ARS
2560 REM *****
2570 REM *****TO DETERMINE THE CONCRETE COMPRESSION FORCE*****
2580 REM *****

```

```

2590 IF ET<0 THEN 2620
2600 C=-.5*B*H*EC*EB \ T1=0
2610 GO TO 3000
2620 S0=X1*((2/(3*ECS)+ET/(4*(ECS^2)))/(1/ECS+ET/(3*(ECS^2))))
2630 LAR=X1-S0
2640 C=-B*FC*ET*X1*(1/ECS+ET/(3*(ECS^2)))
2650 GO TO 3000
2660 REM *****LINEAR STRESS-STRAIN THEORY*****
2670 IF EB<ET THEN 2800
2680 IF X1<H THEN 2910
2690 S1=((X1-H)^3)*(2/(3*ECS*X1)+(ET*(X1-H))/(4*(ECS^2)*(X1^2)))
2700 S1=(X1^2)*(2/(3*ECS)+ET/(4*(ECS^2)))-S1
2710 S2=((X1-H)^2)*(1/(ECS*X1)+(ET*(X1-H))/(3*(ECS^2)*(X1^2)))
2720 S2=(X1*(1/ECS+ET/(3*(ECS^2))))-S2
2730 LAR=X1-S1/S2
2740 ST1=X1*(1/ECS+ET/(3*(ECS^2)))
2750 ST2=(X1-H)^2*(1/(ECS*X1)+(ET*(X1-H))/(3*(ECS^2)*(X1^2)))
2760 ST=ST1-ST2
2770 C=-B*FC*ET*ST
2780 T1=0 \ DT1=0
2790 GO TO 2950
2800 S3=((X1-H)^3)*(2/(3*ECS*X1)+(EB*(X1-H))/(4*(ECS^2)*(X1^2)))
2810 S3=(X1^2)*(2/(3*ECS)+EB/(4*(ECS^2)))-S3
2820 S4=((X1-H)^2)*(1/(ECS*X1)+(EB*(X1-H))/(3*(ECS^2)*(X1^2)))
2830 S4=(X1*(1/ECS+EB/(3*(ECS^2))))-S4
2840 LAR=S3/S4-(X1-H)
2850 ST1=X1*(1/ECS+EB/(3*(ECS^2)))
2860 ST2=(X1-H)^2*(1/(ECS*X1)+(EB*(X1-H))/(3*(ECS^2)*(X1^2)))
2870 ST=ST1-ST2
2880 C=-B*FC*EB*ST
2890 T1=0 \ DT1=0
2900 GO TO 2950
2910 S3=X1*((2/(3*ECS)+ET/(4*(ECS^2)))/(1/ECS+ET/(3*(ECS^2))))
2920 LAR=X1-S3
2930 C=-B*FC*ET*X1*(1/ECS+ET/(3*(ECS^2)))
2940 T1=.5*B*(H-X1)*EC*EB \ DT1=(2*H+X1)/3
2950 T2=0 \ D4=0
2960 IF X1=H THEN T3=((H-DRS)*ET/H)*200000*ARS
2970 IF X1=H THEN 3000
2980 T3=((DRS-X1)*EB)/(H-X1))*200000*ARS
2990 REM *****
3000 REM ***** CHECK EQUILIBRIUM *****
3010 REM *****
3020 TEN=P(R)+T1+T2+T3
3030 CD=C-TEN
3040 IF ABS(CD)<DLIM THEN 3320
3050 IF CD<=0 THEN 3090
3060 IF EB<ET THEN 3130
3070 EB=EB+INC
3080 GO TO 3190
3090 EB=EB-.95*INC
3100 INC=.5*INC
3110 EB=EB+INC
3120 GO TO 3190
3130 IF CD<=0 THEN 3180
3140 EB=EB+INC
3150 INC=.5*INC
3160 EB=EB-INC

```

```

3170 GO TO 3190
3180 EB =EB-INC
3190 IF INC>5.0E-8 THEN 3240
3200 IF ET<0 THEN 3430
3210 INC=-.1*EB
3220 GO TO 3240
3230 INC=-0.01*ET
3240 N1=N1+1
3250 IF ET<0 THEN 3270
3260 GO TO 2570
3270 IF N1=2000 THEN N=N-1
3280 GO TO 2100
3290 REM *****
3300 REM **** CALCULATE MOMENTS ****
3310 REM *****
3320 PH(JJ)=- (ET-EB)/H \ GH(JJ)=ET+(PH(JJ)*DPS)
3330 MH(JJ)=(T1*DT1)+(T2*D4)+(T3*DRS)+(P(R)*DPS)-(C*LAR)
3340 ETH(JJ)=ET
3350 PRINT "MH",JJ,MH(JJ),"ET=",EB=",ET,EB
3360 NEXT JJ
3370 PRINT "P(R)=",P(R)
3380 MMAX=MH(0)
3390 FOR KI=1 TO NINT
3400 KJ=KI-1
3410 IF MH(KI)>MH(KJ) THEN MMAX=MH(KI)
3420 NEXT KI
3430 WINCC=WIN
3440 FOR I=0 TO NS
3450 V=(I-1)*D
3460 IF V<=LAA THEN 3490
3470 MW(I)=.5*W(R)*LAA
3480 GO TO 3500
3490 MW(I)=.5*W(R)*V
3500 IF I<2 THEN MW(I)=0
3510 NEXT I
3520 FOR KK=0 TO NS
3530 IF MW(KK)=0 THEN EB=-P(R)/(AR*EC)-(P(R)*ECC)/(SM*EC)
3540 IF MW(KK)=0 THEN CCT(KK)=-P(R)/(AR*EC)+(P(R)*ECC)/(SM*EC)
3550 IF MW(KK)=0 THEN PHI(KK)=- (CCT(KK)-EB)/H
3560 IF MW(KK)=0 THEN Q(KK)=CCT(KK)+PHI(KK)*DPS
3570 IF MW(KK)=0 THEN GO TO 3740
3580 IF MW(KK)>MMAX THEN W(R)=W(R)-WINC
3590 IF MW(KK)>MMAX THEN WINC=.8*WINC
3600 IF MW(KK)>MMAX THEN W(R)=W(R)+WINC
3610 IF MW(KK)>MMAX THEN GO TO 3440
3620 IF WINC<1 THEN P(R)=P(R)-PINCCC
3630 IF WINC<1 THEN PINCCC=0.8*PINCCC
3640 IF WINC<1 THEN P(R)=P(R)+PINCCC
3650 IF WINC<1 THEN GO TO 870
3660 FOR IJ=1 TO NINT
3670 JJ=IJ-1
3680 IF MW(KK)<=MH(IJ) THEN 3700
3690 NEXT IJ
3700 PROP=(MW(KK)-MH(JJ))/(MH(IJ)-MH(JJ))
3710 PHI(KK)=PROP*(PH(IJ)-PH(JJ))+PH(JJ)
3720 Q(KK)=PROP*(QH(IJ)-QH(JJ))+QH(JJ)
3730 CCT(KK)=PROP*(ETH(IJ)-ETH(JJ))+ETH(JJ)
3740 NEXT KK

```

```

3750 REM ***** AUG. VALUE OF ECP ALONG LENGTH = BECP *****
3760 REM *****
3770 REM ***** STRAIN COMPATIBILITY AND DEFLECTION *****
3780 REM ***** FOR THIRD POINT LOADING *****
3790 REM *****
3800 IN=INT(LAA/D) \ DD=LAA-IN*D \ DIS=(LBB+LAA)*.5
3810 II=0 \ PT=0 \ PB=0
3820 IF II=0 THEN PB=Q(II)*L \ GO TO 3860
3830 IF II=IN+1 THEN PB=(Q(II)+Q(II+1))*DD*.5+Q(II+1)*(D-DD) \ GO TO 3860
3840 IF II>IN+1 THEN PB=Q(II)*D \ GO TO 3860
3850 PB=.5*(Q(II)+Q(II+1))*D
3860 PT=PT+PB
3870 II=II+1
3880 IF II<=NS THEN 3820
3890 ECP=PT/(.5*S+L)
3900 K=0 \ RT=0
3910 IF K=0 THEN RA(K)=PHI(K)*L \ XB(K)=L/2 \ GO TO 3980
3920 IF K=IN+1 THEN RA(K)=(PHI(K)+PHI(K+1))*DD*.5+PHI(K+1)*(D-DD)
3930 IF K=IN+1 THEN XB(K)=(DD*(PHI(K)+2*PHI(K+1)))/(3*(PHI(K)+PHI(K+1)))
3940 IF K=IN+1 THEN 3980
3950 IF K>IN+1 THEN RA(K)=PHI(K)*D \ XB(K)=D/2 \ GO TO 3980
3960 RA(K)=.5*(PHI(K)+PHI(K+1))*D
3970 XB(K)=(D*(PHI(K)+2*PHI(K+1)))/(3*(PHI(K)+PHI(K+1)))
3980 RT=RT+RA(K)
3990 K=K+1
4000 IF K<=NS THEN 3910
4010 REM ***** CALCULATE DEFLECTION AT MID-SPAN *****
4020 I=1 \ DE=0
4030 IF I=IN+1 THEN DEA=((PHI(I)+2*PHI(I+1))*DD^2)/6
4040 IF I=IN+1 THEN DEB=PHI(I+1)*(D-DD)*(DD+(D-DD)/2)
4050 IF I=IN+1 THEN DEC=(PHI(I)+PHI(I+1))*DD/2+PHI(I+1)*(D-DD)
4060 IF I=IN+1 THEN DE=RA(I)*((I-1)*D+(DEA+DEB)/DEC)+DE
4070 IF I=IN+1 THEN 4100
4080 IF I>IN+1 THEN DE=RA(I)*((I-1)*D+D/2)+DE \ GO TO 4100
4090 DE=RA(I)*((I-1)*D+XB(I))+DE
4100 I=I+1
4110 IF I<=NS THEN 4030
4120 TDEL(R)=DE+IDEL
4130 REM *****
4140 REM ***** LOAD INCREMENT *****
4150 REM *****
4160 IF BECP<0 THEN DIF=-BECP+ECP ELSE DIF=BECP-ECP
4170 PRINT " BECP=",BECP,"ECP=",ECP,"TDEL(R)=",TDEL(R)
4180 PRINT " DIF=",DIF,"LPS=",LPS,"P(R)=",P(R),"W(R)=",W(R),"CCT=",CCT(NS)
4190 IF ABS(DIF)<LPS THEN 4330
4200 IF BECP>0 THEN 4220
4210 IF DIF<=0 THEN 4230 ELSE 4250
4220 IF DIF<=0 THEN 4250
4230 W(R)=W(R)+WINCC
4240 GO TO 3440
4250 W(R)=W(R)-WINCC
4260 WINCC=.8*WINCC
4270 W(R)=W(R)+WINCC
4280 IF WINCC<=1 THEN P(R)=P(R)-PINCC
4290 IF WINCC<=1 THEN PINCC=.8*PINCC
4300 IF WINCC<=1 THEN P(R)=P(R)+PINCC
4310 IF WINCC<1 THEN 870
4320 GO TO 3440

```

```

4330 WW=W(R) \ PLO=P(R)
4340 REM *****
4350 REM ***** PRINT OUT RESULTS *****
4360 REM *****
4370 PRINT #1
4380 PRINT #1,"      Prestressing force (N) =";P(R)
4390 PRINT #1
4400 PRINT #1,"      Applied load (N) =";W(R)
4410 PRINT #1
4420 PRINT #1,"Required average value of Ecp=";BECF
4430 PRINT #1
4440 PRINT #1,"Computed Average value of Ecp=";ECP
4450 PRINT #1
4460 PRINT #1,"      Deflection(mm) at mid-span=";TDEL(R)
4470 PRINT #1
4480 PRINT #1,"SECN";TAB(7);"DPS";TAB(12);"X";TAB(20);"M(N.mm)";
4490 PRINT #1,TAB(34);"PHI";TAB(47);"Ecp";TAB(59);"ECT"
4500 PRINT #1,"-----"
--";
4510 PRINT #1,"-----"
--"
4520 PRINT #1
4530 FOR HH=0 TO NS
4540 IF HH=0 THEN DD=(HH*D)-L ELSE DD=(HH-1)*D
4550 PRINT #1 USING"  ##   ##.   ###.##   ##   ##   ^^^^   #.####^    #.####^    #.####^    #.##
##^    ",HH,DPS,DD,MW(HH),PHI(HH),Q(HH),CCT(HH)
4560 NEXT HH
4570 PRINT #1
4580 PRINT #1,"-----"
--";
4590 PRINT #1,"@@@@@@@@@@@@@@@@@@@@@@@@@@@@@@@@@@@@@@@@@@@@@@@@@@@@@@@@@@@@@@@@@@@@@@@@@@@@@@@@@@@@
@@@
4600 R=R+1 \ W(R)=WW \ P(R)=PLO+PINC \ WINC=WIN
4610 IF P(R)=>MP THEN 4630
4620 GO TO 870
4630 CLOSE #1
4640 END

```